Extrusion Cooking

Craft or Science ?

D.J. van Zuilichem

Promotoren: dr. ir. K. van 't Riet, gewoon hoogleraar in de levensmiddelenproceskunde aan de Landbouwuniversiteit Wageningen.

dr. ir. L.P.B.M. Janssen, gewoon hoogleraar in de technische scheikunde aan de Rijksuniversiteit Groningen.

D.J. van Zuilichem

Extrusion Cooking

Craft or Science?

Proefschrift
ter verkrijging van de graad van
doctor in de landbouw- en milieuwetenschappen,
op gezag van de rector magnificus,
dr. H.C. van der Plas,
in het openbaar te verdedigen
op woensdag 29 januari 1992
des namiddags te vier uur in de aula
van de Landbouwuniversiteit te Wageningen.

This thesis has been accomplished at:
Agricultural University Wageningen,
Department of Food Science,
Food and Bioprocess Engineering Group
office: Biotechnion, Bomenweg 2,
P.O. box 8129, 6700 EW Wageningen,
The Netherlands.

Manuscript typing: J. Krauss/S. Nijweide
Photography: J.B. Freeke
Illustrations: W. Stolp/M. Schimmel

aan *Ria*
Dirk
Janneke

Voorwoord

Dit proefschrift is gegroepeerd rond een zestal wetenschappelijke artikelen, waarvoor het onderzoek is uitgevoerd bij de Sectie Proceskunde van de Vakgroep Levensmiddelentechnologie te Wageningen. Het extrusie-onderzoek dateert uit de zeventiger jaren. Sinds 1973 is regelmatig gepubliceerd en gerapporteerd op symposia. Daarom is hoofdstuk 1 méér dan een publicatie, nl. een uitgebreide algemene inleiding, die de stand van zaken beschrijft op het gebied van de levensmiddelen-extrusietechniek. Tevens blijkt hieruit de filosofie achter het onderzoek sinds de aanvang in de zeventiger jaren, toen is begonnen met de bestudering van een eenvoudige enkelschroefextruder van Nederlandse makelij. De complexiteit van de extrusietechnologie zorgde voor een langzame maar gestadige groei van de Wageningse kennis op dit gebied, waarbij een omvangrijke groep collega's en medewerkers nauw betrokken is en zonder wie dit proefschrift niet tot stand zou zijn gekomen. Graag wil ik hier bedanken Willem Stolp, Theo Jager, Eric van der Laan, en de vele studenten die bij experimenten, discussies en presentaties onmisbaar waren. Voor hun wetenschappelijke kritieken en aanmoedigingen ben ik veel dank verschuldigd aan Henk Leniger, Solke Bruin en Klaas van 't Riet, die mij achtereenvolgens in de gelegenheid stelden dit onderzoek te verrichten. Buiten de LU, maar heel nabij in het vak als vriend en promotor is er Leon Janssen, die mij aanmoedigde om een deel van de Wageningse kennis te bundelen in dit proefschrift. Bij de vele contacten met hem bij de TU Delft en bij alle samenwerkingen met de collega's van de Rijksuniversiteit Groningen is er altijd die prettige sfeer van collegialiteit zijn, die zo zeldzaam is.
Van de extruderfabrikanten met wie is samengewerkt wil ik vooral APV-Baker noemen, die zeer genereus onze groep van medewerkers en studenten heeft ondersteund met apparatuur.
Tenslotte wil ik graag de medewerkers van de mechanische werkplaats, de electrowerkplaats, én de servicegroep resp. onder leiding van Johan van de Goor, Guus van Munster, Rink Bouma en Leo Herben bedanken voor de vlotte en deskundige hulp bij de vele modificaties en onderhouds-werkzaamheden aan de vele types extruders, waarop de metingen ten behoeve van dit proefschrift zijn verricht.

Preface

This thesis is written around six publications for which research has been undertaken at the Food and Bioprocess Engineering group of the Department of Food Science in Wageningen. The extrusion research in Wageningen originated in the seventies. Since 1973, results were regularly published and presented at symposia. Because of this, chapter one has more to offer than just a publication; it is more of an extended general introduction which describes the state of the art of food extrusion. It also elucidates the idea behind the extrusion research program when started in the early seventies with a simple single screw extruder of Dutch origin. The know how in Wageningen progressed slowly but steady due to the complexity of extrusion technology. A considerable group of colleagues and co-workers were closely involved in the accomplishment of this thesis. With pleasure, I would like to thank Willem Stolp, Theo Jager, Eric van der Laan and the numerous students who were indispensable for the experiments, discussions and presentations. For the scientific criticism and support I would like to express my gratitude to Professor H.A. Leniger, Professor S. Bruin and Professor K. van 't Riet who respectively offered me the opportunity to undertake this research. From outside the university, I thank Leon Janssen for being a friend, colleague as well as promotor and for encouraging me to write this thesis. The numerous contacts with him and his staff respectively at the Delft Technical University and now at the Rijksuniversiteit Groningen always lead to a cooperation on extrusion topics in a pleasant and rarely found atmosphere. A word of special thanks is reserved for APV-Baker, the extruder manufacturer who supported generously our group of co-workers and students with extruder equipment. Also should be mentioned the great support of our mechanical, electrical and service workshop respectively supervised by Mr. J. van de Goor, Mr. A. van Munster, Mr. R. Bouma and Mr. L. Herben. Their expert assistance was very much needed performing the many modifications and maintenance activities concerning the several extruder types used for the measurements resulting in this thesis.

CONTENTS

Extrusion Cooking, Craft or Science?

CHAPTER 1

GENERAL INTRODUCTION TO EXTRUSION COOKING OF FOOD AND FEED

1.1 Definition and scope

It is not longer ago than the seventies when a food extruder was described as a piece of equipment, consisting out of a barrel and one or two screws. The function of the extruder was believed to receive an agricultural product, to transport it from a feed section to a screw metering section over a compression section. With the help of shear energy, exerted by the rotating screw, and additional heating by the barrel, the food material is heated to its melting point or plasticating-point. In this changed rheological status the food is conveyed under high pressure through a die or a series of dies and the product expands to its final shape.

It is obvious that this more or less phenomenological definition is simple and not complete, since some important properties of the extruder as a food and feed unit operation are not yet mentioned. In the first place one should recognize the cooking extruder to belong to the family of HTST (High Temperature Short Time)-equipment, with a capability to perform cooking tasks under high pressure (van Zuilichem et al. 1975; van Zuilichem et al. 1976). This aspect may be explained for vulnerable food and feed as an advantageous process since small time span exposures to high temperatures will restrict unwanted denaturation effects on

e.g. proteins, aminoacids, vitamins, starches and enzymes. However, one should realize that now physical technological aspects like heat transfer, mass transfer, momentum transfer, residence time and residence time distribution have a strong impact on the food and feed properties during extrusion cooking and can drastically influence the final product quality. Secondly we should realize that a cooking extruder is a process reactor (van Zuilichem et al. 1979; Janssen et al. 1980), in which the designer has created the prerequisites in the presence of a certain screw lay-out, the use of mixing elements, the clearances in the gaps, the installed motor power and barrel heating and cooking capacity, to control a food and feed reaction. This can be a reason "in itself", when only mass is transferred in wanted and unwanted reaction products due to heating, e.g. the denaturation of proteins under presence of water and the rupture of starches, both affected by the combined effects of heat and shear. The reaction can also be provoked by the presence of a distinct biochemical or chemical component like an enzyme or a pH controlling agent. When we consider the cooking extruder to be more than was mentioned originally, a thorough investigation of the different physical technological aspects is more than desirable. This is the motive for the set up of the chapters 1 to 7 and the objective for this study. In cooking extrusion, it is obvious that the study concerns the residence time behaviour, which is done in the chapters 2 and 3 for single and twin screw extruder equipment. The transfer of heat and mass during extrusion-cooking is reported in the chapters 4 and 5. The effect of equipment design on reactor performance has always been very strong. As an example of the outcome of a certain important design feature on the degree of fill in a twin-screw extruder and the resulting unavoidable residence time distribution effects is reported in chapter 6. Finally the capability of an extruder to replace partly a conventional bioreactor, is discussed in chapter 7, in which a process is developed for starch disclosure in a cooking extruder, followed by a saccharification process in a conventional piece of equipment, leading to a calculable process with unique features in bioconversion. The above mentioned

aspects are explained further in the paragraphs 1.2 to 1.7.

1.2 Historical development

Extrusion cooking is nowadays a food and feed processing and manufacturing tool. The significance of it should not be underestimated since the technology is relatively new and also during the last 40 years it is one of the few successfull unit operations for food in Europe that is still developing. Industrial extrusion processes however did not originate in the food sector but in the rubber and plastic polymer industry. In this branche there was a need for continuously operating manufacturing equipment in order to meet the increasing demand for rubber hoses, tubing and sheets for building, householding, farming and starting chemical industry. Between 1855-1880 single screw extruders for rubber products were developed. Just before

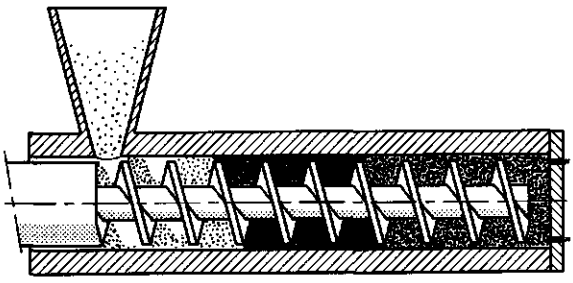

Fig. 1.1 Cold forming extruder

1900 also some applications in the metal branch were described. e.g. the continuous production of tubing out of lead and aluminium and some heat-forming processes used by the steel industry, that can be partly understood as extrusion processes. In those cases single screw extruders were used as friction pumps, while lat the same time a forming task is performed (Fig. 1.1).

At first in 1935 the application of single screw extruders for plasticating thermoplastic materials became more common as a competitor for hot rolling and shaping in hydraulic-press equipment. A plasticating single screw extruder is given in Fig. 1.2, provided with a typical metering screw, developed for this

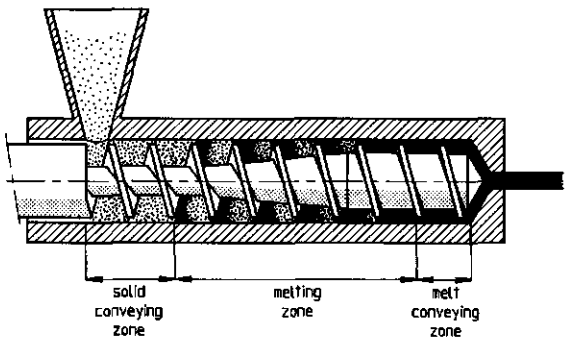

Fig. 1.2a Typical plasticating single screw extruder

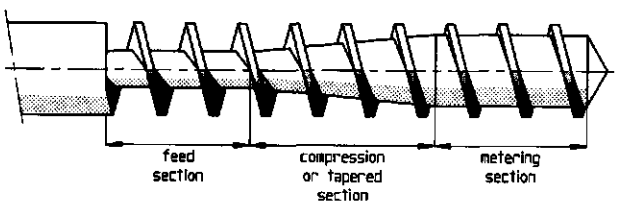

Fig 1.2b Typical plasticating screw

application.

In the mid thirties we notice the first development of twin-screw extruders, both co-rotating and counter rotating, for food products. Nearly in the same period, but shortly after, single screw extruders in the pasta industry became common use for the production of spaghetti and macaroni-type products. In analogy with the chemical polymer industry the single screw equipment was used here primarily as a friction pump and it acts more or less as continuously cold forming equipment, using conveying-type screws (Fig. 1.1). It is remarkable that nowadays the common pasta products are still manufactured in the same single screw extruder equipment with a length over diameter ratio (L/D) of approximately (6 to 7). The main difference with the thirties is that since that period much development work has been done for screw and die-design and much effort has been put into process control, such as sophisticated temperature control for screw and barrel sections, die tempering and, the application of vacuum at the feed port. Finally scale up of the equipment has been done

from a poor hundred kilos hourly production up to several tons. It should be noticed that this progress in pasta extrusion technology mainly has been gained in the time period after 1975. In order to achieve this, combined research was performed by equipment manufacturers and technologists from universities. This has led to the construction of high efficiency screws, improved screw and barrel-design, the development of good steeltypes, reduced wear, and better constructed downstream equipment such as cutters and dryers.

The development of many different technologies seems to be catalysed by World War II, as is the extrusion cooking

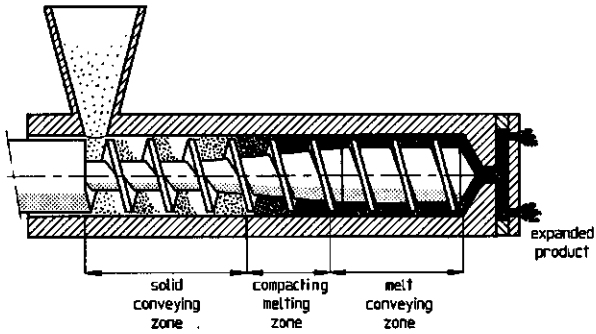

Fig. 1.3 Food extruder for direct expanded products

technology. In 1946 in the US the development of the single screw extruder to cook and expand corn- and rice-snacks occurred (Fig. 1.3). In combination with an attractive flavouring this product type is still popular, and the way of producing snacks with single screw extruder equipment is in principle still the same. A wide variety of extruder designs is offered for this purpose. However it should be mentioned that the old method of cutting preshaped pieces of dough out of a sheet with roller-cutters is still in use, which is due to the fact that complicated shapes of snacks lead to very expensive dies and die-heads for cooking and forming extruders. Here the lack of knowledge of the physical behaviour of a tempered dough and the unknown relations of the transport phenomena of heat, mass and momentum towards physical

and physico-chemical properties of the food in the extruder are clearly noticed. Although modern control techniques offer a big help in controlling the mass flow in single screw extruders, in a lot of cases it is a big advantage to use extruders with better mixing and more steady mass flow, then single screw equipment is offering.

In the mid seventies the use of twin screw extruders for the combined process of cooking and forming of food products has been introduced, partly as an answer to the restrictions of single screw extruder equipment since twin screw extruders provide a more or less forced flow, and partly because they tend to be machinery with better results in scale up from the laboratory extruder types, in use for product development.

1.3 Differences between food-and plasticating-polymers.

When we compare the effects of the polymers in thermoplastics and food we notice that nearly all chemical changes in food are irreversible. A continued treatment after such an irreversible reaction in an extruder should be a temperature, time and shear controlled process leading to a series of completely different functional properties of the produced food (Table 1.1)

Table 1.1 Comparison between thermoplastic- and food polymers

	Plastics	Food
1 Feed to the extruder	Single polymer	Multiple solids, water and oil
2 Composition	Well defined structure and molecular weight	Not well defined. Natural biopolymers, starch, protein, fibre, oil and water
3 Process	Melting and forming. No chemical change. Reversible	Dough or melt-like formation with chemical change. Irreversible continued treatment leads to wanted specific functional properties
4 Die forming	Shape is subjected to extrudate swell	Subjected to extrudate swell and possibly vapour pressure expansion
5 Biochemicals	Use of fillers, e.g. starch	Use of enzymes and biochemicals for food conversion

An answer nowadays of food familiar extruder equipment manufacturers is the design of process lines, where the extruder cooker is part of a complete line. Here the extruder is used as a single or twin screw-reactor, wheras the preheating/ preconditioning step is performed in an especially built preconditioner. The forming task of the extruder has been separated from the heating and shearing. The final shaping and forming has to be done in a second and well optimised post-die forming extruder, processing the food at a lower water level than in the first extruder (Fig. 1.4). In such a process line cooked

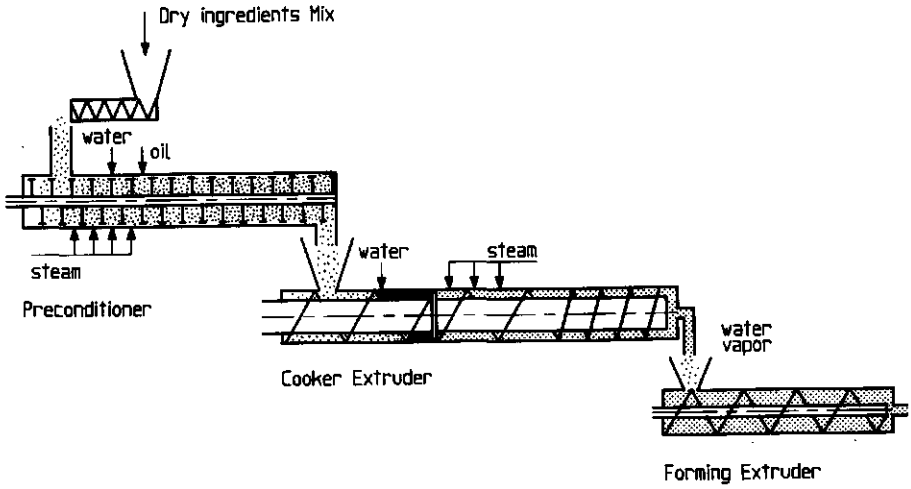

Fig. 1.4 Extruder line for cooked and formed unexpanded food pellets

and preshaped but unexpanded food pellets can be produced. Most benefit is got in handling and controlling the amounts of water in the different stages of the process. In the preconditioner-

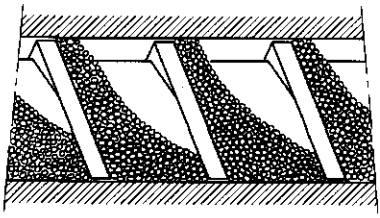

Fig. 1.5 'Archimedes' conveying section

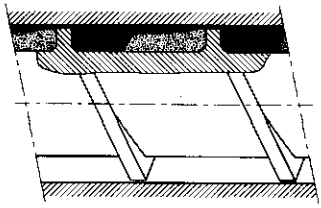

Fig 1.6 Plasticating polymer melting model

water, steam and possibly oil are injected. In the cooker extruder a special screw is operated avoiding steamleakage towards the feed zone and thus having most benefit of the extra steam input, for quicker cooking and higher throughput, caused by the lower viscosity in the cooking zone. After a venting step at the die plate of the extruder a special forming extruder produces a homogeneous, precooked food material at the lowest possible moisture content. The result is a typical food process line differing very much from a comparable extruder line out of the chemical plasticating industry.

With the use of the extrusion equipment in process lines their tasks became more specialised. This encouraged the comparison of extruder performance with that in the plastic industry, which promotes the transformation of the extrusion-cooking craft into a science, taylor made for the 'peculiar' properties of biopolymers.

1.4 Food melting

In analogy with the chemical industry, handling plasticating polymers, a good understanding of the so called food melting phenomena in the different extruder types is needed for equipment design. If that knowledge is available the shearing screw section in the single screw extruder or the melting section of a set of screws of a twin screw extruder can be designed. The first part of each screw is a conveying section, that brings the food material in the direction of the melting In a single screw extruder this conveying screw is designed as an Archimedes-screw allowing a limited filling degree, 'resulting' in a solid bed that only fills up the bottom of the channel and that is pushed by the screw flight (Fig. 1.5). As a result of the pumping towards a "pressure slope" the food material is compacted, the air is pressed out, pressure is developed and the food material is heated by friction and shear. In the plastic polymer industry the melting model of Maddock and Vermeulen (1959) is used (Fig. 1.6), which includes that the screw flight pushes a fast melting solid bed through the compression section of the screw (Fig. 1.2). This melting takes place over the melting distance, different in length, depending on the selected screw pitch, compression ratio and barrel temperature. The melting models by Maddock and Vermeulen (1959) are almost invalid for food material, however the model described by Dekker and Lindt (1976) (Fig. 1.7) is quite well usable and describes more or less the typical way of food melting for a number of food applications. Here the food melting only starts in the way as described by Maddock and Vermeulen (1959) in the first pitches, but immediately after that the solid bed is lifted up by the melt and a time consuming process starts. Hereby, the heat developed over the decreasing friction in the direction of the die, caused by

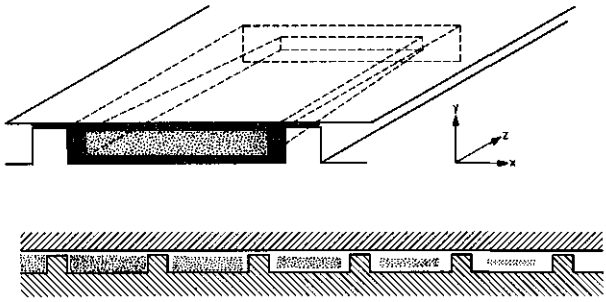

Fig. 1.7 Melting model by Dekker and Lindt

a decreasing viscosity, has to penetrate to the solid bed, which crumbles away and finally is present as a thin solid crust in the middle of the screw channel. Then it depends on the length of the metering section if the available residence time allows to melt down the remaining solid parts of the food biopolymer completely. If the aim of the extrusion cooking process in question is a simple denaturation of the food polymer, without further requirements of food texture, then the experience out of the chemical polymer extrusion field to apply special screw melting parts is advisable, as the melting will be accelerated. In principle the effect of those melting parts is based on improved mixing.

This mixing effect can be based on particle distribution or on shear effects exerted on product particles. For distributive mixing the effects of mixing are believed to be proportional to the total shear given by:

$$\gamma = \int_0^t \frac{dv}{dx} dt \qquad (1)$$

Whereas for dispersive (shear) mixing the effect is proportional with the shear stress (τ):

$$\tau = \mu \frac{dv}{dx} \qquad (2)$$

The group of distributive mixing screws can be divided in the pin

mixing section, the Dulmage mixing section, the Saxton mixing section, the pineapple mixing head, slotted screw flights and the cavity transfer mixing section respectively (Fig. 1.8). The pin mixing section or a variant of this design is used for food in the Buss Co-kneader which is a reciprocating screw provided with pins of special feature, rotating in a barrel provided with pins as well. When we recognize food expanders to be food extruders then much use is made here of the pin-mixing effect, since the barrels of expander equipment, built like the original Anderson design, are provided with mixing pins. The amount of mixing and shear energy is simply controlled by varying the number of pins (Fig. 1.9). Mixing heads like the Dulmage design and the Saxton mixing section as such are not used in food extrusion cooking, although some single screw extruder manufacturers have designs

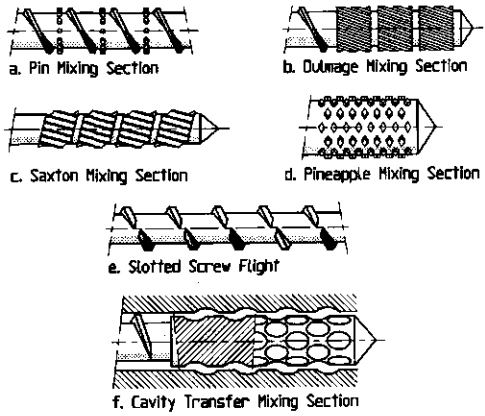

Fig. 1.8 Distributive mixing elements

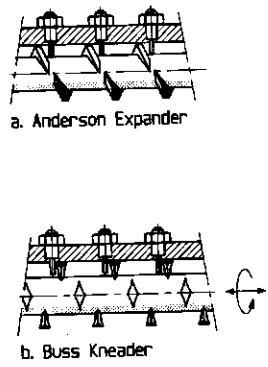

Fig. 1.9 Mixing pin elements Anderson and Buss designs

available, like e.g. special parts of Wenger single screw equipment, where some influence of the mentioned designs is recognizable. The pineapple mixing section or the most simple mixing torpedo has a future in food extrusion cooking due to its simplicity and effectivity. The designs of Fig. 1.8.e and 1.8.f are attractive in food extrusion because of their gentle mixing action, which implies that mixing heads of this design can be used at the end of the metering sections of food extruders

without disturbing the mass-flow at this location too much. In chapter 4 is described how solid saccharose crystals are succesfully melted in a single screw extruder using a torpedo mixing head and how heating and dissolution of saccharose crystals in liquid glucose syrup in a twin screw extruder can be described when a mixing region consisting of a pair of slotted screw flights is present.

Both the designs in Fig. 1.8.e and Fig. 1.8.f are used to correct the non complete melting of food particles in the melting parts of the extruder screws. It is logic that the less expensive slotted screw flight is mostly used, especially in the metering zone, providing the final mixing before the food material enters the die area, at a low level of shear. When we need more

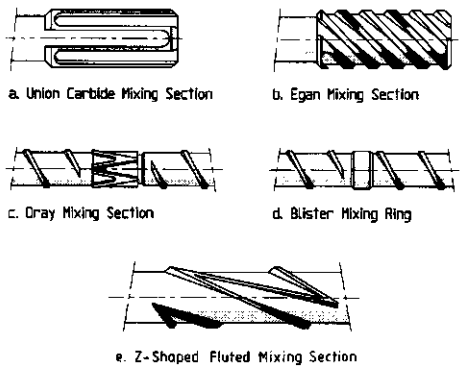

Fig. 1.10 Dispersive mixing element

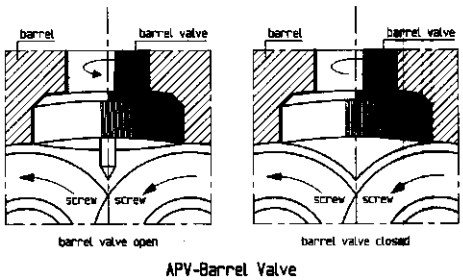

Fig. 1.11 Adjustable barrel-valve by D. Todd (APV-Baker)

dispersive mixing to be exerted to the product, we can make use of the mixing elements, such as the Union Carbide mixing section, the Egan mixing section, the Dray mixing section, the Blister mixing ring or the Z-shaped fluted mixing section (Fig. 1.10). All these designs originate from the plastic industry, but in food extrusion cooking only variants of the Blister mixing ring are used, of which the most remarkable design is the one used in the Baker Perkins equipment, an adjustable barrel valve, constructed by D. Todd (Fig. 1.11). Here an adjustable valve of

which the position can be controlled from the topside of the barrel, is mounted between two Blister rings, placed as a pair in the screwset. The exact function is described in chapter 6. It is expected that the use of such elements in food extrusion cooking will shorten the melting section of the extruder screw and by this will shorten the total length of the screw, due to the ability of the barrel valve to influence the degree of fill in the extruder and increasing the fully filled length as a result. This allows a better dissipation of the motor power over the friction of the product.

In plastic polymer extrusion we will also find the so called barrier flight extruder screws (Fig. 1.12). A well-known design is the one by Maillefer at which the melt is allowed to flow over the screw flight to its own melt channel. A variant on this design is the one by Ingen Housz which can be seen as an optimization of the separation of melt and solids on the screw for plastic polymers.

Up till now in the food and feed industry there is not made any use of those barrier flight screws. In single screw food

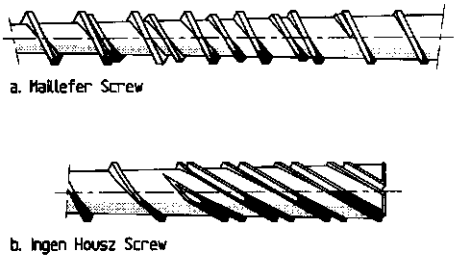

Fig 1.12 Barrier flight extruder screws

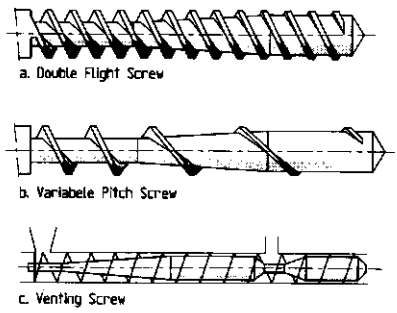

Fig. 1.13 Special screws for single screw extruder

extrusion one will make use of double flighted screws, variable pitch screws and in rare cases a venting screw (Fig. 1.13). Some extruder manufacturers offer modular screw set-ups for single screw designs, making them more flexible than the solid screws out of Fig. 1.13, but it should be said that, especially when

aspects of flexibility are in question, the selection of a twin screw extruder can be justified.

In conclusion it can be said that there is a strong impact of plastic polymer extrusion on the field of food extrusion technology. At first there is the availability of well developed and refined hardware, which includes extruder equipment and instrumentation & control systems. Of course they have to be developed further and/or sifted out to suit specific food applications. Secondly there is the availability of polymer engineering process know-how. Although this know-how is very limited, even for thermoplastic extrusion operations, it has formed the basis of food extrusion engineering analysis as well.

1.5 Rheological considerations

It has already been mentioned that usually non-Newtonian flow behaviour is to be expected in food extruders. A major complication is that chemical reactions also occur during the extrusion process (e.g. gelatinization of starch or starch-derived materials, denaturation of proteins, Maillard reactions), which strongly influence the viscosity function. The rheological behaviour of the product, which is relevant to the modelling of the extrusion process as such, has to be defined directly after the extruder screw before expansion in order to prevent the influence of water losses, cavioles in the material and temperature effects due to the flashing process that occur as soon as the material is exposed to the (environmental) air. A convenient way would be to measure the pressure loss over capillaries with variable diameter and length. However, this method has a certain lack of accuracy, since pressure losses due to entry effects are superimposed on the pressure gradient induced by the viscosity of the material (Bagley 1957). Moreover, since the macromolecules in the biopolymers introduce a viscoelastic effect, the capillary entry and exit effects cannot be established easily from theoretical considerations.

In order to overcome the difficulties mentioned above, several authors (van Zuilichem 1974, 1980, von Lengerich, 1984) prefer

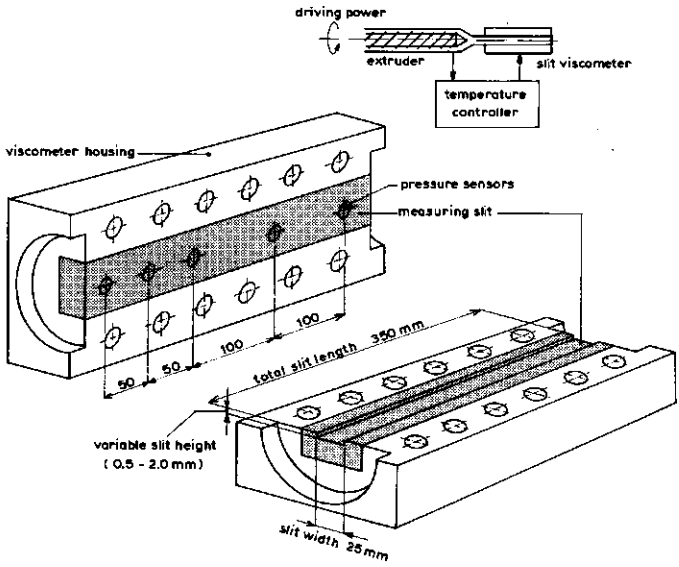

Fig 1.14 Slit viscosimeter

a slit viscosimeter (Fig. 1.14). Here pressures can be measured inside the channel in order to eliminate the entry and exit effects.

It has to be realized that if the pressure gradients have to be measured at different slit geometries, and at different throughputs, the thermal history and the temperature of the material in the slit are changing. In order to determine the exact viscous behaviour of extruded food, a correction for these two variations has to be introduced.

It is well known that within normal operating ranges starches and protein-rich material are shear thinning. This justifies the use of a power law equation for the shear dependency of the viscosity:

$$\eta_a = k|\dot{\gamma}|^{n-1} \qquad (3)$$

in which η_a is the apparent viscosity, $\dot{\gamma}$ stands for the shear rate and n is the power law index.
Metzner (1959) has argued that for changing temperature effects this equation can be corrected by multiplying the power law effect and the temperature dependency, thus giving:

$$\eta_a = k' \, |\dot{\gamma}|^{n-1} \exp(-\beta \Delta T) \qquad (4)$$

The viscosity will also be influenced by the processing history of the material as it passes through the extruder. In order to correct for this changing thermal history it has to be realized that interactions between the molecules generally occur through the breaking and formation of hydrogen and other physico-chemical bonds. This cross-linking effect is dependent on two mechanisms: a temperature effect determines the frequency of breaking and the formation of bonds and a shear effect determines whether the end of a bond that breaks meets a "new" end or will be reattached to its old counterpart. If we assume that this last effect will not be a limiting factor as soon as the actual shear rate is higher than a critical value and that the shear stress levels within the extruder are high enough, then the process may be described by an Arrhenius model, giving, for the reaction constant:

$$K(t) = k_\infty \exp - \frac{\Delta E}{RT(t)} \qquad (5)$$

where ΔE is activation energy, R the gas constant and T the absolute temperature. Under the assumption that the crosslinking process may be described as a first order reaction, it is easy to show that from the general reaction equation:

$$\frac{dC}{dt} = K(1-C) \qquad (6)$$

the following can be derived:

$$1-C = \exp\left(-\int_0^{\tau} \exp-\frac{\Delta E}{RT(t)}\,Dt\right) \qquad (7)$$

in which C denotes the ratio between actual crosslinks and the maximum number of crosslinks that could be attained, and where Dt is a convective derivative accounting for the fact that the coordinate system is attached to a material element as it moves through the extruder. Therefore, the temperature, which is of course stationary at a certain fixed position in the extruder, will be a function of time in the Lagrangian frame of reference chosen. This temperature history is determined by the actual position of the element in the extruder, as has been proved for synthetic polymers by Janssen et al (1975). It is expected that this effect will cancel out within the measuring accuracy and that an overall effect based on the mean residence time τ may be chosen. In combination it may now be stated that the apparent viscosity of the material as it leaves the extruder may be summarized by the following equation:

$$\eta_a = k'' \,|\dot{\gamma}|^{n-1} \exp(-\beta T)\, \exp\left(\int_0^{\tau} \exp-\frac{\Delta E}{RT(t)}\,Dt\right) \qquad (8)$$

Under the restrictive assumption that the constants k, n, ß and ΔE are temperature independent, it is obvious that at least four different measurements have to be carried out in order to characterize the material properly!

It appeared that the proposed procedure can be applied adequately to materials with sufficient homogeneity as there is e.g. in soy and purified starches.

Once the apparent viscosity is known it is possible to plot the value of a power number P* for different Reynolds numbers Re. This is presented for soy in Fig. 1.15 and leads to a value of

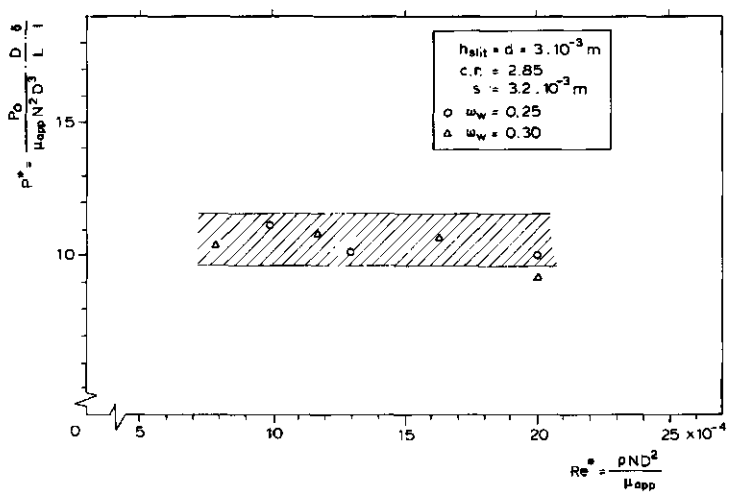

Fig 1.15 Power-number vs -Re- for soy (van Zuilichem et al., 1980)

P*=10 for the single screw extruder in question (van Zuilichem et al., 1980).

The expression for the apparent viscosity in eq. 6 can now be a key factor in the calculation of the dissipated and convectional heat, as will be described in chapter 5.

1.6 Residence time distribution

The irreversible chemical reactions of food materials as mentioned in Table 1 make the time temperature history an important subject in extrusion-cooking. The residence time distribution gives some clues to the time temperature history and it is not surprising that there are more residence time distribution studies known for food,- than for plastic applications (Jager, 1991). Several studies by Wolf and White (1976), Janssen (1979), Pinto and Tadmor (1970), and Bigg and Middleman (1974) have been directed towards experimental verification of residence time distributions in extruders. Measurements performed with radioactive labelled material such as ^{64}Cu are shown for maize grits in Fig. 1.16 and Fig. 1.17. The measurement system consists of a dual detector-set in coincidence mode, allowing to measure accurate RTDs as described by van

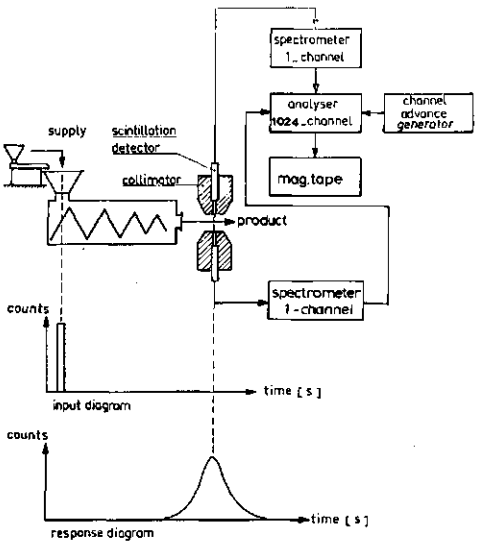

Fig 1.16 Measurement set-up for residence time distributions (Bartels et al., 1982)

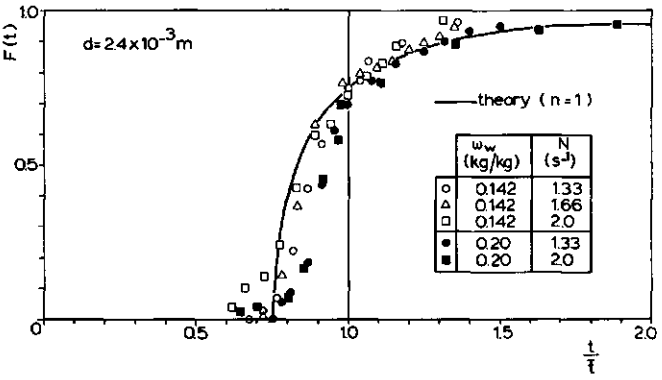

Fig 1.17 F(t) curve for extrusion of corn grits in a single screw extruder (Bruin et al., 1978)

Zuilichem at al. (1988). It can be seen from Fig. 1.17 that, within reasonable limits, the distributions in residence times agree with the theory as it is derived for synthetic polymer extrusion. The same result holds for our soy and maize extrusion measurements as reported in chapter 2. There is some tendency for an early breakthrough at higher rotational speeds when compared with the theory. This was taken from earlier work by van

Zuilichem et al (1973) where measurements with a single screw extruder were reported. When evaluating these measurements careful, the conclusion was made to investigate this problem once again but this time with a better measurement set up. This is shown in the following chapters 2 and 3 for single and twin screw extruders, where in both cases the single detector from the work in 1973 was replaced by a pair of detectors working in coincidence mode. This measuring set up allows very accurate measurements, giving reliable RTD-plots for single and twin-screw extruders.

1.7 Quality parameters

In conclusion, from the foregoing it can be stated that an extruder may be considered as a reactor in which temperature, mixing mechanism and residence time distribution are mainly responsible for a certain viscosity. Quality parameters such as the texture are often dependent on this viscosity. The influence of various extruder variables like screw speed, die geometry, screw geometry and barrel temperature on the produced quality is described by numerous authors for many products e.g. for soy and maize by van Zuilichem (1974,1975,1976,1977) and Bruin et al (1978). However, other extruder process variables like initial moisture content, the intentional presence of enzymes, the pH during extrusion, etc., also play a role. Although a variety of test methods is available a versatile instrument to measure the changes of consistency during pasting and cooking of biopolymers is hardly available. A series of measuring methods is used in the extrusion cooking branch. A compilation of them is given in Fig. 1.18, from which can be seen that an extruded and cooked product is described in practice by its bulk density, its water sorption, its wet strength, its dry strength, its cooking loss and its viscosity behaviour after extrusion for which the Brabender viscosimetry producing amylographs may be chosen, which learn about the response of the extruded material on a controlled temperature, time function (Fig. 1.19).
Only well trained people will understand those Brabender diagrams. For a succesfull description of properties of starches

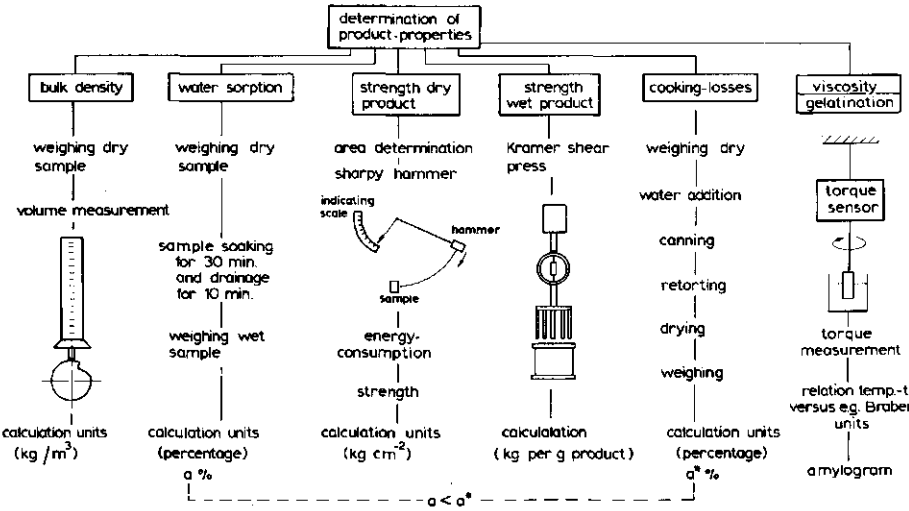

Fig. 1.18 Measuring methods for extruder product properties (Bruin et al., 1980)

and proteins we will need additional chemical data like dextrose-equivalents, reaction rate constants and data describing the sensibility for enzymatic degradation. The task of the food engineer & technologist will be to forecast the relation between those properties and their dependency of the extruder variables. Therefore it is necessary to give a (semi)-quantitative analysis of the extrusion cooking process of biopolymers which can be done when adopting an engineering point of view, whereby the extruder is considered to be a processing reactor. Although the number of extrusion applications justify an optimistic point of view, more experimental verification is definitely needed focussed on the above mentioned residence time distribution, the temperature distribution, the interrelation with mechanical settings like screw compositions, restrictions to flow. And the use of bio-chemicals like enzymes. Enzymes influence directly the viscosity of the biopolymer in the screw channel of the extruder reactor as is investigated in chapter 7 where an extruder cooker is used as a biochemical processreactor. After many of these efforts one will be in a position to give a fair answer to the

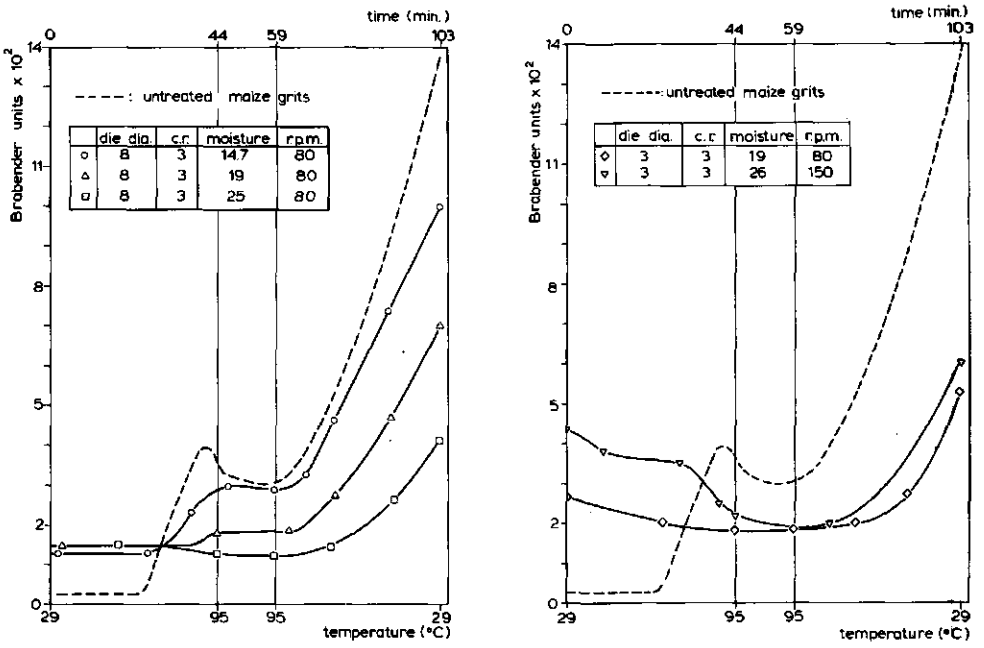

Fig 1.19 Amylograms showing the influence of product moisture content and extruder variables (van Zuilichem et al., 1982)

question if extrusion cooking is a craft or a science.

1.8 Influence of marketing interests on extrusion cooking

In food production the most advanced extrusion processes are found in the snack industry, where the sales are dominated by the combined efforts of the marketing- and the product-development-departments. The product development engineer mostly is somebody who has grown up with the factory and who has a longstanding experience with the raw materials, commonly handled in the extruder-operations, and with the extruder equipment itself. He will run trials with selected raw material compositions and flavours and will develop the dies wanted by the marketeers by extensive trial and error, and finally the new product is there. Such a man or woman is a key factor to the qualification of the developed snack for the supermarket shelf. They can be described as specialists, although their knowledge of the fundamental phenomena in the extruder itself is very poor. Taking into

account that their backgrounds are those of a good operator with feeling for the material, feeling for a certain extruder/die design and recognizing the possibilities of a flavour in combination with the new product, than we will understand that a nearly impossible appeal is done on them in modern times like today, since there is the influence of fashion, trends, new exotic raw materials, etc. The market expects in general every half a year a new succesfull product in the supermarket, with inviting taste, color, bite, outlook, shape regularity, lower fat content, which means that the "specialist" in question should know much more about the transport phenomena in the extruder-equipment.

In other branches of the food industry a comparable situation is found as in the snackfood branch where the extrusion cooking technology has been introduced. The confectionery industry, the baking industry, the pharmaceutical industry and the animal feed industry can be mentioned. Here the extruder cooker still is a relatively new piece of equipment and specialists in this field expect the extruder cooker to be a process tool capable to help the industry to develop new series of products. For this purpose one can make use of the unique property of the extruder cooker to be a high temperature/pressure short residence time (HTST) piece of equipment, capable e.g to replace conventional process lines in its own.

References

Bagley, E.B., (1957). End corrections in the capillary flow of polyethylene. J. App. Physics, 28, 624.

Bartels, P.V., Janssen, L.P.B.M., van Zuilichem, D.J., (1982). Residence time distribution in a single screw cooking extruder.

Bigg, D. M., Middleman, S. (1974). Mixing in a single screw extruder. A model for residence time distribution and strain. Ind. Eng. Chem. Fundam., 13, 66-71.

Bruin, S., van Zuilichem, D.J., Stolp, W. (1978). A review of fundamental and engineering aspects of extrusion of biopolymers in a single screw extruder. J. Food Process Eng., 2, 1-37.

Dekker, J. (1976). Verbesserte Schneckenkonstruktion fur das Extrudieren von Polypropylen. Kunststoffe, 66, 130-135.

Jager, T. (1991). Residence time distribution in twin-screw extrusion. Thesis of the Agricultural University of Wageningen.

Janssen, L.P.B.M. (1978). Twin Screw Extrusion. Elsevier Scientific Publishing Company, Amsterdam.

Janssen, L.P.B.M., Noomen, G.H., Smith, J.M. (1975). The temperature distribution across a single screw extruder channel. Plastics and Polymers, 43, 135-140.

Janssen, L.P.B.M., Smith, J.M. (1979). A comparison between single and twin screw extruders. Proc Int. Conf. on Polymer Extrusion. Plastics and Rubber Institute, London, June, 91-

99.

Janssen, L.P.B.M., Spoor, M.W., Hollander, R., Smith, J.M. (1979). Residence time distribution in a plasticating twin screw extruder. AIChE, 75, 345-351.

von Lengerich, B.H. (1984). Entwicklung und Anwendung eines rechner unterstützten systemanalytischen Modells zur Extrusion von Stärken und stärkehaltigen Rohstoffen. Thesis TU-Berlin, 1984 FB 13, Nr. 165.

Maddock, B.H. (1959). Technical Papers, Vol. V, 5th Annual Technical Conference SPE. New York.

Menges, G., Klenk, P. (1967). Aufschmelz- und Platiziervorgange beim Verarbeiten von PVC hart Pulver auf einem Einschnecken-extruder. Kunststoffe, 57, 598-603.

Metzner, A.B. (1959). Flow behaviour of thermoplastics In: Processing of Thermoplastic Materials, ed. E.C. Bernhardt. Van Nostrand-Reinhold, New York.

Pinto, G., Tadmor, Z. (1970). Mixing and residence time distribution in melt screw extruders. Polym. Eng. Sci., 10, 279-288.

Wolf, D., White, D.H. (1976). Experimental study of the residence time distribution in plasticating screw extruders. AIChE, 22, 122-131.

van Zuilichem, D.J. (1976). Theoretical aspects of the extrusion of starch-based products in direct extrusion cooking process. Lecture Intern. Snack Seminar, German Confectionery Institute, Solingen.

van Zuilichem, D.J., Bruin, S., Janssen, L.P.B.M., Stolp. W. (1980). Single screw extrusion of starch and protein rich

materials. In: Food Process Engineering Vol. 1: Food Processing Systems, ed. P. Linko, V. Mälkki, J. Olkku, J. Larinkariels, Applied science, London, 745-756.

van Zuilichem, D.J., Buisman, G., Stolp, W. (1974). Shear behaviour of extruded maize. IUFoST Conference, Madrid, September, 29-32.

van Zuilichem, D.J., Jager, T., Stolp. W., de Swart, J.G. (1988). Residence time distributions in extrusion cooking. Part III: Mathematical modelling of the axial mixing in a conical, counter-rotating, twin-screw extruder processing maize grits. J.Food.Eng., 8 109-127.

van Zuilichem, D.J., Lamers, G., Stolp, W. (1975). Influence of process variables on quality of extruded maize grits. Proc. 6th Europ. Symp. Engineering and Food Quality. Cambridge.

van Zuilichem, D.J., de Swart, J.G., Buisman, G. (1973). Residence time distribution in an extruder. Lebensm. Wiss. u. Technol., 6, 184-188.

van Zuilichem, D.J., Witham, I., Stolp. W. (1977). Texturisation of soy flour with a single-screw extruder. Seminar on extrusion cooking of foods. Centre de Perfectionnement des Cadres Industries Agricoles et Alimentaires, (C.P.C.I.A.) Paris.

van Zuilichem, D.J., Stolp, W., Jager, T. (1982). Residence time distribution in a single screw cooking extruder. Lecture at intern. Snack Seminar, Zentralfachschule der Deutschen Süsswarenwirtschaft, Solingen.

Notation

C	Concentration	[kgm^3]
Dt	Convective derivative	[-]
k	Consistency factor of power-law model	[Ns^nm^{-2}]
k_∞	Frequency factor	[1/s]
K(t)	Reaction constant	[1/s]
n	Flow behaviour index of power-law model	[-]
P^*	Power number	[-]
R	Gas constant	[$kJmol^{-1}K^{-1}$]
Re	Reynolds number	[-]
T	Temperature	[K]
v	Velocity	[m/s]
x	Channel depth	[m]
β	Temperature correction constant	[-]
ΔE	Activation energy	[kJ/mol]
γ	Shear	[-]
$\dot{\gamma}$	Shear rate	[1/s]
η	Apparent viscosity	[Nsm^{-2}]
μ	Dynamic viscosity	[Nsm^{-2}]
τ	Shear stress	[Nm^{-2}]

CHAPTER 2

RESIDENCE TIME DISTRIBUTIONS IN SINGLE-SCREW EXTRUSION COOKING.

ABSTRACT

Residence time distributions were measured in a single screw extruder fed with maize grits and defatted soya flakes. ^{64}Cu was used as a tracer. The influence of four variables has been studied; moisture content, feed rate, rotational speed of the screw and die diameter. Rotational speed and die diameter are the most important variables affecting the mean residence time. The residence time distributions curves are analysed with a model containing a plug flow component and a number of CSTRs in cascade. For maize this model contains four to ten CSTRs. The fit of this model, however, can be improved. With the proteinaceous material soya, the model contains two or three CSTRs, and a better fit is reached, than with maize. The residence time distribution model is used to compare the measurements with models developed for plastic melt extrusion.

THIS CHAPTER HAS BEEN PUBLISHED AS:

van Zuilichem, D.J., Jager, T., Stolp, W., and de Swart, J.G. (1988). Residence Time distribution in Extrusion Cooking, Part II: Single-screw extruders processing maize and soya. J. of Food Eng. 7, 19-210

2.1 Introduction

Cooking extruders are nowadays frequently described as "High Temperature Short Time reactors", in which a range of biopolymer reactions occur, such as gelatinization and cross linking of starch, browning and protein denaturation. The process time, together with factors such as shear and temperature, is very

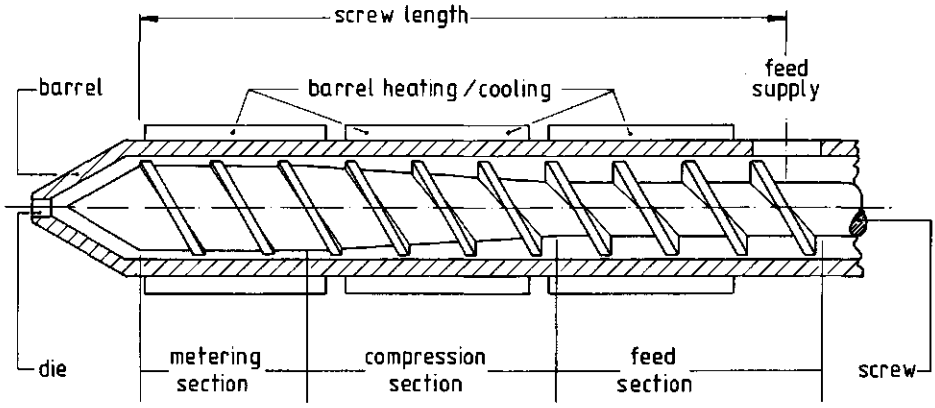

Fig 2.1 Simplified extruder scheme (van Zuilichem et al., 1988)

important to these reactions, which means that every element of food should be subjected to more or less the same extrusion history. However in a single-screw extruder (fig. 2.1) the particles experience variations in extrusion history due to extruder geometry, energy input and rheological effects. This will result in a residence time distribution (RTD) which is dependent on such engineering aspects as extruder design and the rheological behaviour of the materials extruded. For a good quality product it is necessary that the biopolymer reactions are controlled by the extrusion conditions, which requires knowledge of mechanisms of mixing and flow behaviour. It is possible to calculate the RTD from defined velocity profiles, but, more importantly, the RTD can be measured by suitable experiments. From the RTD, information about the degree of mixing, residence time expectancy of the fluid elements and the degree of uniformity of the stress exerted on the fluid elements during

their passage through the extruder can be gained. A theory suitable for predicting the RTD-curves and flow rates during extrusion of biopolymers in a single-screw extruder is not available at present, as most biopolymers undergo chemical reactions during extrusion-cooking, which significantly change the rheology during extrusion (Bruin et al., 1978).

Earlier work was performed using a measuring system containing a single detector (van Zuilichem et al., 1973). Residence time distributions could be described by a model consisting of a serial combination of a plug flow and a cascade of CSTRs. The determination of the number of CSTRs required additional measurements. This model gives no information on the rheology of the extruded materials, but should be regarded as an intermediate between rheologically-defined theoretical models and measured RTD curves.

2.2 Theory

A single-screw extruder can be regarded as a continuous rectangular channel, formed on three sides by the screw surface and on one side by the barrel. For modelling, this channel is usually regarded as a straight channel having three dimensions,

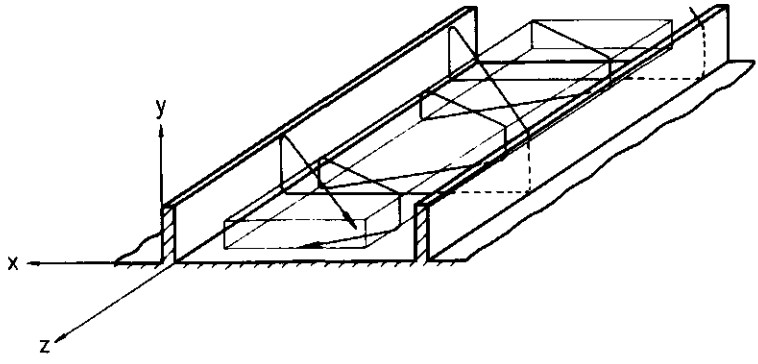

Fig 2.2 Flow pattern in the channel of a single screw extruder (Janssen, 1978)

with the screw stationary and the barrel wall moving. This is

demonstrated in fig. 2.2 which omits the barrel wall. The simplest profiles of the velocity (v) in the x-y plane of the extruder channel arise when the material is Newtonian with a temperature-independent viscosity and when the radial components near the flights are neglected. This last assumption is reasonable when the screw channel depth is less than 10% of its width. Such approximate profiles were derived about 30 years ago (Carley and Stub, 1962):

$$v_x = U_z \xi (1-P+P\xi) \qquad (1)$$

and:

$$v_x = U_x \xi (2-3\xi) \qquad (2)$$

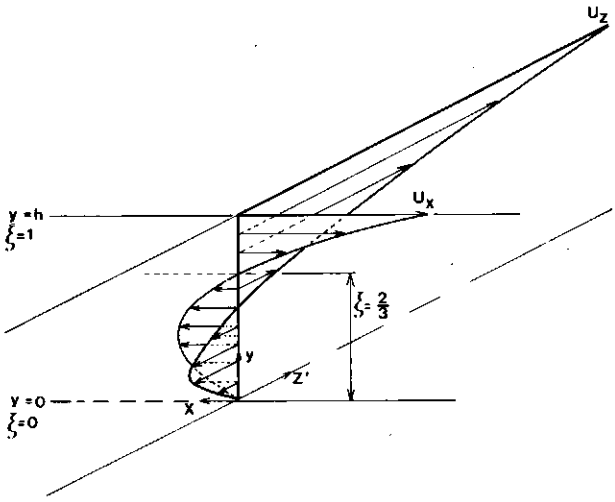

Fig 2.3 Two dimensional flow profile for a constant viscosity Newtonian liquid (Bruin et al., 1978)

in which U is the relative velocity of the barrel wall with respect to the centre line of the screw, P is the ratio between pressure flow and drag flow, and ξ is the dimensionless particle level within the channel in the y-direction. Due to the nature of the velocity profiles, a particle will circulate in the x,y-plane. Fig. 2.3 shows the velocity profiles in the x-y and

y-z plane. The result is that the particles all flow down the channel in a helical path with a net positive component in the z-direction (fig. 2.2). The shortest path can be found at 2/3 of the channel height. Pinto and Tadmor (1970) have analysed the RTD's resulting from these velocity profiles. The exit age distribution (E(t)) for Newtonian liquids then becomes:

$$E(t) = \frac{9\pi N D_e \sin Q \cos Q (1-\frac{P}{3}) \xi^3 \{(\xi-1)\sqrt{1+2\xi-3\xi^2}\}^3}{2L(6\xi^2-4\xi-1)\sqrt{1+2\xi-3\xi^2+3\xi^3}-1} \qquad (3)$$

in which N is the screw rotational speed and Q the flight angle. This result is shown in figure 2.4 together with the F-diagram for complete backmixing and for plug-flow. The mean residence time is equal to the hold-up divided by the volumetric output rate. The minimum residence time is approximately 3/4 of the mean residence time. The shape of the F-curve is independent of the pressure built-up in the extruder and of the rotational speed, only the mean residence time will be affected. The RTD's for a power-law fluid in an isothermal, single-screw extruder have been analysed by Bigg and Middleman (1974). As the temperature and the viscosity in a food extruder are inhomogeneous the validity of these RTD-curves for describing a food extruder are limited. Power-law behaviour, which is more appropriate to biopolymers than Newtonian behaviour was described by them as:

$$\eta = M\left(\left(\frac{\delta v_x}{\delta y}\right)^2 + \left(\frac{\delta v_z}{\delta y}\right)^2\right)^{(n-1)/2} \qquad (4)$$

in which η is the coefficient of dynamic viscosity and M and n are power-law constants. When n=1 the fluid is Newtonian. In figure 2.4 a power-law RTD (Bigg and Middleman,1974) is included. The minimum residence time in this case of the power-law RTD-curves depends greatly on the values of the rheological coefficients. Slip phenomena at extruder surfaces also influence the velocity profile (Holslag and Ingen-housz, 1980). When a thin

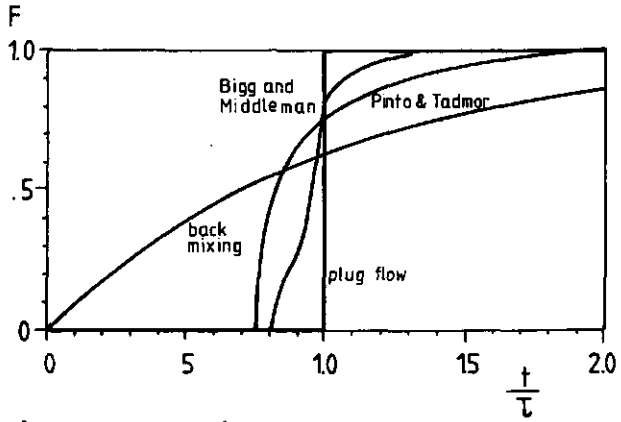

Fig 2.4 Comparison of four F-curves (Bigg et al., 1974)

layer of water is present on the barrel or the screw surface, the food-material can slip over the surfaces. The barrel of a single-screw, food-extruder is usually grooved to prevent slip. As the surface of the screw is polished, slip is most likely to occur there. This is contrary to the assumption of a zero velocity at the barrel and screw surfaces made by Pinto and Tadmor (1970), and by Bigg and Middleman (1974). A confirmatory indication of such slip was found by an increase in the difference between the measured and predicted outputs, when the rotational speed increases (van Zuilichem et al., 1983). A model describing slip conditions and a non-isothermal, power-law viscosity condition was considered impracticable, as the number of variables is too large. The RTD measurements are described by a model consisting of a plug flow and a cascade of W perfect mixers, as described in eq. 5:

$$E(R) = \frac{W\,(WR)^{W-1}\,e^{-WR}}{(W-1)!} \qquad (5)$$

in which R is a dimensionless time, calculated from the plug-flow time t_p and the mean residence time τ, as in:

$$R = \frac{t - t_p}{\tau(1 - t_p)} \qquad (6)$$

The introduction of this plug-flow time increases the asymmetry of the E-curve.

2.3 Experimental

RTD measurements were carried out with a 48 mm diameter, single-screw, Almex Battenfeld-extruder using a screw with a compression ratio of 3:1. Aspects investigated were the influence of the feed rate, rotational speed, die diameter, and moisture content on the RTD-curves. During measurements all other variables were kept constant. Two materials were used : defatted soya-flakes and coarsely milled degerminated maize grits. In both materials the mean size of the particles was about 1 mm. Defatted

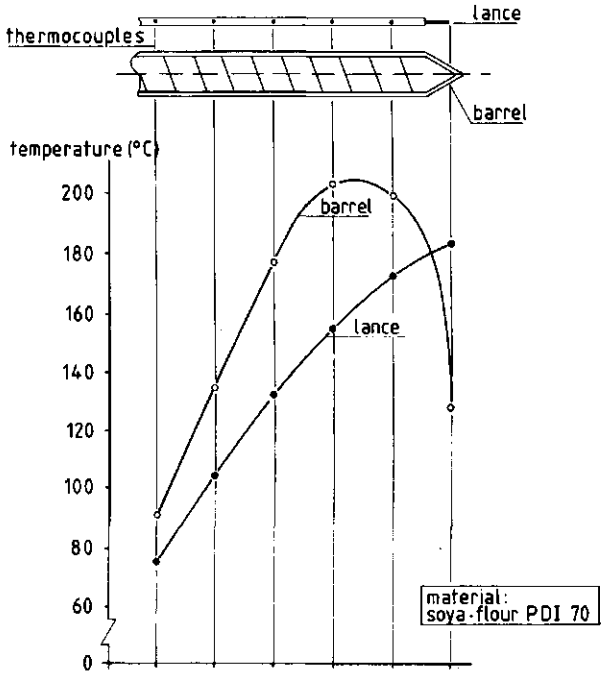

Fig 2.5 Temperature profiles maintained for these experiments (van Zuilichem et al., 1977)

soya-flakes contain 56% protein and the extruded product is well known in the pet-food industry. During extrusion of the soya a temperature profile was imposed with a maximum of 200°C and a die temperature of 125°C (Fig. 2.5). The lance temperature approximates the screw temperature. The maximum pressure was 100 bar. Maize grits containing 85% starch and 8% protein were extruded adiabatically with a maximum temperature of 200°C and a maximum pressure of 300 bar.

2.3.1 Measuring the residence time distribution

To measure the RTD a radioactive tracer technique, with ^{64}Cu as a tracer, was chosen because of its accuracy, safety and chemical inertness. The tracer was used in the form of cuprous chloride mixed with some of the feed material. In earlier work (van Zuilichem et al., 1973) a single detector was used, reacting to all gamma quanta at the energy level characteristic of ^{64}Cu, which also detects somewhat before and after the plane of detection. For the present work a coincidence detector was used as described by van Zuilichem et al. (1988).

2.4 Results

2.4.1 General

The influence of the rotational speed, die resistance and moisture content on the mean residence time, the dimensionless minimum residence time, the number of equivalent CSTRs and the so-called "non-Newtonian" character of the F-curves are shown in Tables 2.1, and 2.3. The number of CSTRs is used here as an indication of the amount of axial mixing in the extruder. The "non-Newtonian" character is a measure of the difference between the RTD curve of a power-law fluid and that of a Newtonian fluid. This difference is most prominent just after the minimum residence time (see fig. 2.4). The measured RTD curves are compared with a Newtonian RTD curve, to estimate the difference between them in terms of the area between the curves just after

Table 2.1 Influence of the die resistance, moisture content and rotational speed on the RTD curves for soya and maize extrusion

	Soya			*Maize*		
	Die resistance	*Moisture content*	*Rotational speed*	*Die resistance*	*Moisture content*	*Rotational speed*
Mean residence time τ	*m*	—	∨	∧	—	∨
t_{min}/τ	*m*	—	∨	*m*	—	∨
Number of CSTRs	—	—	—	*m*	∨	*m*
Deviation from Pinto and Tadmor (1970) model 'non-Newtonian' character	—	—	—	∨	∨	∧

— No significant effect.
m Mixed effects.
∧ Positive effect of variables.
∨ Inverse effect of variables.

Table 2.2 Results for soya

N (*r.p.m.*)	*Die diameter* (*mm*)	*Moisture content* (%)	*No. of CSTRs W* (—)	t_{min}/τ (—)	τ (*s*)
80	4·0	24·5	3	0·80	66
100	4·0	24·5	3	0·77	58
120	4·0	24·5	3	0·60	38
80	6·0	23·6	2	0·89	102
120	6·0	23·6	2	0·72	49
80	8·0	22·9	2	0·84	63
120	8·0	22·9	3	0·77	34
80	8·0	19·8	2	0·74	62
80	8·0	26·9	3	0·80	59

the minimum residence time. The measured RTD curves were arranged according to their rotational speed, die resistance and moisture content on their "Non-Newtonian" character. The qualitative effect of these variables is indicated in Table 2.1. Linear inverse correlations between mean residence time and rotational speed have been found for both soya and maize. Fig. 2.6 shows this correlation for a non-Newtonian dough. With both maize and soya, the influence of the die-resistance on the mean residence time is significant (see Tables 2.2 and 2.3).

The minimum residence time decreases faster than the mean

Table 2.3 Results for maize

N (r.p.m.)	*Die diameter* (mm)	*Moisture content* (%)	*No. of CSTRs W* (—)	t_{min}/τ (—)	τ (s)
80	1·9	14·4	4	0·56	71
90	1·9	14·4	5	0·56	65
100	1·9	14·4	11	0·56	60
120	1·9	14·4	10	0·49	41
80	3·0	14·4	10	0·62	59
100	3·0	14·4	5	0·58	48
120	3·0	14·4	10	0·55	41
120	3·0	18·3	12	0·52	44
120	3·0	21·9	5	0·54	41

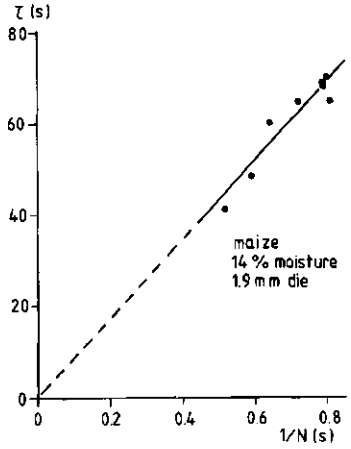

Fig 2.6 The relation between the mean residence time τ and the inverse of the rotational speed (van Zuilichem et al., 1988)

residence time with increasing rotational speed, as can be seen in Tables 2.2 and 2.3, where the ratio of minimum residence time and mean residence time ($t_{min}\tau^{-1}$) decreases with increasing rotational speed of the screw (N).

2.4.2 Soya

The RTD-curves for soya in fig.2.7 show a near-plug-flow behaviour, which resembles the model of PINTO and TADMOR. These curves can be simulated reasonably with the RTD model of eq. 6, using two or three perfect mixers and a plug-flow time which is approximately equal to the minimum time. The number of equivalent CSTRs in table 2.2 varies slightly between two and three, which

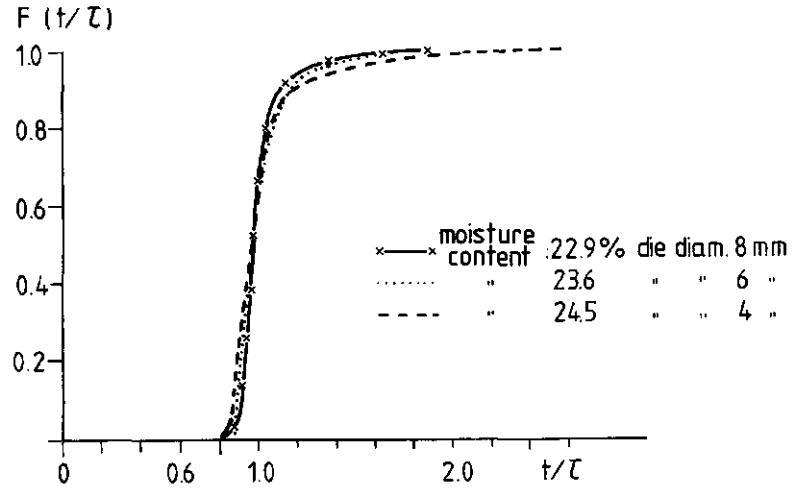

Fig 2.7 F-Diagram for soya extrusion at 80 rpm (All Figures and tables; van Zuilichem et al., 1988)

is not significant, as the two best values where two or three in all cases. This signifies that the axial mixing in the extruder is almost independent of the moisture content in the range 20-26%, of die diameter and of the rotational speed of the screw. An explanation for this phenomenon can be found in a reaction of the soya-proteins: soya forms a texture in the extruder (van Zuilichem et al., 1979) which favours plug flow.The ratio of the minimum and mean residence time in table 2.2 is affected by the rotational speed and the die-resistance, which is at variance with the Pinto and Tadmor model. The mean residence time with a 6 mm die is larger than with the 4 and 8 mm dies, while the effect on the ratio of minimum to mean residence times is unsystematic. The effect on the mean residence time might be caused by differences in the location and extent of the texturizing process, which can affect the hold-up in the extruder.

2.4.3 Maize

The first aspect for investigation was the effect of the feed rate on the RTD. Remarkably, both the mean residence time and the minimum residence time decreased by only 5% when the feed rate changed from choked feeding to starved feeding. It is obvious

that this behaviour is provoked by the combination of acompressive screw with a very small die diameter. This explaines a drastic decrease in hold-up of the maize dough in the extruder with decreasing output (fig. 2.8), and a decrease in the spread

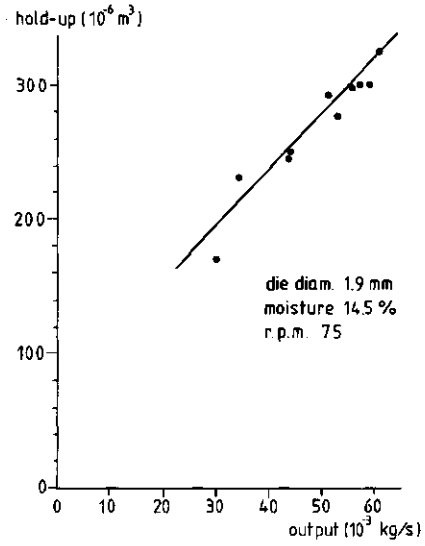

Fig 2.8 Hold-up vs. output of maize grits during extrusion at different feed rates

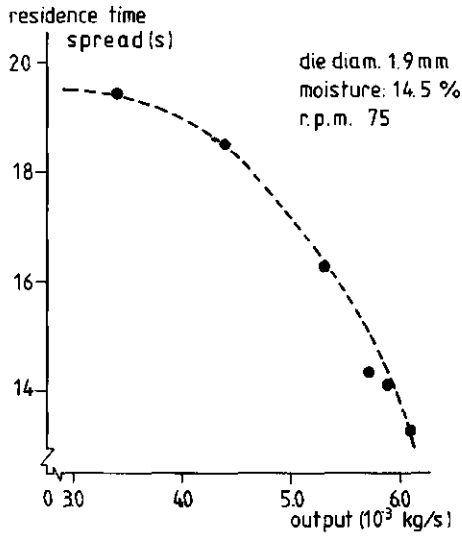

Fig. 2.9 Relationship between the spread of the residence time and the feed rate

of the residence times (fig. 2.9). The general shape of the F-curves was not influenced by the feed-rate. Regarding the pressure in the extruder it can be seen in fig. 2.10 that the pressure drop across the die is proportional to the output. In fig. 2.11 the pressure inside the extruder is plotted, measured at four positions along the screw length. The F-curves for maize grits (figs. 2.12, 2.13 and 2.14) resemble the F-curves for non-Newtonian liquids predicted by Bigg and Middleman. The so-called "non-Newtonian" character is the difference, between the Pinto and Tadmor model and the RTD measurements in the period of time before the peak-time, which is expressed as an area. The "non-Newtonian" character becomes prominent when the rotational screw speed increases, but decreases when the moisture content of the maize dough increases. The fit of the maize RTD

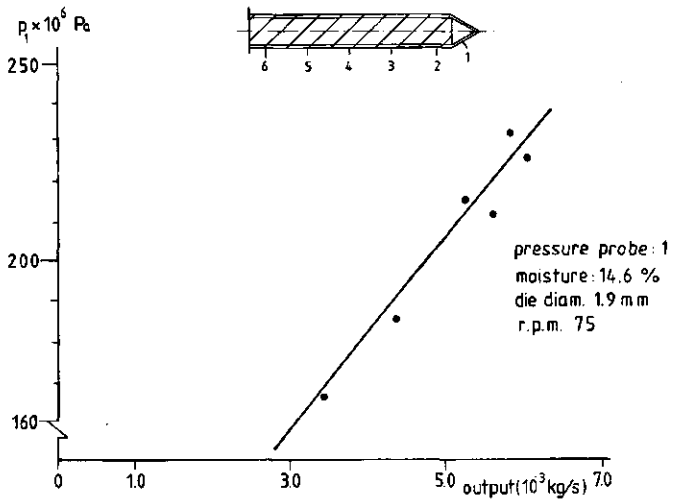

Fig. 2.10 Relationship between pressure before the die and throughput for maize grits

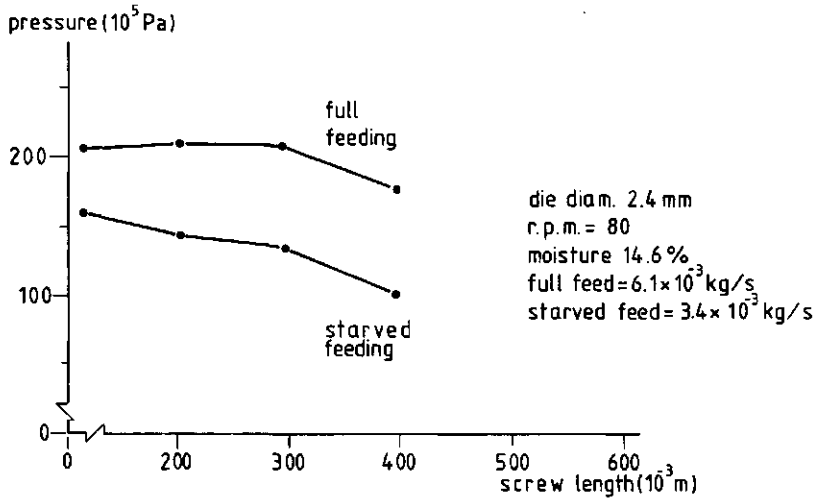

Fig. 2.11 Pressure in the screw channel for maize extrusion when feeding at maximum rate and half the maximum rate

measurements with F-curves calculated from eq. 5 was not as good as with soya. A systematic relationship to the number of CSTRs could not be found (tables 2.1 and 2.3). The influence of increasing die-resistance on the mean residence time and the "non-Newtonian behaviour" are opposite to the influence of increasing rotational speed. A smaller die gives a longer mean residence time and a more distinctly "non-Newtonian" character.

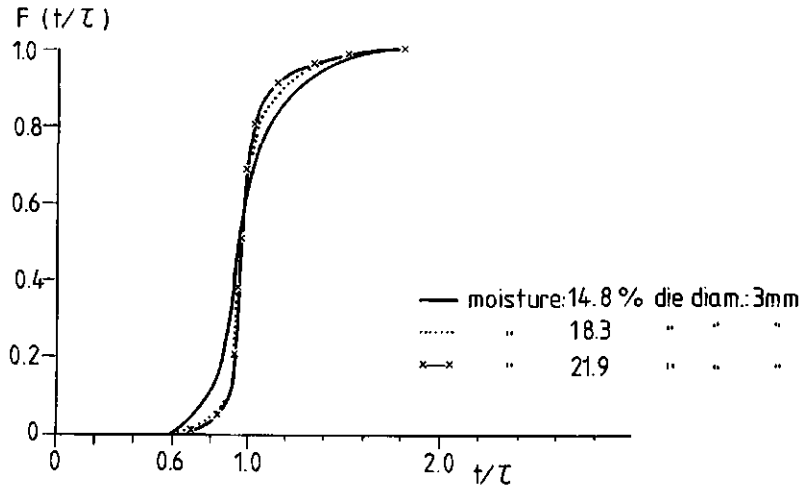

Fig. 2.12 The influence of moisture content of maize on the shape of the F-function at 80 rpm

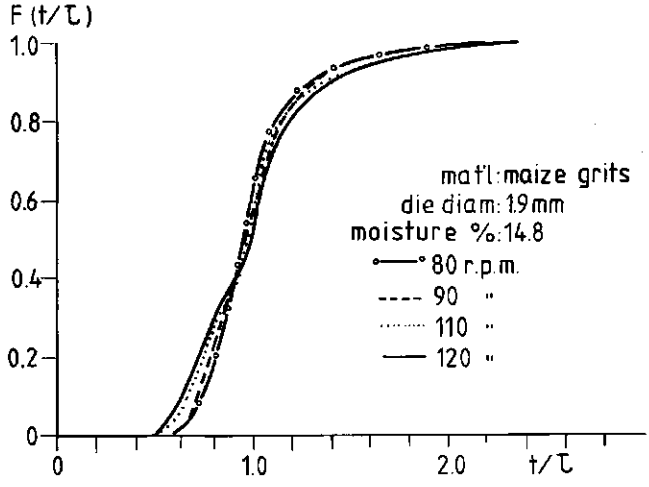

Fig. 2.13 The influence of rpm and the shape of the F-function with die-diameter 1.9mm

The moisture content affects the number of CSTRs and the "non-Newtonian" character, but not the mean or the minimum residence time. It was expected that an increase in the moisture content would reduce the viscosity and change the rheological constants in eq. 4. According to the power-law model of Bigg and Middleman this would affect both the mean and average residence time. Also the changes in the number of perfect mixers without

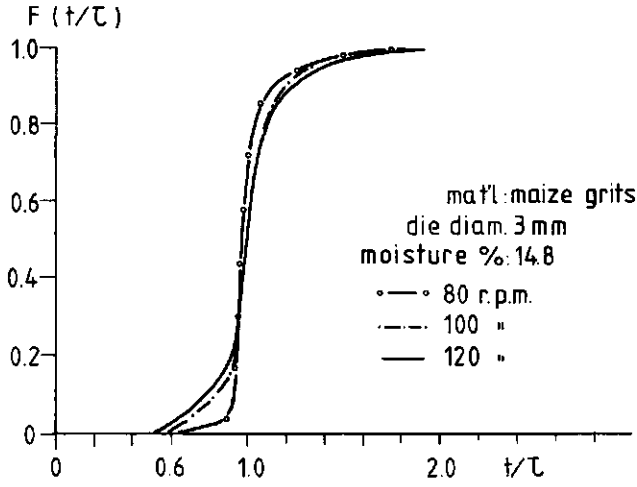

Fig. 2.14 The influence of rpm and the shape of the F-functioon with die-diameter 3mm

changes in the minimum residence time are atypical for this model.

2.5 Conclusions

The rotational speed and the die diameter are the most important variables affecting the mean residence time. The influences of the moisture content and of the feed rate is small. Compared with maize, soya shows less axial mixing, which could be caused by the change in texture of soya within the extruder. As the texturizing of soya could affect the RTD it is recommended that the RTD of soya extrusion is studied in relation to product quality. With maize grits an increase in the feed rate or the moisture content decreases the spread of the RTD. In these situations the model of Bigg and Middleman (1974) predicts considerable changes in the minimum residence time, which was not found in the RTD. A possible, but farfetched hypothesis is that such changes are compensated for by changes in the RTD of the first part of the extruder, where the power-law model is not valid as the maize is here still present in the form of grits. The moisture content should affect the viscosity which should change the mean residence time according to the models of Pinto and Tadmor (1970) and of Bigg and Middleman (1974). The mean residence time is not in fact found to be affected by changes in the moisture content,

while, with maize grits, the width of the RTD-curves decreases when the moisture content increases, without changing the minimum residence time. This can be explained by the less farfetched hypothesis that the thickness of the maize dough layer, of which the velocity is influenced by slip, decreases when the moisture content increases, resulting in a decrease in axial mixing combined with a decrease in viscosity. This hypothesis requires slip to be a dominant factor in the RTD of maize grits. With soya, texturizing is another possible hypothesis. The RTD-curves of soya resemble the Pinto and Tadmor (1970) model and the RTD-curves of maize resemble the power-law rheology RTD-curves of Bigg and Middleman (1974). However some significant features of the measured RTD-curves are not predicted by these models and so their validity for biopolymers are not proven.

References

Bigg, D. Middleman, S. (1974). Mixing in a single screw extruder. A model for residence time distribution and strain. Ind. Eng. Chem. Fund. (13) 66.

Bruin, S., van Zuilichem, D.J., Stolp, W., (1978). A review of fundamental and engineering aspects of extrusion biopolymers in a single screw extruder. Journal of Food Process Engineering. V(2) (1) 1.

Carley, J.F., Strub, R.A., (1962). Basic concepts of extrusion. Ind. Eng. Chem., (45) 970.

Holslag, R.H., Ingen-Housz, J.F., (1980). Gleitphänomenen in einem Extruder. Lecture at Zentral Fachschule der Deutschen Süsswarenwirtschaft. Solingen.

Janssen, L.P.B.M. (1978). Twin Screw Extrusion. Elsevier Scientific Publishing Company, Amsterdam.

Pinto, G., Tadmor, Z., (1970). Mixing and residence time distributions in melt screw extruders. Polym. Eng. Sci., (10) 279.

van Zuilichem, D.J., Bruin, S., Janssen, L.P.B.M., Stolp, W., (1980). Single-screw extrusion of starch and protein-rich materials. Proc. of 2nd Int. Congress on Eng. and Food. Helsinki, aug. 1979. 745-56.

van Zuilichem, D.J., Reijnders, M.P., Stolp, W., (1983). Enkelschroefsextruders: berekeningswijzen, gedrag en prestaties. P.T. Procestechniek. 12, 15-18. 3.

van Zuilichem, D.J., de Swart, J.G., Buisman, G., (1973). Residence time distribution in an extruder. Lebensm.-Wiss. u. Technol. 6(5) 184-188.

van Zuilichem, D.J., Stolp, W., Witham, I., (1977). Texturization of soya with a single screw extruder. Lecture at; European seminar on extrusion cooking of foods, C.P.C.I.A., Paris

van Zuilichem, D.J., Jager, T., Stolp, W., de Swart, J.G., (1988). Residence time distribution in extrusion-cooking part 1: coincedence detection. J. Food Eng., 7, 147-58.

Notation

D_e	Dispersion coefficient	$[m^2s^{-1}]$
E(t)	Exit age distribution	$[s^{-1}]$
F(t)	Cumulative exit age distribution	[-]
η	Dynamic viscosity	$[Nsm^{-2}]$
n	Power-law coefficient	[-]
N	Rotational speed in revolutions per second	$[s^{-1}]$
M	Power-law constant	[-]
L	Length of extruder screw	[m]
P	Ratio between pressure flow and drag flow	[-]
Q	Angle of screw flight	[rad]
R	Dimensionless time	[-]
t_{min}	Minimum residence time	[s]
t_p	Plug flow time	[s]
U	Relative velocity of barrel wall and screw	$[ms^{-1}]$
v	Fluid velocity	$[ms^{-1}]$
W	Number of perfect mixers	[-]
x,y,z	Subscripts indicating relative directions	[-]
ξ	Dimensionless particle height (y-direction)	[-]
τ	Mean residence time	[s]

CHAPTER 3

MODELLING OF THE AXIAL MIXING IN TWIN-SCREW EXTRUSION COOKING

ABSTRACT

A mathematical model was developed to simulate the axial mixing in a twin-screw extruder. A comparison is made between the residence time distributions (RTD) predicted by it and measurements on an actual counter-rotating, twin-screw extruder working on maize grits. The measured residence time distribution curves were characterised by their average residence times and Peclet numbers. The model developed contains an infinite series of CSTR's (Continuous Stirred Tank Reactors), each one representing four screw chambers. The leakage flows between the screw chambers are described in the model as backmixed flows. With this model, a fairly close simulation of the measured residence time distribution could be made. Mixing in the compression zone proved to be independent of screw speed in the range 40-80 rpm. Peclet numbers of 26-34 were measured for the total length of the extruder. As far as biochemical reactions occuring mainly in the high temperature compression zone
(120-150°C) are concerned, the upstream axial mixing at the low temperatures of the feed zone (60-100°C) may be neglected, in calculating an effective Peclet number for the extruder. This results in calculated effective Peclet numbers of 49 to 61, where as values of 26-34 were measured.

THIS CHAPTER HAS BEEN PUBLISHED AS:

van Zuilichem, D.J., Jager, T., Stolp, W., de Swart, J.G. (1988). Residence Time Distributions in Extrusion Cooking, Part III:Mathematical Modelling of the Axial Mixing in a Conical, counter-rotating, Twin-Screw Extruder processing Maize Grits. J. of Food Eng.,8 109-127.

3.1 Introduction

Although twin-screw extruders are known to be excellent reactors for processes such as the enzymic hydrolysis of starch (Chouvel et al., 1983), starch gelatinization and liquefaction (Linko et al., 1983), formation of amylose-lipid complexes (Mercier et al. 1980) and ethanol production (Ben-Gera et al., 1983), knowledge of reaction conditions in the reactor part of the extruder is incomplete. This is illustrated by a quotation from Linko et al. (1983) :"Current uses of HTST extrusion cooking are basically physical, chemical and biochemical transformations, yet only recently has an extrusion cooker been studied as a reactor. Better understanding of the basic phenomena taking place in the high temperature, high pressure and shear environment of the reactor is necessary ". The phenomena mentioned are mainly studied in three fields of research : engineering, rheology and biopolymer-chemistry. Engineering is concerned with the geometry of the reactor and with control and measurement (Janssen, 1978; van Zuilichem et al., 1983; Savolainen and Karling, 1985). Rheology covers all aspects of material flow (Launay and Lisch, 1983; Bush et al., 1984). Transformations and modifications of starch, lipids, sugars, cellulose and proteins are studied in the field of chemistry and biochemistry (van Zuilichem et al., 1983; van Zuilichem et al., 1985). Individual competence across all these fields is rare, which makes the study of complex phenomena in the extrusion of biopolymers interdisciplinary. The combining of efforts in these fields is greatly helped by mathematical models which can describe the complex phenomena studied. Publications on measurements of axial mixing in starchy doughs in twin-screw extruders (Olkku et al., 1980; Bounie and Cheftel, 1986 ;Altomare and Ghossi, 1986) do not contain any axial mixing model which is generally accepted. In the study reported herein a model was developed to simulate axial mixing in a twin-screw extruder. This model was used to translate residence time distribution curves, measured on a conical, counter-rotating, twin-screw extruder fed with maize grits, into mass-flows probably occurring inside the extruder. The refinement of this

model into a more complex one which can describe the extrusion process for a particular rheology, seems possible.

3.2 Theory

As the material processed passes through a twin-screw extruder, the chambers decrease in size whilst temperature and pressure increase. Leakage flows between chambers in the compression zone are caused by pressure gradients between the chambers. In Fig. 3.1 the leakage flows are identified by the particular gaps through which they pass. In this way tetrahedron, calender, side and flight leakage flows can be distinguished (Janssen, 1978). Flight leakage is that over the flights of the screws. The calender leakage is that through the gap formed between the flight of one screw and the bottom of the channel of the other screw: This material remains in the same screw channel. Side leakage is that through the gap between the flanks of the flights of the two screws from the lower to the upper side of the intermeshing zone of the screws and the tetrahedron gap is the only gap through which the material is transported directly from one screw to the other. This gap is a result of the angle of the flight walls in relation to the channel bottom of the screws. In the compression zone the pressure gradient is large enough to promote leakage but in the transport zone no leakage flows are

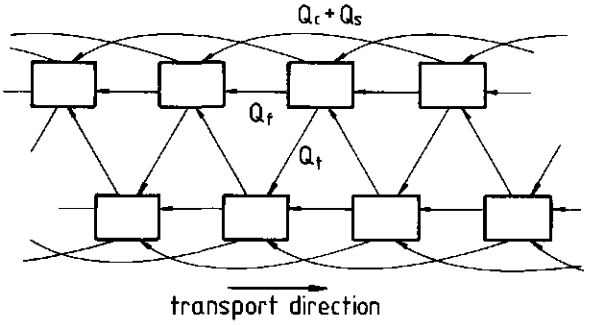

Fig. 3.1 Model of a twin screw extruder with two start screw. Q_c, Q_s, Q_f and Q_t are leakage flows through the calender, flight and tetrahedron gaps respectively (Janssen, 1978)

to be expected. Axial mixing in twin-screw extruders has been

studied mostly in relation to plastics or model fluids having rheological and other physical properties different from those of starches. One important difference is the compressibility of the material. When grits pass through the feed zone of a twin-screw extruder they become water-soluble by gelatinization, which increases their compressibility. Albers (1976) gives specific densities of PVC as a function of temperature and pressure (Fig. 3.2). The PVC is heated for one hour to a certain temperature and then compressed for one minute, after which

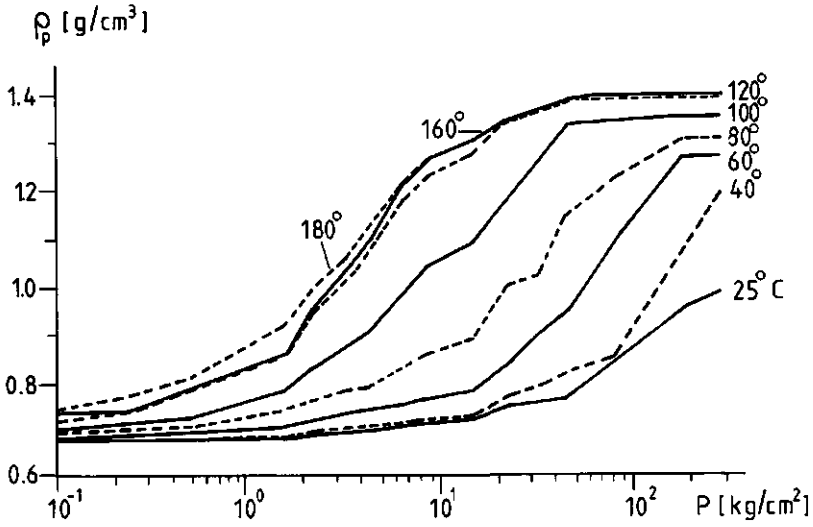

Fig 3.2 Density ρ of dryblend PVC (Halvic 227) related to pressure and temperature (Albers, 1976)

procedure the density is measured. Measuring the specific density of starch under high temperature and pressure is, however, more complicated as the physical and chemical properties of starches will change rapidly when heated. As water functions in extrusion-cooking as a solvent for starch, it is clear why the porosity of a starchy dough in a counter-rotating, twin-screw, extruder readily becomes zero at a lower pressure than that for PVC granules. Because of this, and the absence of leakage flows in the transport zone, it follows that there is a rapid increase in density when the maize dough enters the compression zone. For maize grits a maximal specific density of about 1350 kgm^{-3} can be

found in the compression zone. The specific density in the transport zone was evidently much less. The residence time distributions are characterised by their mean residence times and Peclet numbers (Pe). The Peclet number which is discussed by van Zuilichem et al. (1988a), characterizes the spread of the RTD and is defined as:

$$Pe = \frac{\bar{v}l}{D_e} \qquad (1)$$

in which l is the extruder length, D_e the axial dispersion coefficient and $\bar{v}$ the axial velocity of the extruder chambers. The larger the value of Pe, the smaller the spread of the residence time. In order to calculate the residence time distributions from the axial mixing profiles, the mixing of leakage flows in the chambers cannot be neglected. When a leakage flow enters a chamber, and mixes poorly with the contents of the chamber, it can merge directly with a leakage flow which is leaving that chamber. This will increase the Peclet number.

3.3 Materials and methods of measurement

The extruder used was a Cincinnati CM 45 conical counter-rotating, twin-screw, extruder. The screws used were the 1552 type (see Table 3.1 and Fig. 3.3). The extruder was fed with maize grits containing 25% moisture (wet weight) with a composition of 85% starch and 8% protein, on a dry basis. The size distribution is given in Table 3.2. The diameter of the die was 20 mm. The residence time distribution was measured by the coincidence technique described by van Zuilichem et al. (1988b) which measures the ^{64}Cu activity at the die outlet (Fig. 3.4). Half way along the screws, above the midpoints, two single detectors were placed each normal to a screw. Both the single and the coincidence detectors are described by van Zuilichem et al. (1988a). The two "midpoint" single detectors have a symmetrical sight angle, which leads to an erroneous Peclet number being measured, but this error is small (0.4%) because of shielding by

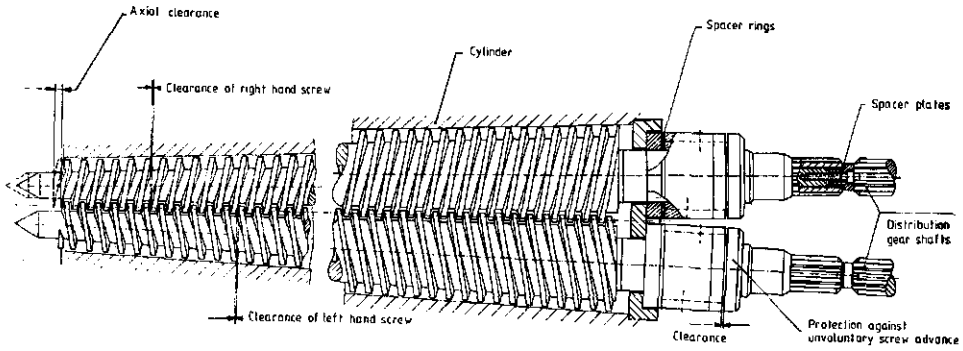

Fig. 3.3 Conical, counter-rotating, twin screw extruder (Cincinnatt). (van Zuilichem et al., 1983)

Table 3.1 Dimensions of screw set 1552 (van Zuilichem et al., 1988)

Length	1·00 m
Calender gap	0·5 mm
Flight gap	0·2 mm
Maximum diameter	90 mm (one screw)
Minimum diameter	45 mm (one screw)
Volumetric compression ratio	2·1–1
Number of chambers per screw	42
Number of thread starts	2

Table 3.2 Size distribution of maize grits used (Moisture content 13.1%, wet basis) (van Zuilichem et al., 1988)

Size (mm)	*Fraction (%)*
<0·50	0·8
0·50–0·60	1·7
0·60–0·70	9·2
0·70–0·85	26·5
0·85–1·00	54·2
>1·00	7·5
Total	99·9

the screws and barrel. By van Zuilichem et al. (1988a) it was shown that measurements with the coincidence detector do not result in different average residence times or Peclet numbers. The Peclet numbers were determined as described by Todd (1975), by calculating the ratio of the residence times for which 16% and 64% of the tracer has passed the detector. This ratio was

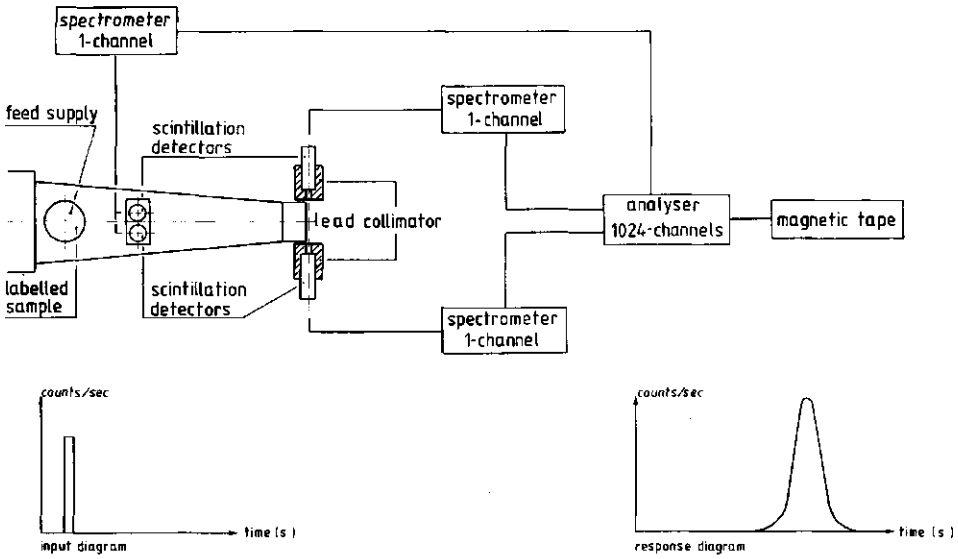

Fig 3.4 Block diagram of the arrangement for measuring of residence time distributiion (van Zuilichem et al., 1982)

compared with that for an RTD model which gives similar RTD's. The Peclet number for the model with the same ratio was then used as the Peclet number of the RTD measurement. The dispersed plug flow RTD model, described by Levenspiel (1972) and discussed in chapter 2 was used as RTD model.

3.4 Simulation model

In the simulation model each C-shaped chamber of the extruder screw-set is considered to be a CSTR. The contents of these chambers are changed by leakage flows, represented in the model as backmixing flows. A complete extruder simulation according to the leakage flow equations of Janssen (1978) should calculate the tetrahedron, calender, flight and side leakage flows, which requires a large number of assumptions. To minimize the number of assumptions, the block-diagram of Fig. 3.1 is simplified by summation of the contents of corresponding chambers of different screws and summation of the contents of corresponding chambers of different channels on one screw. The simplified model derived from the block-diagram of Fig. 3.1 can be found in Fig. 3.5. The leakage flows between chambers in the simplified model are the

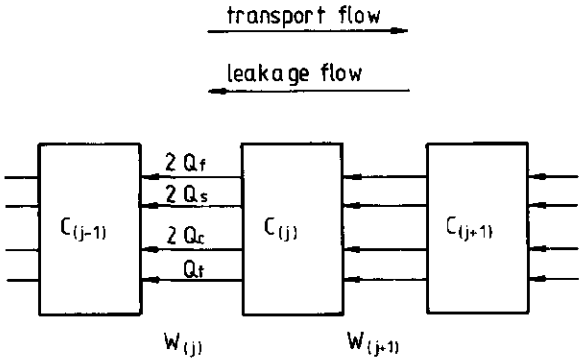

Fig. 3.5 Leakage flow pattern when leakage flows are completely mixed with chamber contents (van Zuilichem et al., 1988)

summation of the tetrahedron leakage flow (Q_t), the side leakage flow (Q_s), the flight leakage flow (Q_f), and the calender leakage flow (Q_c), Thus:

$$W(j,t) = Q_t+2Q_s+2Q_f+2Q_c \qquad (2)$$

in which W(j,t) is the leakage flow leaving chamber j at time t. The CSTRs of the model are described by a chamber volume V(j), a chamber tracer content (C) and a location (L) in the simulated extruder. The location variable (L) can vary between L=0, corresponding to the first chamber in the feed zone of the extruder, and L=1, which corresponds to the location at the die outlet. The location variable increases with time to simulate the transport of screw chambers in the extruder. The chamber volume V(j) of a single CSTR from the simplified block-diagram of Fig 3.5,. is the total volume of the four chambers summed to form this single CSTR. The chamber volume is calculated according to equations of Janssen (1978), but adapted for the conical aspect of the extruder used. The degree of fill, H(j) is the ratio of actual fill to maximum possible fill in the j-th chamber of the extruder. The material fed at time t=0 contributes to the degree of fill of all chambers during its residence in the extruder.

The leakage flows in the compression zone of the extruder are simulated by two variables for each chamber of the simulation

model, a coefficient describing the magnitude of the leakage flows A(j), and a mixing coefficient G(j), which describes the degree of mixing of the leakage flows with the chamber content. The leakage flow leaving chamber j at time t is calculated as:

$$W(j,t) = C(j,t) \cdot A(j) \cdot U \cdot \Delta t \cdot e^{(-A(j) \cdot U \cdot \Delta t)} \qquad (3)$$

in which U is the rotational velocity of the screws. Without exponential term the tracer content C(j,t) left after one turn of the screw is dependent of the time interval Δt, as W(j,t) is proportional to C(j,t). By the introduction of the exponential term this dependency disappears. In the compression zone of the model the leakage flow leaving chamber j enters chamber j-1. A fraction G_j of this leakage flow mixes with the chamber contents of the (j-1)th chamber and the remaining fraction (1-G) of the leakage flow, enters the (j-2)th chamber. This calculation procedure is repeated n times until the remaining fraction $(1-G)^n$ reaches the (j-n-1)th chamber with a zero leakage flow coefficient, where it mixes completely with the chamber contents. The mixing of leakage flows and chamber contents in the feed zone section of the model is slightly different from the mixing model in the compression part. Here a fraction G of the leakage flow leaving chamber j, mixes with the content of chamber (j-1), while the remaining fraction (1-G) is directly transported to the first chamber of the feed zone. After each time-interval a new tracer content (C) of all chambers is calculated. After a number of such intervals corresponding in total to one screw rotation, the j-th chamber becomes the (j+1)th chamber. The degree of fill can be calculated from the total amount of tracer which has been inside the j-th chamber during the residence time distribution measurement as:

$$H(j) = \frac{V(1) \cdot I}{V(j)} \int_{t=0}^{t=\infty} C(j,t)\, dt \qquad (4)$$

In which C(j,t) is the fraction of the tracer material which is present in chamber j at time t. The summation of C(j,t) in time is proportional with the degree of fill in chamber j. The minimum

value of this summation is 1.00, which occurs for a zero leakage flow entering this chamber. In this case the degree of fill in this chamber can be calculated by the degree of fill of the first chamber under the feed hopper by the feed rate for a zero porosity, I, corrected for the differences in the chamber volumes, V(j). The average residence time (τ) is dependent on the degree of fill in all 21 CSTRs and the feed rate, as in:

$$\tau = \frac{\sum_{j=1}^{j=21} H(j)}{I \cdot U} \qquad (5)$$

The upper part of eqn. 5 gives the filled volume in the extruder, while the lower part gives the volumetric feed rate , Q.

3.5 Optimization method

Simulation models with a large number of variables require an efficient search method in order to find an optimum or near-optimum solution with a modest computation time (Sisson, 1969). Such a search method can consist of a subdivision of the model into smaller sub-models, the optimization of these sub-models, and optimization of the complete model using the optimal solutions of the sub-model (Mesarovic, 1973). The proposed model here is subdivided into the feed zone, the transport zone and the compression zone. The complete model has seven input variables, namely: the feed rate (I), three variables ($S_1 \ldots S_3$) describing the leakage flow profile in the compression zone section of the model and three variables ($S_4 \ldots S_6$) describing the leakage flow profile in the feed zone section of the model (see Fig. 3.6). S_1 and S_4 are the values of the leakage flow coefficient A, constant for all chambers in the zone described. The value of the leakage flow coefficient A in all other chambers in the model is zero. S_2 and S_5 are the number of chambers in the zones described. S_3 and S_6 are the values of the mixing coefficient G, constant for all chambers in the zones described. There are five output variables, $O_1 \ldots\ldots O_5$, for the model, which are respectively, the greatest degree of fill found

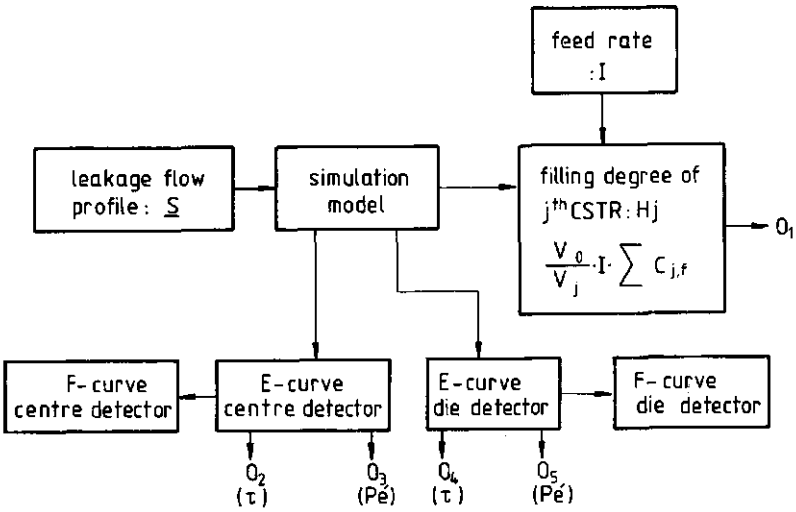

Fig. 3.6 Input and output simulation model (van Zuilichem et al., 1988)

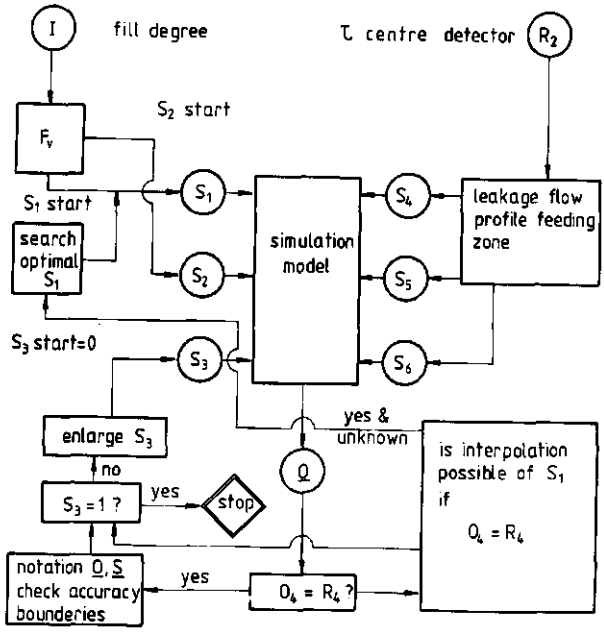

Fig. 3.7 Optimization procedure (van Zuilichem et al., 1988)

in the compression zone part of the model (O_1), the average residence times at two locations in the model corresponding to the locations of the two detectors (O_2,O_4), and the derived

Peclet-numbers (O_3,O_5). O_2 and O_3 are the "die outlet" output variables. The variables O_1....O_5 correspond to five variables R_1....R_5 measured on the actual extruder. Table 3.3 shows which input variables and output variables are dependent and which are independent. The feed zone model is used separately by searching for values of the input variables S_4....S_6 at which the output variables O_2 and O_3 are within the accuracy intervals of the measured variables R_4 and R_5. For the optimization of the compression zone model it is necessary to know this solution for the feed zone model. A rapid strategy, described in Fig. 3.7, to optimize the sub-models is based on feed-back, and uses some generalizations and assumptions.

For each group of residence time distribution measurements a leakage flow profile for the feed zone could be developed with only one variable ,the leakage flow coefficient S_4.
The maize dough in the compression zone was assumed to have zero porosity, which means that R_1=1.00. The average residence time O_2 and the maximum degree of fill in the compression zone O_1 are dependent as can be seen from eq. 5. Because of this dependence and the assumption, that R_1=1 , the number of leaking chambers S_2 in the compression zone, which is an integer variable, has one value, for which (R_1-O_1) is minimal, while O_2=R_2. The number of chambers S_2 can be estimated from a function F(v) derived from eq. 5, which calculates the average residence time in the compression zone from the number of fully-filled chambers. When S_2 is known, a value for S_3 is chosen, and the value of S_1 for which O_2=R_2 is searched for.

A constant leakage flow coefficient (A) for all chambers of the compression zone results in a degree of fill less than 1.00 in the chamber next to the die. A constant degree of fill of 1.00 for all chambers in the compression zone is possible, with another optimizing procedure, less efficient in calculation time. This slow procedure only gives a small improvement in the accuracy of the Peclet number of the model.

Table 3.3 Influence of input variables S and I on output variables (O-variables) (van Zuilichem et al., 1988)

	O_1	O_2 *and* O_3	O_4 *and* O_5
I	x	o	o
S_1 S_2 S_3	x	o	x
S_4 S_5 S_6	o	x	x

x = Dependent
o = Independent

3.6 Results

The RTD measurements are labelled with the letter combination 'exo' and a number, which indicates the sequence of the

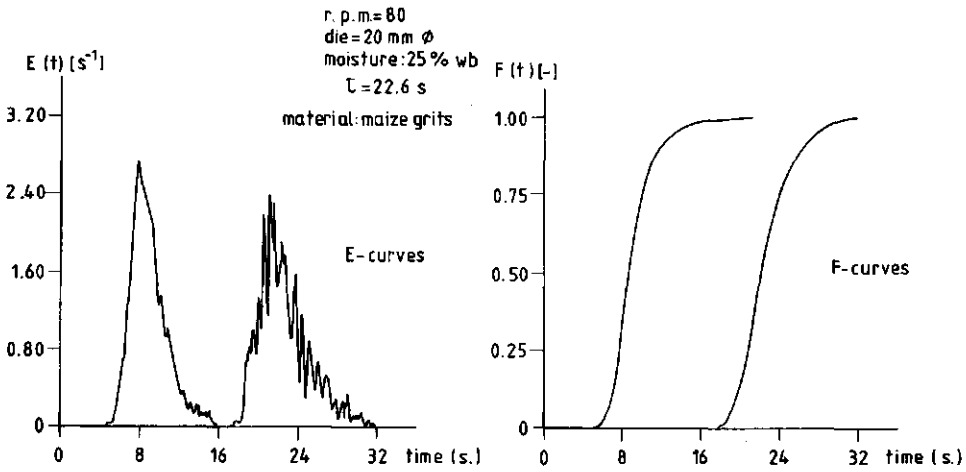

Fig 3.8 Extinction curves measured at the die and the midpoint positions (van Zuilichem et al., 1982)

measurements. An example of the measured RTD's is given in Fig. 3.8. Combination of average residence times and Peclet numbers measured at the centre detector, could not be simulated by assuming the total mixing of leakage flows and chamber content (S_6=0). The simulated average residence time and/or the Peclet number tended to be too high. A leakage flow profile was developed suitable for simulating the centre detector measurements 'exo(2)', 'exo(3)' and 'exo(4)'. In this leakage flow profile, all leakage flows from chambers four and five move directly to chamber one. Table 3.4 shows the differences between

the measured (R-variables) and simulated (O-variables) RTD's to be small. The mean residence time (R4) is inversely proportional to the rotational speed of the screws. From these measurements it is not clear which main variable affects the velocity profile in the feed zone, and hence the Peclet number (R_5).

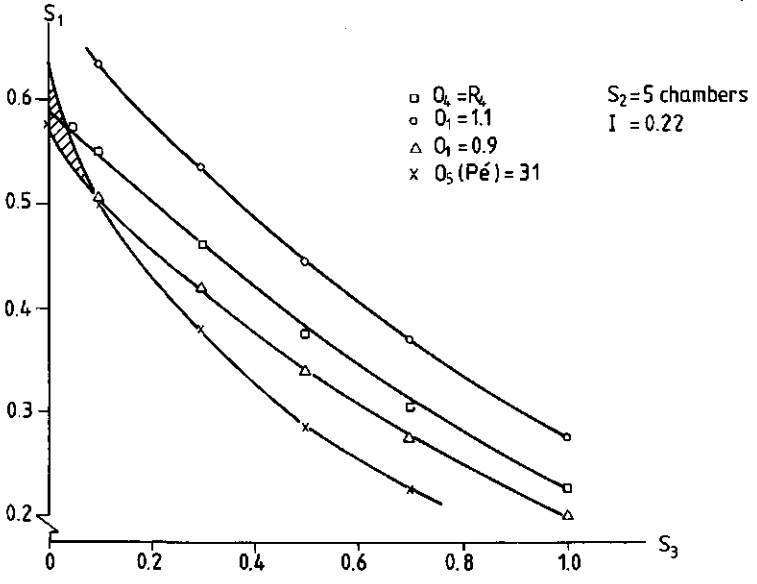

Fig. 3.9 Simulations are valid for optimal values of the leakage flow coefficient S_1 and the chamber mixing coefficient S_3 in the hatched areas of the curve for experiment 'exo 2'

The leakage flow profile variables in the feed zone were quantified so as to make the F-curve entering the compression zone match the measurements of the midpoint detector. The simulation of the feed zone was not affected by leakage flows in the compression zone, as can be seen from Table 3.3. In Fig. 3.9, 3.10 and 3.11 all possible combinations of the coefficients related to the magnitude of leakage flow S1 and the extent of chamber mixing S_3 are given for three measurements. Some values from Fig. 3.9, 3.10 and 3.11 are shown in Table 3.5. The four lines in each figure are: the combinations of S_1 and S_3 which result in the simulated average residence time at the die detector (O_2=R_2), the upper and lower boundaries of accuracy for the maximal degree of fill in the compression zone (O_1) and for the Peclet number (O_5). The hatched areas give all possible

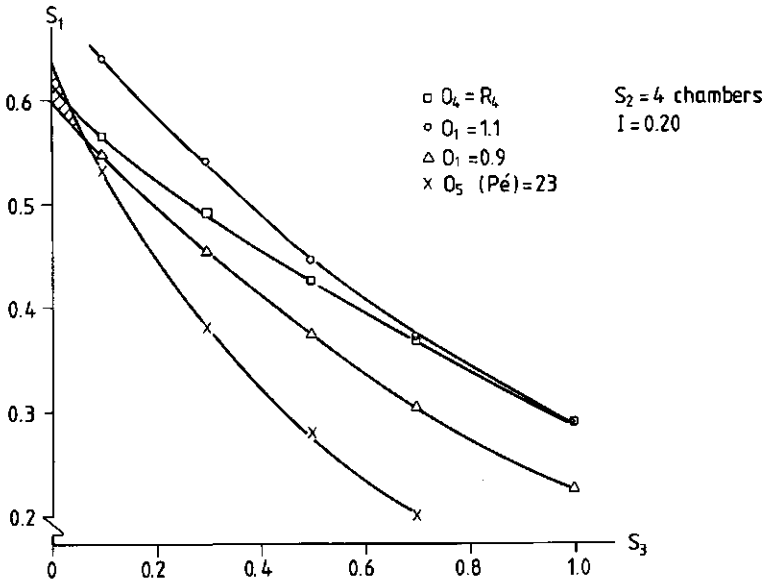

Fig. 3.10 Simulations are valid for optimal values of leakage flow coefficient S_1 and the chamber mixing coefficient S_3 in the hatched areas of the curve for experiment 'exo 3'

combinations of S_1 and S_3 if the number of chambers in the compression section is infinitely variable instead of an integer. In the hatched fields the correct values of the Peclet numbers can only be simulated within a limited range of the chamber mixing coefficient S_3. In four out of six measurements, S_3 ranged from 0.0 to 0.1 (Fig. 3.9, 3.10). The other two measurements gave a value of S3 ranging from 0.0 to 0.7 (Fig. 3.11). These intervals are greatly influenced by small changes in the Peclet number. On the lines for which $O_2=R_2$, where the mean residence time is kept at a constant value, the chamber mixing coefficient has a suprisingly small effect on the Peclet number. An increase in S_3 from 0.0 to 0.4 resulted in a decrease in the Peclet number from 29 to 25. Therefore such a determination of the chamber mixing coefficient requires a very accurate measurement of Peclet numbers. When simulations are made without backmixing in the feed zone, and the compression zone is dimensioned as given in Table 3.5, Peclet numbers increase, as can be seen in Table 3.6. These Peclet numbers are large in comparison with those for other extruder types having comparable hold-up volumes, as can be seen

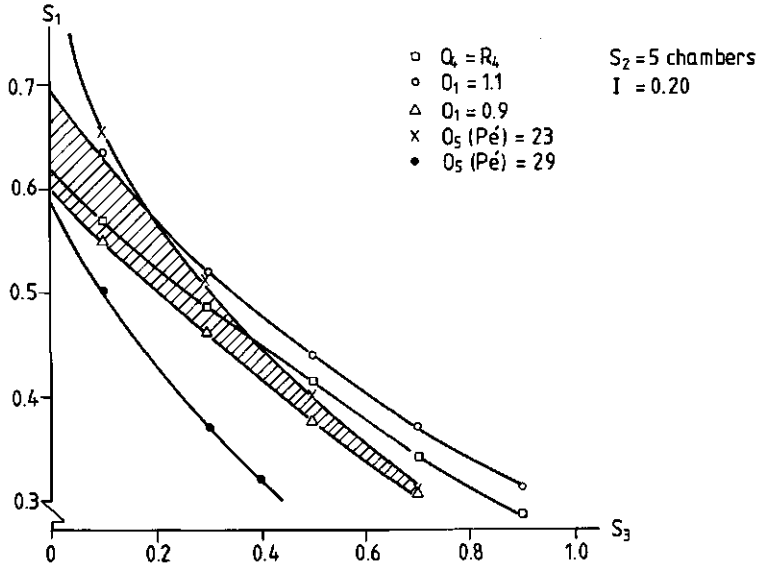

Fig. 3.11 Simulations are valid for optimal values of the leakage flow coefficient S_1 and the chamber mixing coefficient S_3 in the hatched areas of the curve for experiment 'exo 4'

Table 3.4 (van Zuilichem et al., 1988)

Measurement of Mean Residence Time (R_2) and Peclet Number (R_3), Simulation Results for Mean Residence Time (O_2) and Peclet Number (O_3), and Simulation Input Variable S_4, of Mid-point Detector, as Influenced by the Rotational Screw Speed U, Employing a Constant Feed-rate (I)

Experiment	$U\ (s^{-1})$	I	$R_2(s)$	$O_2\ (s)$	R_3	O_3	S_4
exo 2	0·67	0·22	18	18	7	7·4	0·41
exo 3	1·00	0·20	14	14	5	5·4	0·53
exo 4	1·33	0·20	9	9	8	7·4	0·41

Table 3.6

Peclet Number Measured at the Die Detector and Peclet Number as Output Variable of a Model Without Axial Mixing in the Feed Zone

Experiment	*exo 2*	*exo 3*	*exo 4*
Peclet number measured, R_5	34	26	26
Peclet number simulated, O_5	55	61	49

in Table 3.7. The nearly doubled Peclet numbers in Table 3.6 give

Table 3.5 (van Zuilichem et al., 1988)

Leakage Flow Profile (S-Variables) in the Compression Zone Necessary to Simulate the Mean Residence Time (R_4) and Peclet Number (R_5) Measured at the 'Die' Detector. The Calculated Peclet Number (O_5) is Given for Three Values of the Chamber Mixing Coefficient S_3

Experiment	*exo 2*	*exo 3*	*exo 4*
Screw speed, U (s^{-1})	0·67	1·00	1·33
Feed rate ratio, I	0·22	0·20	0·20
Average residence time measured, R_4 (s)	45	31	23
Peclet number measured, R_5	34	26	26
Accuracy range of R_5	31–37	23–29	23–29
Fully filled chambers in compression zone of simulation model, S_2	5	4	5
$S = 0·00$ (leakage flow coefficient simulated Peclet number)			
S_1	0·59	0·61	0·62
O_5	31	23	29
$S_3 = 0·05$ (leakage flow coefficient simulated Peclet number)			
S_1	0·58	0·58	0·59
O_5	31	23	28
$S_3 = 0·40$ (leakage flow coefficient simulated Peclet number)			
S_1	[a]	[a]	0·45
O_5	[a]	[a]	25

[a] O_5 cannot be simulated within the accuracy range of R_5.

information on the axial mixing at temperatures above the selected temperatures of the feed zone (60-100°C), ignoring mixing effects at temperatures below 100°C. In Fig. 3.12 the F-curves for axial mixing above the selected temperatures of the feed zone, and above or at 150°C, are given. Due to the absence of mixing in the feed zone part of the model, these curves tend to become more uniform. This uniformity is due to the equal mixing profiles of these three measurements in the compression zone. The coefficient describing the magnitude of the leakage flow is, assuming a constant value for the mixing coefficient S_3, independent of screw velocity and the number of chambers in the compression zone (see Table 3.5). Variations in the Peclet numbers measured at the die are largely due to variations in

Table 3.7 (van Zuilichem et al., 1988)

Peclet Numbers for Three Extruder Types

Extruder type	*Peclet number*	τ *(s)*	*Feed rate (g s^{-1})*	*Hold-up volume (m^3)*
Single screw[a]	10–20	60	11	5×10^{-4}
Co-rotating, twin-screw[b]	10–30	55	10	4×10^{-4}
Counter-rotating, twin-screw with axial mixing in the feed zone	26–34	30	25	6×10^{-4}
Counter-rotating, twin-screw without axial mixing in the feed zone	55–61	20	25	4×10^{-4}

[a]Calculated from Van Zuilichem *et al.* (1988*a*).
[b]Van Zuilichem, unpublished data.

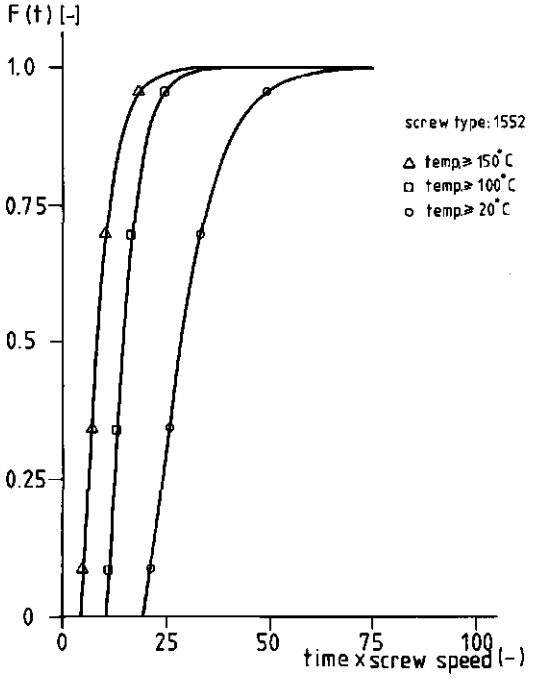

Fig. 3.12 Calculated F-curves for the die location for experiment 'exo 4' in which only the axial mixing in sections with a temperature above the indicated temperature is simulated

leakage flows in the feed zone.

3.7 Conclusions

The assumption of a constant leakage flow coefficient in four or five chambers of the compression zone gives a possible leakage flow profile on which a model simulation of a working twin-screw extruder can be based, within the limits of accuracy of the measurements. In the model the effect of the coefficient describing the mixing of chamber contents and leakage flows on the Peclet number proved to be minor. The coefficient for the mixing of chamber contents and leakage flows could not be determined, due to the restricted number of measurements and the small effect of this coefficient on the Peclet number. The average residence time in the feed zone is inversely proportional to the rotational speed of the screws. When a counter-rotating, twin-screw extruder is used as a reactor for starch conversions occurring mainly in the compression zone of the extruder, the Peclet numbers measured have to be corrected for the axial mixing in the feed zone, as this mixing is not relevant to the reactions. Thus a measured Peclet number of 26 to 34 becomes an effective Peclet number of 49 to 61.

References

Albers, F., (1976). Beitrag zur Dimensionierung der Schnecken von einen Gegenlaufig kammenden Doppelschneckenextrudern. Dissertation Montanuniversität Leoben.

Altomare, R.E., Ghossi, P. (1986). An analysis of residence time distribution patterns in a twin screw cooking extruder. Biotechnology Progress, 2 157-163.

Ben-Gera, I., Rokey, G.J., Smith, O.B.(1983). Extrusion cooking of grains for ethanol production. J. Food Eng., 2, 177-187.

Bounie, D., Cheftel, J.C. (1986). The use of Tracers and Thermosensitive Molecules to Assess Flow Behaviour and Severity of Heat Processing During Extrusion-Cooking. In: Pasta and Extrusion Cooked Foods. ed. C. Mercier, C. Cantarelli. Elsevier Applied Science Publishers, London, 148-158.

Bush, M., Milthorpe, R.F., Tanner, R.I. (1984). Finite element and boundary element methods for extrusion computations. J. Non- Newtonian Fluid Mech., 16, 37-51.

Chouvel, H., Chay, P.B., Cheftel, J.C. (1983). Enzymatic hydrolysis of starch and cereal flours at intermediate moisture contents in a continuous extrusion reactor. Lebensm.-Wiss.u-Technol., 16, 346-353.

Janssen, L.P.B.M. (1978). Twin screw Extrusion. Elsevier Scientific Publications, Amsterdam.

Launay, B., Lisch, J.M. (1983). Twin screw extrusion cooking of starches: flow behaviour of starch pastes expansion and mechanical properties of extrudates. J. Food Eng., 2, 157-175.

Levenspiel, O. (1972). Chemical Reaction Engineering, 2nd Ed..

John Wiley & Sons, New York.

Linko, P., Linko, Y., Olkku, J. (1983). Extrusion cooking and bioconversions. J. Food Eng., 2, 243-257.

Mercier, C., Charboniere, R., Grebaut, J., de la Gueriviere, J.F. (1980). Formation of amylose-lipid complexes by twin screw extrusion cooking of manioc starch. Cereal Chem., 57 (1) 4-9.

Mesarovic, M.D. (1973). On vertical decomposition and modeling of large scale systems. In: Decomposition of large scale problems, ed. D.M. Himmelblau. North-Holland Publishing Company, Amsterdam, (American Elsevier Publishing Co., Inc.), 323-340.

Olkku, J., Antila, J., Heikkinen, J., Linko, P. (1980). Residence time in a twin screw extruder. In: Food Proces Engineering Vol. 1: Food processing Systems, ed. P. Linko, V. Mälkki, J. Olkku, J. Larinkari. Applied Science Publishers, London, 791-794.

Sisson, R.L. (1969). Simulation: uses. Progress in Optimization Research, Vol. iii, ed. S. Arinofsky. John Wiley & Sons, New York, 17-70.

Savolainen, A., Karling. R, (1985). The influence of screw geometry on the extrusion of soft PVC. J. Appl. Polym. Sci., 30, 2095-2104.

Todd, D. (1975). Residence time distribution in twin screw extruders. Polym. Eng. Sc., 15, 437-442.

van Zuilichem, D.J., Bruin, S., Janssen, L.P.B.M., Stolp, W. (1980). Single screw extrusion of starch and protein rich materials. In: Food Proces Engineering Vol. 1: Food processing Systems, ed. P. Linko, V. Mälkki, J. Olkku, J.

Larinkari. Applied Science Publishers, London, 745-756.

van Zuilichem, D.J., Tempel, W.J., Stolp, W., van't Riet, K. (1985). Production of high boiled sugar confectionary by extrusion cooking of sucrose. J. Food Eng., 4, 37-51.

van Zuilichem, D.J., Stolp, W., Janssen, L.P.B.M. (1983). Engineering aspects of single-and twin screw extrusion cooking of biopolymers. J. Food Eng., 2, 157-175.

van Zuilichem, D.J., Jager, T., Stolp, W., de Swart, J.G. (1988a). Residence time distributions in extrusion-cooking. Part I: coincidence detection. J. Food Eng., 7, 147-158.

van Zuilichem, D.J., Jager, T., Stolp, W., de Swart, J.G. (1988b). Residence time distributions in extrusion-cooking. Part II: Single-screw extruder processing maize and soya. J. Food Eng., 7, 197-210.

van Zuilichem, D.J., Stolp, W., Jager, T., (1982). Seminar koch und extrudiertechnieken, Lecture at: Zentralfachschule der Deutschen Süsswarenwirtschaft,Solingen.

Notation

A(j)	Leakage flow coefficient of CSTR j	[-]
C(j,t)	Fraction of tracer content in CSTR j at time t	[-]
D_e	Axial dispersion coefficient	[m^2s^{-1}]
exo	Series of residence time distribution measurements	[-]
E	Exit age distribution	[s^{-1}]
F	Cummulative exit age distribution	[-]
G(j)	Chamber mixing coefficient of chamber j	[-]
H(j)	Degree of fill of j th CSTR	[-]
I	Ratio of feed rate to maximum feed rate	[-]
j	CSTR number	[-]
l	Extruder length	[m]
L	Dimensionless extruder length	[-]
O_1	Greatest fill degree in compression zone model	[-]
O_2	Average residence time in reference to midpoint location in model	[s]
O_3	Peclet number in reference to midpoint location in model	[-]
O_4	Average residence time in reference to die location in model	[s]
O_5	Peclet number in reference to die location in model	[-]
Pe	Peclet number	[-]
Q_c	Dimensionless calender leakage flow	[-]
Q_f	Dimensionless flight leakage flow	[-]
Q_s	Dimensionless side leakage flow	[-]
Q_t	Dimensionless terahedron leakage flow	[-]
R_1	Degree of fill in the compression zone	[-]
R_2	Average residence time in reference to midpoint detector position	[s]
R_3	Peclet number in in reference to midpoiunt detector position	[-]
R_4	Average residence time in reference to die detector	

	position	
R_5	Peclet number in reference to die detector position	[-]
S_1	Value of A in compression section of the model	[-]
S_2	Number of CSTRs in the compression section of the model for which A>0	[-]
S_3	Chamber mixing coefficient G in the compression section of the model	[-]
S_4	Value of A in the feed section of the model	[-]
S_5	Number of CSTRs in the feed section of the model for which A>0	[-]
S_6	Chamber mixing coefficientG in the feed zone	[-]
t	Time	[s]
U	Rotational speed of the screws	[s^{-1}]
$\bar{v}$	Mean axial velocity	[ms^{-1}]
V(j)	Volume of j^{th} CSTR	[m^3]
W(j,t)	Leakage flow out of CSTR j at time t	[-]
τ	Average residence time	[s]
Δt	Time interval	[s]

CHAPTER 4

CONFECTIONERY AND EXTRUSION COOKING TECHNOLOGY

ABSTRACT

The capabilities of cooking extruder equipment in confectionery production is investigated. Sugar crystals are converted to a seedingfree clear melt using a single screw extruder. The production of high-boiled sugar confectionery by means of a twin-screw extrusion-cooker (e-c) has been investigated and is described. The products are crystal free and uncoloured. The water content is low, even though no evacuation systems were used to remove excess water. The heat transfer in the e-c may be calculated by a stepwise procedure over the length of the extruder. The results indicate that the e-c is an effective heat exchanger. The model developed enables the time needed for dissolution of the crystals to be estimated. It is concluded that use of an e-c for this purpose is both possible and attractive.

THIS CHAPTER IS BASED UPON THE PUBLICATIONS:

van Zuilichem, D.J., Alblas, B., Reinders, P.M. and Stolp, (1983a). A comparative study of the operational characteristics of single and twin screw extrusion of biopolymers. In Thermal Processing and Quality of Foods, ed. P. Zeuthen, J.C. Cheftel, C. Eriksson, M. Jul, H. Leniger, P. Linko, G. Varela, G. Vos, Elsevier Applied Science Publishers, London\New York, 1984.

van Zuilichem, D.J., Tempel, W.J., Stolp. W and K. van 't Riet (1985). Production of high boiled sugar confectionery by extrusion cooking of sucrose:liquid glucose mixtures. J.Food Engng. 4 , 37-51.

Sugar Confectionery Manufacture, pp 311-330. Ed. Blackie/van Nostrand REINHOLD/New York 1990.

4.1 Introduction

Among other applications, cooking extruders can be used to produce confectionery. As such extrusion cooking technology is not a new technology, since pasta products are commonly extruded and shaped since the thirties and sausage is produced for a hundred years on extruder-like equipment. The real novelty is that "cooking" extruder equipment is offered to the food industry, which means that a heating process is introduced in which a controlled food-chemical or -biochemical reaction takes place.

The chemical polymer industry started up the use of extruder equipment since the fourties with the so called melting-extruders based on design concepts of mixer compounders. The food industry discovered the cooking extruder since the fifties and used the equipment in the beginning for the production of cooked and expanded snacks on basis of corngrits and other cereals. Most of the equipment used were so called single screw extruder concepts, whilst twin screw extruder equipment dates back since the sixties. A technological reason for the use of twin screw extruders is the need for equipment capable to handle high viscosities as they are known in the confectionery branch or to process low and high viscosities in a distinct recipe at the same time in one piece of equipment. Although most of the confectionery-articles are unique in its own it is clear that the basic components are sugar (sucrose), starch syrups (treacle) and starch or flours (see Table 4.1).

Table 4.1.Generalised composition of some confectioneries (van Zuilichem et al., 1985

Materials	Liquorices	Soft liquorice	Clear gums	Wine gums
Products				
sucrose	x	x	x	x
syrups	x	x	x	x
starch	x	x	x	x
wheat flour		x		
block liquorice	x	x		
caramel	x			
NH_4Cl	x	x		
additives	x			
gelatines	x	x		
water	x	x	x	x

At the same time water is always part of the recipe and this is just the reason for the selection of extruder equipment as an innovative tool in this area, since drying costs are determining for a great deal the price of the goods. Cooking extruders offer a possibility to process confectionery-goods at lower process moisture conditions compared with conventional processing, which will lead to attractive savings.

4.2 Problem description

At the conventional confectionery-processes water is used to dissolve sucrose crystals at preset temperatures, described by Honig (1953). The products are casted in cornstarch and the water is removed to conditions required for a long shelf life. For this operation careful and time consuming drying is necessary at temperatures between 45-60°C. The low diffusivity constants for water in sugarlike materials determine the rate of drying.
It is clear that these methods are energy consuming. It would be more attractive to develop a cooking method at which the water

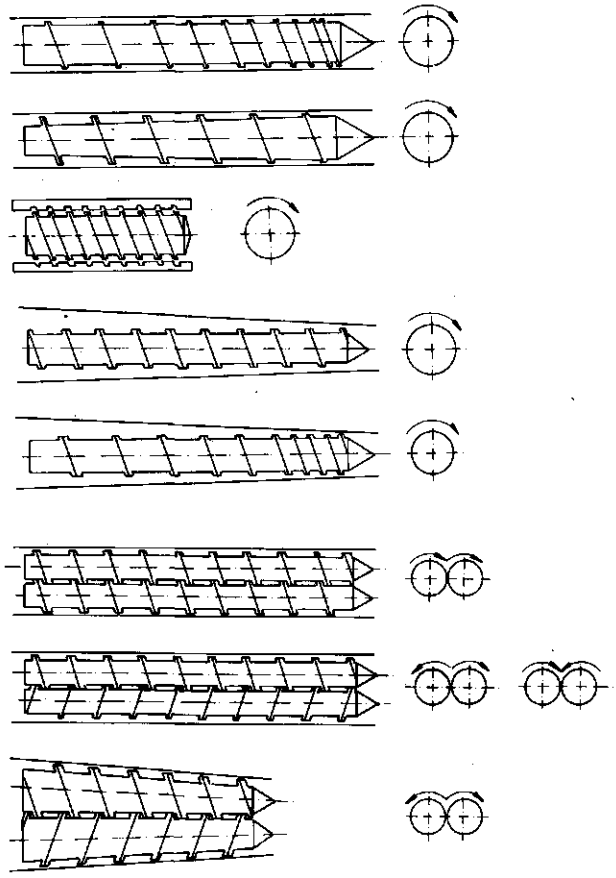

Fig 4.1 Existing food extruder models (van Zuilichem et al., 1976)

percentage is as close as possible to the moisture level of the end product (see Table 4.2). Such a wish may be fullfilled by the selection of an appropriate extruder for this purpose. The available extruder-designs can be divided in single and twin screw extruders (see Fig. 4.1).

Table 4.2. Typical shelf life/moisture for some confectioneries

Product	Moisture (%)	Shelf life (in months)
chocolate		
bakery	1	6/8
milk	2	6/8
pure	1	6/8
toffees	6 à 7	8
hard boilings	2 à 3	12
agar gels	24	6/8
cream	12 à 13	6
whipped cream	6	8
fondant	12	10
wine gums	12	12
soft gums	22	6/8
fudge	7	5/6
gelatine gels	22	6/8
marshmallows	12	4
pastilles 1	18	4
pastilles 2	11	18
pectine gels	22	6/8
tablets	1	18
turkish delight	20	5
liquorice	8/18	8/9

The twin screw extruder designs consist of corotating and counterrotating designs and closely intermeshing, so called self-wiping extruders. The most important difference between single screw extruders and closely intermeshing twin screw extruders is that single screw extruders are so called "open channel" equipment, with no restriction prohibiting backflow of the material, whereas the closely intermeshing twins consists of a series of C-shaped chambers, which pump the material from feed port to the die (see Fig. 4.2).

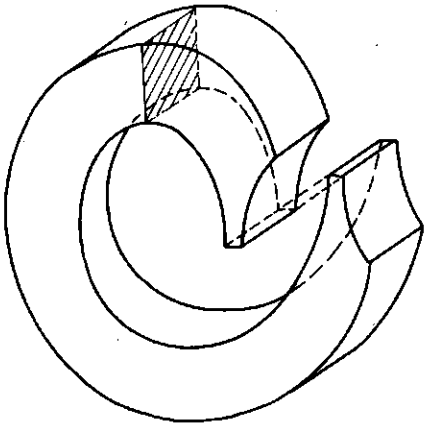

Fig 4.2 C-shaped chamber of twin screw extruder (Janssen, 1978)

4.3 Status quo of realised extrusion cooking -processes

It is possible to replace the conventional continuous cooking of confectionery at high solids content by twin screw extrusion cooking, optionally followed by moulding and drying in starch or other moulds. This may not be very spectacular as the post extruder process is still conventional but the aim is to save energy by preparing the melt at lower moisture contents. Another possibility is the use of extrusion cooking in the manufacture of gum confectionery cooking extrusion. Here forming-extrusion is already being used to produce liquorice, gums, chewing gum, caramels and marsh-mallows. These products have been well investigated by extruder manufacturers, mostly in combination with starch-producers. For example Staley has patented the use of the cold water swelling Miragel 463 for confectionery extrusion in US-patent no. 4567055. The patent describes the extrusion of maltose syrup, fructose syrup and Miragel 463 at 121 °C. Regular cold swelling starches are claimed not to lead to translucent products. It is obvious that product development in this area is very well possible and necessary, but a good knowledge of the behaviour of the basic components in extruders should be understood.

4.4 Extrusion of starch

The commercial attractive starch sources are: maize, potato, rice, manioc, wheat or sago. It is well known that starches have a gelatinisation temperature between 60 and 80 °C. (See Table 4.3).

Table 4.3 Gelatinisation of starches. (van Zuilichem et al., 1976)

Basic starches	Gelatinisation temperature (°C)
Corn starch	62-72
Potato starch	56-66
Wheat starch	52-63
Rice starch	61-78
Tapioca	58-70
Sago	60-72

The composition of starches consists in most cases of amylose and amylopectin in a ratio 1 : 4. An exception is Waxy-maize as shown in the table 4.4.

Table 4.4 Starch composition (van Zuilichem et al., 1976)

	Ratio (%)	
	Amylose	Amylopectin
Corn starch	24-26	74-76
Potato starch	22-23	Approx. 77
Tapioca	19-20	Approx. 80
Sago	20-26	74-80
Waxy maize	<1	>99

As shown in Figure 4.3 amylose consists of a chain of α-1,4 glucan elements. On the other hand, amylopectin shows a branched structure of α-1,4 glucan and α-1,6 elements. The aim of an extruder, when processing these polysaccharides, is to damage cell walls of the starch particles and to seperate them more or less by breaking or reducing the size of the molecular chains. For this purpose the product application is very important. For

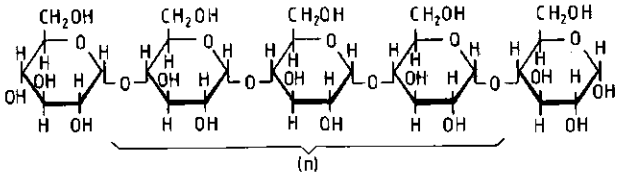

Amylose, α 1.4 glucan

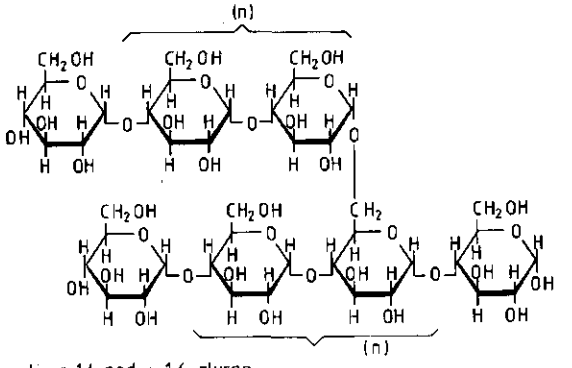

Amylopectin, α 1.4 and α 1.6 glucan

Fig. 4.3 Molecular structure of amylose and amylopectin (van Zuilichem et al., 1982b)

human consumption it is necessary, for reasons of digestibilty to gelatinize the starch almost completely, for animal foodstuff this is not the case as the ability of animals to digest partly gelatinized starches, due to enzyme activity, is much better. For confectionery products, however, the starch must be completely cooked.

4.5 Extrusion of dry sucrose-crystals

Sucrose crystals are one of the main recipe-components used in the mixtures in the confectionery-industry. It is necessary to study the melting behaviour of sucrose in an extruder, as this

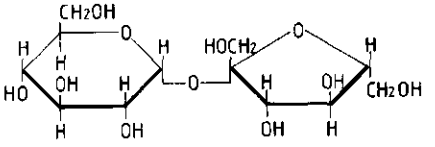

Fig. 4.4 Molecular structure of sucrose (van Zuilichem et al., 1982b)

stage offers the potential to save a considerable amount of energy used for the cooking step. Sucrose is composed of glucose and fructose units. The structural formula of sucrose is given in Figure 4.4.

For application in the confectionery industry sucrose should be present as a clear melt at high temperatures (> 160 °C) that can easily be cast in preformed maize-starch moulds, and that can easily be mixed with other components.
The extruded product must meet these requirements. At the same time it is necessary to know the possible degree of caramellization caused by the high temperature levels in extruders. Furthermore one should also be aware of the possibility of inversion of sucrose, which means chemically that the dissaccharide is split up into the two monosaccharide components, glucose and fructose. Finally one will be interested in the viscosity developed in an extruder, which will determine directly the capacity of the extruder equipment and the energy consumption.

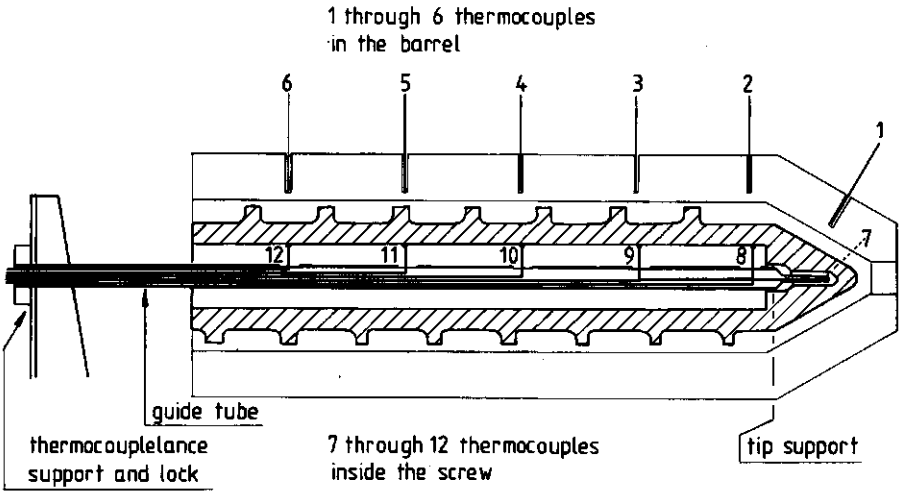

Fig. 4.5 Thermocouple arrangement for screw and barrel

The extruder used by van Zuilichem et al. in 1983 was a 50 mm single screw extruder originating from the Battenfeld design. The screws used were of the compressing type, with constant pitch and compression ratio's of 3 : 1, 2 : 1 and 1.15 : 1. Temperatures of barrel and screw were measured with thermocouples. The screws used were hollow. A thermocouple-lance, supported in the nosetip of the screw and at the rear of the extruder, were used to measure the temperature profile in the screw side (See Fig. 4.5)

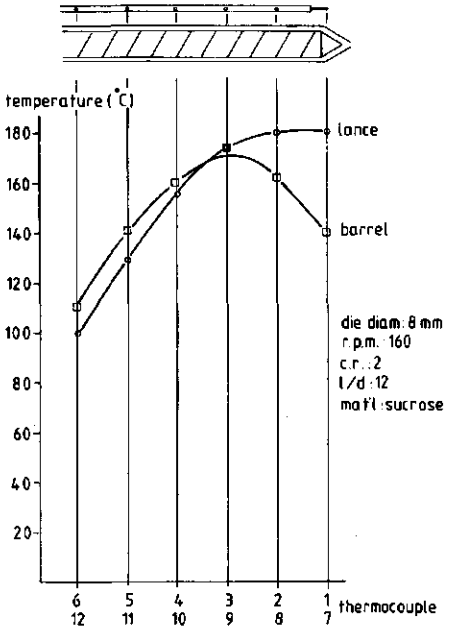

Fig. 4.6 Screw and barrel temperature profile for sugar melting (van Zuilichem et al., 1982a)

The sugar was supplied to the extruder by a simple vibratory metering device. At first a good temperature distribution had to be found in order to create a sufficient melting of the dry crystals. The necessary temperature profiles could be controlled very well and an example is shown in Fig 4.6. It can be seen that the sugar is sheared on the screw side resulting in a quite high "lance" temperature profile in connection with an extruder barrel profile going from ± 130 °C above ± 170 °C, to 150 °C at the barrel outlet. This temperature profile was measured at 160

r.p.m., with a screw compression ratio of 2 : 1 and length/diameter of the screw, l/d = 12. The die used had a slit of 8 mm. With this setup the process is unstable and the throughput is fluctuating.

A maximum throughput of molten sucrose is plotted in Fig. 4.7 for screw compression ratio's 3 : 1, 2 : 1 and 1.15 : 1 at the range 160 - 200 r.p.m. A maximum throughput of the melt of over 90 kg/hr proved to be possible at 200 r.p.m., using a 3 : 1 compression screw. The molten sugar exhibited an amorphous structure and had lost its crystalline nature when it was sampled directly at the extruder die. After some time of storage the samples showed a slight recrystallisation due to very small seeding crystals.

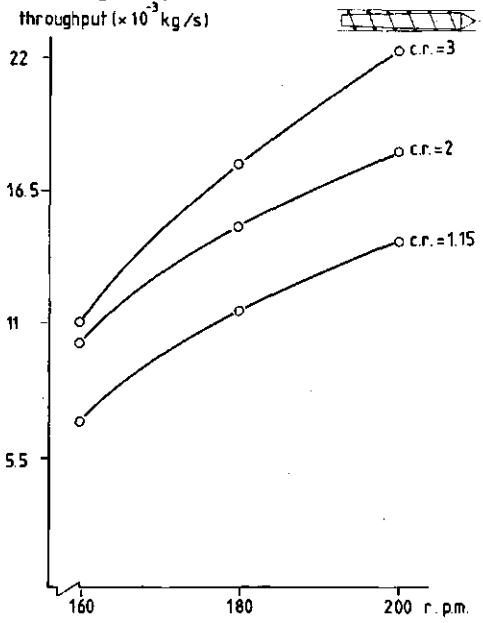

Fig. 4.7 Maximum throughput for sucrose (van Zuilichem et al., 1982b)

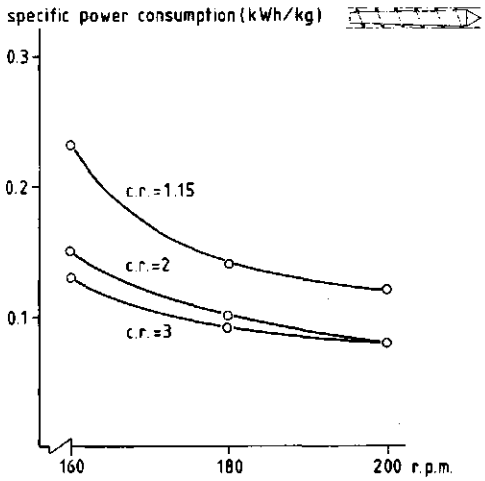

Fig. 4.8 Specific power consumption for sucrose (van Zuilichem et al., 1982b)

Of interest is the average specific power consumed necessary in the above mentioned trials. This is shown in Fig. 4.8 for three different screw compression ratios. At compression ratios of 3:1

and 2:1 power consumption was low ≈ 0,1 kWh/kg. The lower compression ratio of 1,15 : 1 needed a specific power consumption of at least 0,15 kWh/kg. When motor power only is considered, the figures are much lower, in the region of (0,04 - 0,05) kWh/kg for screws with compression ratio's of 2 : 1 and 3 : 1. The difference in power is provided by the electric heaters that intermittently heated the barrel and the heat losses to the environment (See Fig. 4.9).

The melt must be produced at the higher r.p.m. values used, in order to avoid scaling in the die and recrystallization of molten sugar. The reducing ability of the sugar after this dry extrusion was measured by the method of Nierle and Tegge and no considerable inversion could be determined at the circumstances mentioned. Some colour measurements were also performed, using

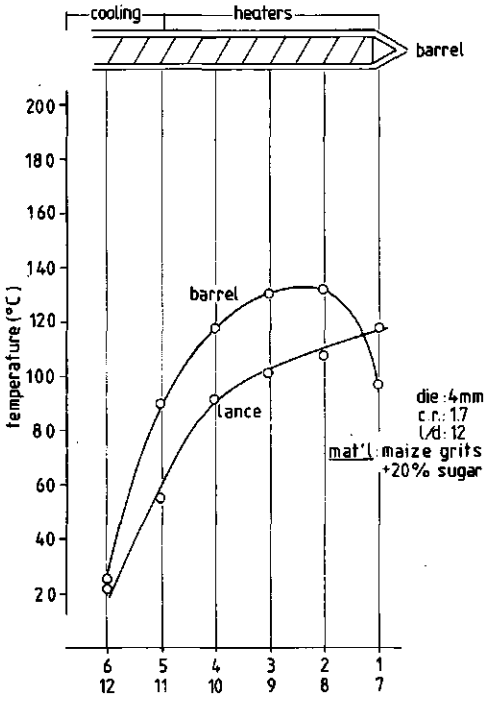

Fig. 4.9 Temperature profiles for the extrusion of a maize-sugar mix (van Zuilichem et al., 1981)

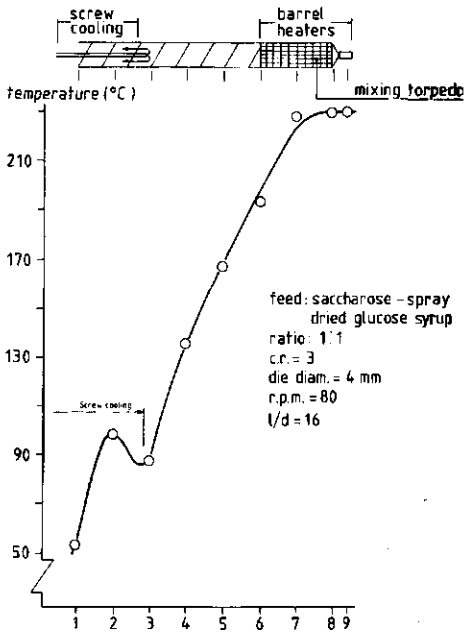

Fig. 4.10 Temperature profile for dry saccharose-glucose mixtures (van Zuilichem et al., 1990)

the standardized Icumsa method nr. 4, according to De Whalley

(1964). Clear melts without any recrystallisation are produced when a steep temperature profile is applied at a cooled screw provided with a so called mixing torpedo. (see Fig. 4.10). Colour ratings are below Icumsa 50. In this way a single screw extruder can be used as a relatively economical melting tube for dry sucrose crystals.

4.6 Extrusion of sucrose-starch mixtures

In the confectionery industry many products, based on starchy materials like rice, wheat and sometimes corn, are used as candy bar fillers. In Fig. 4.10 a temperature profile is given for a single screw extruder processing a candybar filler out of corn and sucrose in a ratio 4 : 1. Such a product can still be handled by a single screw extruder without difficulties. If the percentage of sucrose required, is higher then 20%, a twin screw extruder is a good machine for such a product, because the forced flow needed for such a high viscosity mixture is easily provided by the C-shaped chambers. A single screw extruder, however, is in this case already problematic.

4.6.1 Extrusion of sucrose-syrup mixtures

The extrusion cooking of this type of mixture forms the basis of confectionery-products. Due to the unattractive low viscosity of the starch-syrups a single screw extruder will be unsuitable for such a job, but a closely intermeshing twin screw extruder can easily be used.

In the conventional method of producing the melt from which hardboiled sweets are formed, water is added to the other ingredients in a cooking vessel. The advantage of an extrusion-cooker (e-c) is that dissolution can be performed without the addition of any water. Thus by using an e-c the time- and energy-consuming step of evaporation of the excess water can be obviated. A twin-screw e-c is able to perform this function, as it has a large heat exchange capacity combined with a favourable residence-time pattern. The positive forward transport mechanism together with the lateral mixing action of the screw result in a plugflow-like pattern combined with radial (interchamber)

mixing. This results in a well-controlled, limited residence-time whilst at the same time a well-mixed material is processed. Evidence for this plugflow character is given by Jager (1983) who defined S as the ratio of the time taken for 16% and 84% of an injected tracer to pass a reference point at the end of the e-c. Jager found that in a twin-screw e-c S tends to be in the region of 0.3-0.5, which is an attractive value. Jager also explained that the higher the viscosity of the material, the greater the variance of residence-time distribution, due to back-flow. Because the material used in the confectionery production described here has a relatively low viscosity at e-c temperatures, S could be even higher in this case, which implies even more favourable conditions in the e-c.

The sucrose crystals dissolve in the water present in the glucose syrup. In this process the time and temperature (and pressure, in combination with the temperature), determine whether the crystals will disappear and whether undesirable colour development will occur. A schematic representation is given below:

Time		Crystal dissolution
Temperature	→	Off-colour development
Pressure		Water evaporation

The residence-time must not be less than the minimum time needed to dissolve the crystals completely at the prevailing temperature. On the other hand, the temperature must be low enough to avoid the formation of off-coloured products.
There is no melting of sugar crystals involved since working temperatures are in the region of 130-150 °C and the melting temperature of sucrose is 186 °C. Shear effects can also be neglected since Brinkman numbers are below 0.001, while Graetz numbers are above 10^5, for the working points of the extruder used.

Coloration of sugars or off-color development at high temperatures is due to caramelization. Unfortunately there are no exact quantitative data available on the relationship between

sugar temperature and degree of coloration. The reason for this is that, once the initiating reaction has started, a complex of condensation, fragmentation and dehydration reactions follows. The starting reaction is known, however. Shallenberger & Birch (1975) point out that colour formation begins with the 1,2-enolisation of a sugar reducing end (see Fig. 4.11).
Since sucrose does not contain a reducing end, the colouring of the mixture considered here is most probably due to the glucose syrup. An experiment with material in test-tubes heated in a temperature-controlled glycerine bath, sustained this view.
Tubes filled with glucose syrup discoloured to twice the intensity attained by tubes filled with a 1 : 1 sucrose: glucose syrup mixture, which indicates that the 50% sucrose in the latter tubes may be regarded as a colour diluent agent. These tests also showed that colour development increases linearly with time and is following an Arrhenius model for the dependence on

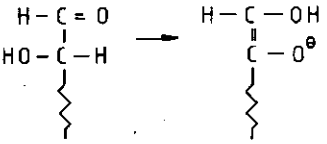

Fig. 4.11 Schematic representation of the 1,2 enolization of a sugar reducing-end (van Zuilichem et al., 1985)

temperature. This means that the temperature is especially important. The test tube experiment showed that the reaction mixture should not be subjected to temperatures higher than 155°C for appreciable times.

The important question that must be answered is whether the bulk material flowing in an extruder will reach the temperature of the heated extruder wall. Van Zuilichem et al. (1983a) presented a calculation method for the mass temperature, which results in the following equation:

$$\phi_{wall} = 5.71 \frac{\rho^3 \lambda_m^4 C_p^2}{\eta} N^{0.5} D_w D_s^{0.5} (T_w - T_m)_z Z^{-0.5} \qquad (1)$$

In which ϕ_{wall} = cumulative heat flow into the bulk material over length z(W), ϱ = mass density (kg m^{-3}), λ = mass thermal conductivity (J s^{-1} m^{-1} K^{-1}), C_p = mass heat capacity (J kg^{-1} K^{-1}), N = rotational speed of screws (revolutions per second, r.p.s.), D_w = barrel diameter (m), D_s = screw diameter (m), T_w = barrel temperature (K), T_m = mass temperature (K), Z = distance along heated length of extruder (m) with Z = 0 at feed entrance, η = bulk viscosity (N s m^{-2}).
This result needs to be corrected for the volumetric chamber filling degree U which is defined as the part of the volume of a C-shaped chamber that is actually filled with material.

$$U = \frac{Q_m}{2nNV_i\rho} \qquad (2)$$

in which Q_m = mass flow (kg s^{-1}), V_i = volume of one C-shaped chamber at the entrance of the extruder (m^3), n = number of screw channels. Multiplication by the factor U is necessary and can be done, although there is no linear relationship between the volumetric filling degree and the surface provided for heat exchange. However, since U is about 0.5 in the feed section of the extruder, the effective heat exchange surface there is also about 0.5 of the total surface available, considering the circular geometry of the extruder. Thus, simple multiplication by U will hold in this case. Including the heating supplied via the screws (van Zuilichem et al., 1983a) and multiplying by the factor U, the following expression for the total heat flow into the bulk, ϕ_{tot}, can be constructed:

$$\phi_{tot} = 11.44\left(\frac{\lambda_m^4 C_p^2}{\eta\rho^3}\right)^{1/6} (D_s^{1/2}D_w + D_s^{3/2})\,(T_w - T_m)\,z\left(\frac{Z^{1/2}}{2nV_i}\right)\left(\frac{Q_m}{N^{1/4}}\right)^{2/3} \qquad (3)$$

Equation (3) can be differentiated with respect to Z to obtain ϕ_{tot}, the heat flow per unit (m) of linear distance from the feed point.
Next, the heat balance

$$\phi'_{tot} = Q_m C_p \Delta T_b \qquad (4)$$

is used, in which T_b is the rise in temperature of the bulk over an arbitrary small distance Δz along the extruder. For ΔZ = 1 cm,

$$\Delta T_b = \frac{0.01\phi'_{tot}}{Q_m C_p} \qquad (5)$$

In this way the temperature development of the bulk along the extruder can be calculated for every centimeter, using the calculation scheme shown in Fig. 4.12. In this way, a temperature profile of the bulk material in the extruder may be obtained (Fig. 4.13). Corresponding heat transfer coefficients, α , are found to be in the region of 1000 W m^{-2} K^{-1}.
The conclusion is that only at high throughputs and high rotational speeds the bulk temperature does not reach the wall temperature. In other cases it may be concluded that the barrel temperature is reached quickly. The extruder is thus seen to be an effective heat exchanger.
This conclusion is confirmed by the experiments reported below.

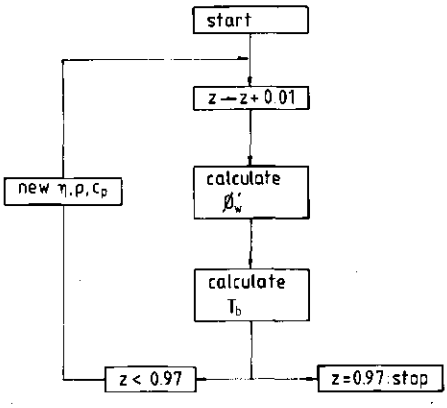

Fig. 4.12 Calculating scheme for temperature development (van Zuilichem et al., 1985)

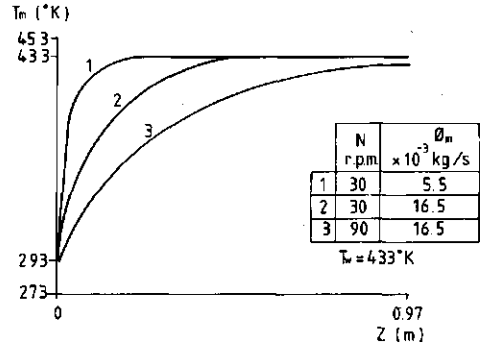

Fig. 4.13 Temperature profiles of bulk in extruder (van Zuilichem et al., 1985)

4.6.2 Time: dissolution of crystals

The time needed for complete dissolution of a sucrose crystal may be expressed as:

$$t = t(dp_0)_T \qquad (6)$$

in which dp_0 = particle diameter at t = 0 m, T = temperature (K). Following Levenspiel (1972), using a material balance and assuming that diffusion of sugarmolecules is the rate-determining step:

$$Q_m = \frac{1}{\pi d_p^2}\frac{dS_s}{dt} = k_c \Delta C \qquad (7)$$

in which S_s = quantity of material in the particle (kg), d_p = particle diameter at time t (m), k_c = mass transfer coefficient (m s^{-1}), ΔC = concentration-difference driving force (kg m^{-3}), Q_m = material flux (kg m^{-2} s^{-1}).

The driving force ΔC, the difference in the concentration of sugar at the surface of the crystal and in the bulk, is

$$\Delta C = C^* - C_{bulk} \qquad (8)$$

in which the concentration at the crystal surface is taken to be C* (the saturation concentration at the prevailing temperature) and C_{bulk} is the concentration of sucrose present in the water. Following the assumption of Janssen (1978) and van Zuilichem et al. (1983b) the bulk material at any linear position is considered to be perfectly mixed radially so that C_{bulk} is uniform in a plane at any z-location.

For the solubility of sucrose in water the Hoynak and Bollenback (1966) formula is the best available:

$$\%\ solubility = \frac{25200}{400 - T} \qquad (9)$$

T=t in units (w/w) and for t=t°C. This formula is expected to be quite reliable and accurate for the higher temperature regions. For the calculation of densities out of the percentages from eq.(9), the sensitive relation 9a is used.

$$C^* = 100/(\%sol/1550 + (100 - \%sol)/1000) \qquad (9a)$$

Based on Honig's (1953) data a solubility coefficient is used in order to correct for the non-ideal nature of the solution. In a solution of two sugars in water, the presence of each sugar hinders the solubility of the other. In case of mixtures of 1:1 sucrose and glucose, the solubility coefficient is 0.85. Table 1 can thus be constructed. It is also necessary to estimate C_{end}, the final concentration of sucrose present in the water. From a mass-balance on a glucose-solids-free basis, i.e. assuming 50% sugar in 10% water, C_{end} = 83.33% or 1241.5 kg m^{-3}.
S_s is calculated from the relationship

$$S_s = \varrho V = \varrho \frac{1}{6} \pi d_p^3 \qquad (10)$$

from which differentiating.

$$dS_s = \varrho \frac{\pi}{2} d_p^2 d(d_p) \qquad (11)$$

Now, k_c can be estimated by comparing the flow pattern around a spherical crystal with a Brian-Hales creep flow, following Sherwood.

Table 4.5 Saturation concentrations of sucrose in water versus temperature (van Zuilichem et al., 1985)

T (°C)	C*(%)	C*(kg m^{-3})
150	84-83	1271.4
145	84-00	1254.8
144	83-67	1248.4
143	83-34	1241.6

et al. (1975). They proposed a relationship between the dimensionless mass transfer number $k_c d_p/2ID$ and the flow characteristic, represented by the Péclet number (Pé):

$$\frac{k_c d_p}{2ID} = (4.0+1.21Pé^{\frac{2}{3}})^{\frac{1}{2}} \qquad (12)$$

in which ID is the diffusion coefficient of sucrose in water at the corresponding temperature (m^2/s)
This expression reduces to $k_c d_p/2 = 2$, when the relative velocity between crystals and bulk material is zero, which is the case assumed here.

Equation (7) can now be written as:

$$\frac{1}{\pi d_p^2} \cdot \frac{\varrho \pi d_p^2 d(d_p)}{2dt} = \frac{ID}{d_p}(C^*-C_{bulk})$$

or

$$d_p d(d_p) = \frac{ID}{\varrho}(C^*-C_{bulk})\,dt \qquad (13)$$

In order to determine the concentration C_{bulk}, use is made of:

$$C_{bulk} = C_{end} - C_{end}\left(\frac{d_p}{d_{p0}}\right)^3 \qquad (14)$$

Equation (13) then becomes:

$$d_p d(d_p) = \frac{ID}{\varrho}(C^* - C_{end}) + \frac{D}{\varrho}\frac{C_{end} d_p^3}{d_{p0}^3} dt \qquad (15)$$

so

$$t = \int_{d_{p0}}^{0} \frac{d_p d(d_p)}{k_1 + k_2 d_p^3} \qquad (16)$$

In the Appendix 4.1 it is shown that the dissolution time t thus becomes:

$$t = A\left(\ln(1+C'^{\frac{1}{3}}) + \ln(C'^{\frac{2}{3}} - C'^{\frac{1}{3}} + 1) + \tan\left(\frac{2}{\sqrt{3}}C'^{\frac{1}{3}} - \frac{1}{\sqrt{3}}\right) - \tan\left(\frac{1}{\sqrt{3}}\right)\right) \qquad (17)$$

where

$$A = \frac{\varrho d_{p0}^2 \sqrt{3}}{54 ID C_{end}^{\frac{2}{3}} (C^* - C_{end})^{\frac{1}{3}}}$$

and in which

$$C' = \frac{C_{end}}{C^* - C_{end}} \qquad (19)$$

To find data for ID , van der Lijn's (1976) results for maltose/water mixtures are used. These data are extrapolated and concentration effects are ignored (Table 4.6). The results of this calculation procedure for this particular combination is shown in Table 4.7.

The conclusion from these calculations is that the two

Table 4.6 Diffusion coefficients for maltose water systems (van Zuilichem et al., 1985)

$T(°C)$	$\mathbb{D}\ (m^2 s^{-1})$
150	$2{\cdot}5 \times 10^{-9}$
145	$1{\cdot}9 \times 10^{-9}$
144	$1{\cdot}8 \times 10^{-9}$
143	$1{\cdot}7 \times 10^{-9}$

Table 4.7 Calculated dissolution times for sugar crystals of different diameter at different temperatures (van Zuilichem et al., 1985)

$T(°C)$	$t\ (s)$	t if $d_{p0} = 0{\cdot}0005\ m$	t if $d_{p0} = 0{\cdot}001\ m$
150	$2{\cdot}43 \times 10^8 d_{p0}^2$	60·7 s	243 s
145	$4{\cdot}97 \times 10^8 d_{p0}^2$	124·2 s	497 s
144	$7{\cdot}42 \times 10^8 d_{p0}^2$	185·5 s	742 s
143	$64{\cdot}00 \times 10^8 d_{p0}^2$	1600·0 s	6400 s
142·96	∞	∞	∞

determining factors are the operating temperature and the size of the sucrose crystals. It is obviously of crucial importance that the temperature of the bulk exceeds the saturation temperature for an 83.33% sucrose solution. The temperature may be lower when water is added or the ratio of syrup to sucrose is increased. However, when water is added, problems may be expected with excess water in the final product.

The size of the crystals is also very important. When the particle size is in the region of 0.1 mm, as is the case with icing sugars, the residence time in the extruder is amply sufficient to obtain a clear product. This calculation also shows that it will be difficult to produce a crystal-free product when normal-sized sugar crystals (d_{p0} = 1 mm) are used.

4.8 Water content

When the product leaves the extruder its pressure drops immediately and water evaporates from it, reducing its temperature. The temperature drop measured in this work is from 150 to 80°C, corresponding to a heat loss of

$$\Delta T \cdot C_p = (150-80)\, C_p = 70 \cdot 2.5 \cdot 10^3 = 1.75 \cdot 10^5 J\ kg^{-1} \qquad (20)$$

Assuming that effectively all this heat goes in evaporating water

from the product, with a latent heat of evaporation of 2250 kJ kg^{-1}, the water evaporated is

$$(1.75 \cdot 10^5) / (2250 \cdot 10^3) = 78\ g\ kg^{-1}\ \text{product} \qquad (21)$$

The initial water content is 100 g kg^{-1} (i.e. 10%) and the final water content is thus 100-78 = 22 g kg^{-1}, or some 2%, which is the desired level in the product.

4.9 Experimental results and conclusions

Tests have been performed with a Cincinnati Milacron CM45 twin screw e-c. (For a drawing of conical screws similar to those used see Fig. 4.14). The results of the test are shown in Table 4.8 T_{end} is the temperature of the bulk material just before it leaves

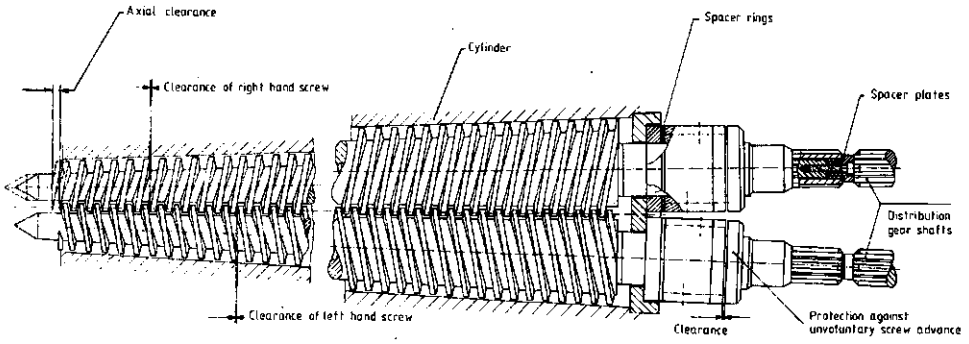

Fig. 4.14 Example of a conical twin screw extruder (Cncinnati) (van Zuilichem et al., 1983)

the extruder. The feed end diameter of the screws is 90 mm, and the die end diameter is 45 mm. The total length of the screws is 970 mm.

The colour of the product was measured by the ICUMSA method number 4, which essentially measures the light extinction at 420 nm. Water content was measured by the Karl Fischer method. Presence of crystals in the product was detected by use of a polarizing microscope. A temperature profile of 130-140-150 means that the barrel temperature is 130°C at the feed section and then rises towards the end of the extruder to 150°C.

These tests confirm that the bulk material indeed attains the

Table 4.8 Results of extrusion tests at different temperatures, throughputs and rotational speeds (van Zuilichem et al., 1985)

T_{barrel} (°C)	ϕ_m (kg h^{-1})	N (r.p.m.)	T_{end}	Colour (I)	Water (%)	Crystallinity
140	20	40	139	54	3·5	–
140	20	60	138·5	43	3·2	–
140	40	60	138	41	3·5	–
130	20	40	129	39	5·3	–
130	20	60	128·5	38	5·0	–
130	40	60	127·5	30	5·1	–
130-140-150	20	40	142	82	3·1	–
130-140-150	20	60	140	58	3·2	–
130-140-150	40	60	136	47	3·2	–

wall temperature. The product did not contain any sugar crystals, and there was little coloration.
The water content of the product is low, considering that no special water-removal action was undertaken. If such was done, even lower values could be reached.

It is clear that the important factors are:
(1) for the dissolution of the crystals:
- the barrel temperature
- the size of the crystals at the entrance of the extruder

(2) for the colour of the product:
- the final bulk temperature attained

(3) the water content of the product
- the final bulk temperature attained
- any special provision for removal of water

References

Honig, P. (1953). Principles of Sugar Technology, Elsevier, Amsterdam.

Hoynak, P.X., Bollenback, G.N. (1966). This is Liquid Sugar, Refiners Syrup Inc., New York.

Jager, Th. (1983). Residence time distribution in a twin screw extruder. Internal Research Report, Agricultural University, Wageningen.

Janssen, L.B.P.M. (1978). Twin-screw Extrusion, Elsevier, Amsterdam-New York.

Levenspiel, O. (1972). Chemical Reaction Engineering, Wiley and Sons, New York.

Van der Lijn, J. (1976). Simulation of heat and mass transfer in spray drying. Dissertation, Agricultural University, Wageningen.

Shallenberger, R.S., Birch, G.G. (1975). Sugar Chemistry, AVI Publishing Co., Westport, Connecticut.

Sherwood, T.K., Pigford, R.L., Wilke, C.B. (1975). Mass transfer, McGraw Hill, New York.

van Zuilichem, D.J., Alblas, B., Reinders, P.M., Stolp, W. (1983a). A comparative study of the operational characteristics of single and twin screw extruders. Proceedings Cost '91, Athens (concluding seminar).

van Zuilichem, D.J., Stolp, W., Janssen, L.B.P.M. (1983b). Engineering aspects of single and twin screw extrusion of

biopolymers. J. Food Engng., 2, 157-175.

van Zuilichem, D.J., Tempel, W.J., Stolp, W., K. van 't Riet (1985). Production of high boiled sugar confectionery by extrusion cooking of sucrose/liquid glucose mixtures. J. Food Engng., 4, 37-51.

van Zuilichem, D.J., Stolp, W., van 't Riet, K., (1985). Twin screw rextrusion cooking of sugar doughs. I.C.E.F. IV., Edmonton.

van Zuilichem, D.J., Stolp, W., (1976). Theoretical aspects of extrusion of starch based products in a direct extrusion cooking process. Lecture at: Zentral fachschule der Deutschen Süsswarenwirtschaft, Solingen.

van Zuilichem, D.J., Stolp, W., (1982a). Survey of the present extrusion cooking techniques in the food and confectionery industry. Lecture at: Zentralfachschule der Deutschen Süsswarenwirtschaft, Solingen.

van Zuilichem, D.J., Stolp, W., (1982b). Extrusion of sucrose crystals. Lecture at: Zentralfachschule der Deutschen Süsswarenwirtschaft, Solingen.

van Zuilichem, D.J., Stolp, W., (1981). Standortsbestimmung und Ausblicke über de Einsatz von Koch-Extrudern zur Herstellung von Zuckerwaren. Lecture at: Zentralfachschule der Deutschen Süsswarenwirtschaft, Solingen.

Notation

ϕ_m'	Heat flux per m extruder length	[J/sm]
λ_m	Heat conductivity	[J/smK]
C_p	Heat capacity	[J/kgK]
ρ	Density of the mixture	[kgm^{-3}]
η	Dynamic Viscosity	[Nsm^{-2}]
R_w	Barrel inner diameter	[m]
R_s	Screw diameter	[m]
T_w	Barrelwall temperature	[K]
T_m	Productmass temperature	[K]
Q_m	Throughput	[kg/s]
Z	Coordinate alongside barrel	[m]
m	Number of extruder screws	[-]
V_{in}	Volume of C-shaped chamber	[m^3]
N	Number of revolutions	[s^{-1}]
ϕ_m	Throughput	[kg/s]
ΔT	Temperature rise of product mass	[K]
ΔZ	Small increase of coordinate Z	[m]
t	Dissolution time	[s]
R_0	Sucrose crystaldiameter at Z=0	[m]
D	Coefficient of diffusion	[m^2/s]
C_{end}	Final concentration given as density	[kg/m^3]
C^*	Maximum solubility at given temperature	[kg/m^3]
C'	$C_{end}/(C^*-C_{end})$	[-]
x_s	Molecular fraction	[-]
T	Final product temperature	[K]
%sol	Solubility of sucrose in water	[-]

Appendix 4.1

$$t = \int_{d_{p0}}^{0} \frac{d_{p0}\,\mathrm{d}(d_{p0})}{k_1 + k_2 d_{p0}^3} = \frac{1}{k_1}\int \frac{d_{p0}\,\mathrm{d}(d_{p0})}{1 + \frac{k_2}{k_1} d_{p0}^3} \quad (16)$$

$$\alpha = d_{p0}\left(\frac{k_2}{k_1}\right)^{1/3} \rightarrow t = \frac{1}{k_2^{2/3} k_1^{1/3}} \int \frac{\alpha\,\mathrm{d}\alpha}{1+\alpha^3}$$

$$(1+\alpha)^3 = (1+\alpha) \times (1-\alpha+\alpha^2)$$

$$\frac{\alpha}{(1+\alpha)(\alpha^2-\alpha+1)} \rightarrow t = \frac{1}{k_2^{2/3} k_1^{1/3}}\left(\int \frac{-\frac{1}{3}\,\mathrm{d}\alpha}{(1+\alpha)} + \int \frac{(\frac{1}{3}\alpha+\frac{1}{3})}{(\alpha^2-\alpha+1)}\,\mathrm{d}\alpha\right)$$

$$= \frac{-\frac{1}{3}}{(1+\alpha)} + \frac{(\frac{1}{3}\alpha+\frac{1}{3})}{(\alpha^2-\alpha+1)}$$

$$t = \frac{1}{k_2^{2/3} k_1^{1/3}}\left(\int \frac{-\frac{1}{3}\,\mathrm{d}\alpha}{(1+\alpha)} + \int \frac{\frac{1}{6}(2\alpha-1)\,\mathrm{d}\alpha}{\alpha^2-\alpha+1} + \int \frac{\frac{1}{2}\,\mathrm{d}\alpha}{\alpha^2-\alpha+1}\right)$$

$$t = \frac{1}{k_2^{2/3} k_1^{1/3}}\left(\int \frac{-\frac{1}{3}\,\mathrm{d}\alpha}{(1+\alpha)} + \int \frac{\frac{1}{6}(2\alpha-1)\,\mathrm{d}\alpha}{\alpha^2-\alpha+1} + \int \frac{\frac{1}{2}\,\mathrm{d}\alpha}{(\alpha-\frac{1}{2})^2+\frac{3}{4}}\right)$$

$$t = \frac{1}{k_2^{2/3} k_1^{1/3}}\left(\int \frac{-\frac{1}{3}\,\mathrm{d}\alpha}{(1+\alpha)} + \int \frac{\frac{1}{6}(2\alpha-1)\,\mathrm{d}\alpha}{\alpha^2-\alpha+1} + \frac{\frac{4}{3}\cdot\frac{1}{2}\cdot\mathrm{d}\alpha}{\frac{2}{\sqrt{3}}\cdot(\alpha-\frac{1}{2})^2+1}\right)$$

$$t = \frac{1}{k_2^{2/3} k_1^{1/3}}\left(\int \frac{-\frac{1}{3}\,\mathrm{d}\alpha}{(1+\alpha)} + \int \frac{\frac{1}{6}(2\alpha-1)\,\mathrm{d}\alpha}{\alpha^2-\alpha+1}\right.$$

$$+\int \frac{\frac{1}{3}\sqrt{3}\cdot \mathrm{d}\left(\frac{2}{\sqrt{3}}\cdot(\alpha-\frac{1}{2})^2\right)}{\frac{2}{\sqrt{3}}\cdot(\alpha-\frac{1}{2})^2+1}\Bigg)$$

$$t=\frac{1}{k_2^{2/3}k_1^{1/3}}\left(-\tfrac{1}{3}\ln(1+\alpha)+\tfrac{1}{6}\ln(\alpha^2-\alpha+1)+\tfrac{1}{3}\sqrt{3}\tan\left(\frac{2}{\sqrt{3}}(\alpha-\tfrac{1}{2})\right)\right)$$

$$\alpha=\frac{d_p}{d_{p0}}\left(\frac{C_{end}}{C^*-C_{end}}\right)^{1/3}$$

$$C'=\frac{C_{end}}{C^*-C_{end}}$$

$$k_1=\frac{\mathbb{D}}{\rho}(C^*-C_{end})$$

$$k_2=\frac{\mathbb{D}}{\rho}\left(\frac{C_{end}}{d_{p0}^3}\right)$$

$$\rightarrow\quad t=\frac{\rho d_{p0}^2\cdot\sqrt{3}}{54\mathbb{D}C_{end}^{2/3}\cdot(C'-C_{end})^{1/3}}\cdot\left(\ln\left(1+\frac{d_p}{d_{p0}}C'^{1/3}\right)+\ln\left(\frac{d_p^2}{d_{p0}^2}C'^{2/3}-\frac{d_p}{d_{p0}}C'^{1/3}+1\right)+\tan\left(\frac{2}{\sqrt{3}}\frac{d_p}{d_{p0}}C'^{1/3}-\frac{1}{\sqrt{3}}\right)+K\right)$$

K is now found by using the boundary values, $t=0$, $d_p=d_{p0}$

$$K=\frac{\rho d_{p0}^2\sqrt{3}}{54\mathbb{D}C_{end}^{2/3}(C^*-C_{end})^{1/3}}\left(\ln(1+C'^{1/3})+\ln(C'^{2/3}-C'^{1/3}+1)+\tan\left(\frac{2}{\sqrt{3}}C'^{1/3}-\frac{1}{\sqrt{3}}\right)\right)$$

So at the desired final condition, when $d_p = 0$, t becomes:

$$t = \frac{\rho d_{p0}^2 \sqrt{3}}{54 \mathbb{D} C_{end}^{2/3} (C^* - C_{end})^{1/3}} \left(\ln 1 + \ln 1 + \tan\left(-\frac{1}{\sqrt{3}}\right)\right)$$

$$+ \frac{\rho . d_{p0}^2 \sqrt{3}}{54 \mathbb{D} C_{end}^{2/3} (C^* - C_{end})^{1/3}} \left(\ln (1 + C'^{1/3}) + \ln (C'^{2/3} - C'^{1/3} + 1) \right.$$

$$\left. + \tan\left(\frac{2}{\sqrt{3}} C'^{1/3} - \frac{1}{\sqrt{3}}\right)\right)$$

from which:

$$\dot{t} = \frac{\rho . d_{p0}^2 \sqrt{3}}{54 \mathbb{D} C_{end}^{2/3} (C^* - C_{end})^{1/3}} \left(\ln (1 + C'^{1/3}) + \ln (C'^{2/3} - C'^{1/3} + 1) \right.$$

$$\left. + \tan\left(\frac{2}{\sqrt{3}} C'^{1/3} - \frac{1}{\sqrt{3}}\right) - \tan\left(\frac{1}{\sqrt{3}}\right)\right)$$

CHAPTER 5

MODELLING OF HEAT TRANSFER IN A CO-ROTATING TWIN SCREW FOOD EXTRUDER

ABSTRACT

The main problem in modelling heat transfer in twin screw food extruders, is to include all variables in a complete analysis. However, the solutions found in the various models, concern mainly the metering section which is assumed to contain only molten material. To predict the heat transfer process for food processing in the feed and compression section is far more complex and well fitting models for these sections have not been developed yet.
The heat transfer model suggested gives, through combination of existing theories, an extension towards predicting the performance of food extruders.
The model gave promising results, when tested on a APV Baker Perkins twin screw food extruder. Wheat flour was used as raw material to acquire the data.

THIS CHAPTER IS BASED UPON THE PUBLICATIONS:

van Zuilichem, D.J., van der Laan, E., Kuiper, E. (1990). The development of a heat transfer model for twin screw extruders, J. of Food Engng.,11,187-207.

van Zuilichem, D.J., van der Laan, E. Janssen, L.P.B.M (1991). submitted for publication.

van Zuilichem, D.J. van der Laan, E., Stolp, W.(1991), Modelling of heat transfer in a co-rotating twin screw extruder, Applied Food Extrusion Science, Edt. Kokini, Ho, Karwe.

5.1 Introduction

Extrusion cooking processes normally involve mixing, melting and the application of intensive energy to the product at high pressures within a short period of time. This results in varying degrees of starch modification, protein denaturation and other physico-chemical reactions. When the product leaves the die, the temperature and pressure drop abruptly and the product expands.

There are two major types of extruders: the single-screw and twin-screw extruder. The latter type is divided into co-rotating and counter rotating depending on how one screw rotates in relation to the other.

Counter-rotating intermeshing twin-screw extruders are positive displacement-pumps which form closed 'C'-shaped chambers between the screws while minimizing the mixing and the backflow due to pressure build-up. In co-rotating extruders, the material is transported steadily from one screw to the other. The flow mechanism can be described by a combination of dragflow and positive displacement caused by the pushing action of the screw-set in the intermeshing region. The co-rotating type generally works at a higher screw speed than the counter-rotating twin screw extruder.

Although sophisticated screw configurations with as many as eight or nine screw sections exist nowadays, one can basically identify three different screw sections:

(1) the feed section; which ensures that sufficient solid material is transported into the screw;
(2) the compression section; in which the material is heated and worked into a dough mass during passage through this section;
(3) the metering section; in which the screw configuration feeds the die constantly with material. The viscous dissipation of mechanical energy is typically large in this section so that the temperature increases rapidly. The high

shear rate in the screw also enhances internal mixing to produce temperature homogeneity in the extruder.

5.2 The basic model for a single screw extruder

It is interesting to look at the flow patterns inside an extruder as they provide an insight into the mechanism of mixing, and facilitate estimation of residence time distributions, prediction of flow rates, pressure drop and power consumption (Bruin et al. 1978). Fig. 5.1 gives an outline sketch of the flow channel in

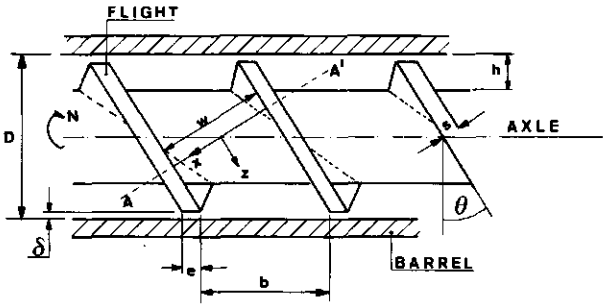

1. SECTION OF EXTRUDER WITH DEFINITION OF GEOMETRY

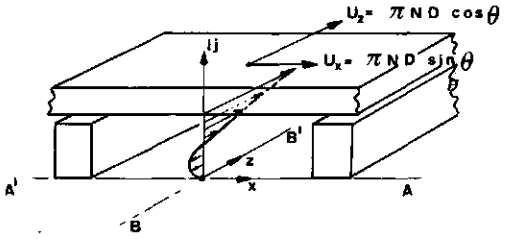

2. SIMPLIFIED FLOW GEOMETRY (SECTION AA')

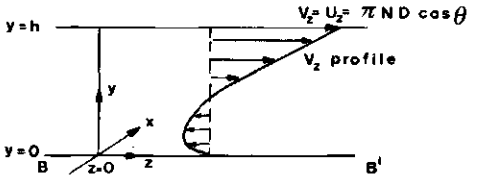

3. FLOW PROFILE IN COORDINATE SYSTEM USED (SECT. BB')

Fig. 5.1 Definition of geometry and simplified flow geometry for a single screw extruder (Bruin et al., 1978)

a single screw extruder. For simplification, the barrel is assumed to be rotating around the stationary screw. The basic problem in describing flow patterns inside the extruder is that the flows in the compression and metering section are non-newtonian and non-isothermal. Therefore the equation of motion as well as the equation of energy should be solved to obtain the exact flow patterns. The general procedure is indicated schematically in Fig. 5.2 The set of equations can only be solved with some approximations. The most important are the assumptions of steady state, negligible inertia and gravity forces and of fully developed incompressible fluid flow. With these assumptions the flow in a slit of height h and width W, with one wall moving with a velocity πND and against a pressure gradient dp/dz is determined. The velocity of the barrel wall can now be divided into two components: in the cross channel direction: $U_x = \pi ND\sin\theta$ and in the channel direction $U_y = \pi DN\cos\theta$.

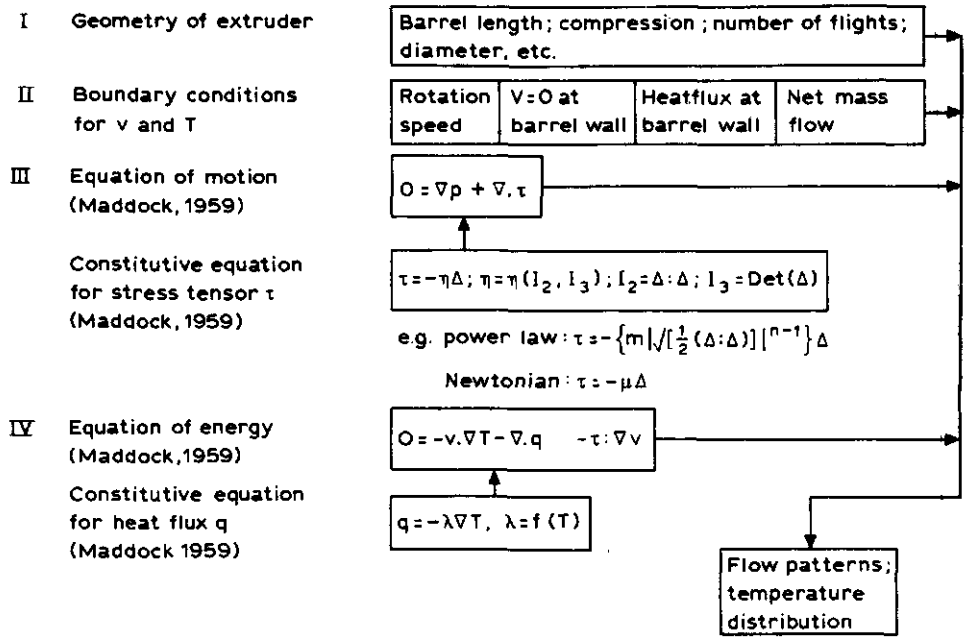

Fig. 5.2 Schematic approach for calculation of flow patterns in an extruder (Bruin et al., 1978)

The velocity distributions in the x and z-directions can be

calculated seperately and combined to give the total flow profile. The flow in the z-direction is the result of two driving forces: the drag caused by the z component of the relative velocity of the barrel (U_z) and the pressure gradient in the z-direction because of the gradual pressure build up in the z-direction. With these assumptions and simplifications the solution of the equation of motion and the energy equation is possible. The most simple case arises when the material behaves as a newtonian fluid with temperature-independent viscosity and

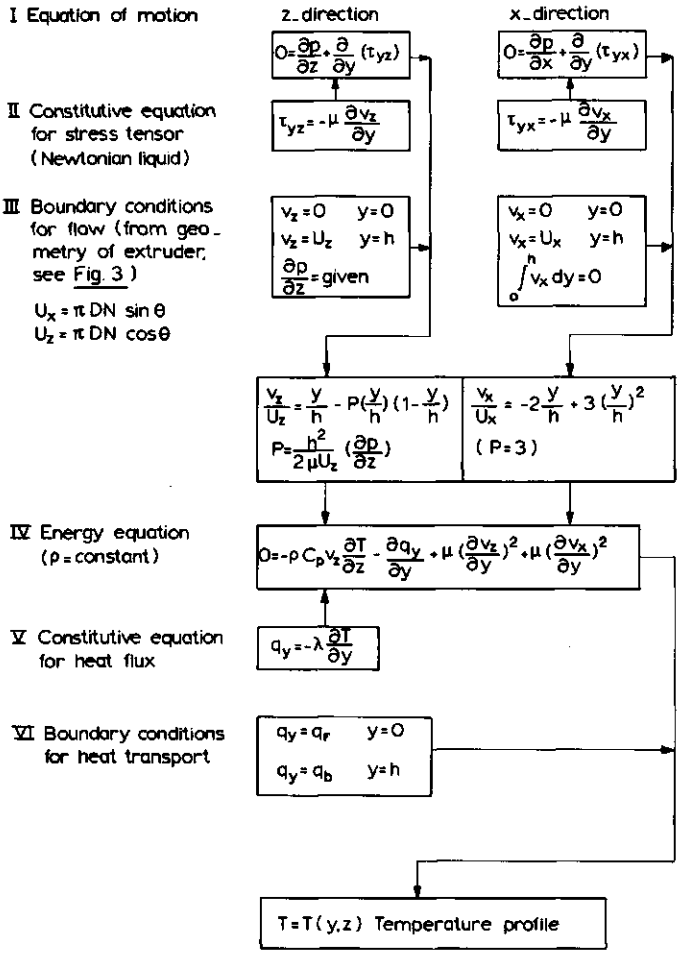

Fig 5.3 Calculation scheme for flow patterns in a single screw extruder for an incompressible Newtonian fluid with constant heat conductivity and viscosity (Bruin et al., 1978)

when the velocity components in the y-direction near the flights are neglected. The latter assumption is a reasonable approximation for shallow channels (h/w<0.1). Fig. 5.3. illustrates how velocity profiles could be derived and successively the heat flux at the barrel surface and the screw root can be calculated. It is interesting to note that the equation of energy is fairly difficult to solve even for this simple rheological behaviour because of the convection term. Only when adiabatic extrusion is assumed and temperature gradients in the y-direction are assumed to be negligible, a relatively simple result can be obtained.

5.3 Various models

5.3.1 Introduction

The main problem in modelling heat transfer is to include all variables in a complete analysis. This appeared to be impractical because of the computational effort involved. In many practical cases, however, some of the variables can be neglected as being unimportant for the particular set of conditions under consideration. This means that it is possible to make some assumptions and to derive a solution which is useful under certain operating conditions. Care has to be taken, however, that the model should not be used for an unjustified extrapolation to other circumstances.

The solutions found in the various models concern mainly the metering section which is assumed to contain only molten material. This has been solved for a complex, three dimensional, non-isothermal, non-newtonian flow of viscous temperature sensitive fluid (Martin et al., 1969). It is far more complex to predict the heat transfer process in the feed and compression section and well- fitting models for these sections have not yet been found.

In practice, most food materials for extrusion show a non-

Newtonian rheological behaviour. Several authors have analyzed such situations (Griffith 1962, Pearson 1966 , Yankov 1978, Yacu (1985)). They produced models which gave a better understanding of the extrusion of non-Newtonian materials. Griffith used a numerical analysis to solve the differential equations for fully developed velocity and temperature profiles for single screw extrusion of power-law fluids. Pearson solved the equations of motion and energy for transverse channel flow and a superimposed temperature profile for power-law fluids. Results were presented in terms of dimensionless parameters of output, pressure and the Brinkman numbers. Yankov used finite-difference techniques to solve the equations of motion for non-Newtonian fluids, where he assumed that temperature did not change along the channel. One could, however,doubt the accuracy of these models because of the assumptions used in solving the several equations. This is especially true when the power-law approximation for the food behaviour was used. Yacu gave the most thorough description of non-Newtonian behaviour. With some alterations, this approach is partly incorporated in the LU model which is discussed in section 5.6

5.3.2 Dimensionless numbers

To describe properly the heat transfer in an extruder, is it useful to introduce several dimensionless numbers. With these numbers it is often possible to see whether particular assumptions are correct. The following dimensionless numbers are most frequently used in heat transfer analyses:

Peclet: The ratio of heat transfer by convection to heat transfer by conduction;

$$Pe = \frac{UH}{a} \qquad (1)$$

Nusselt: The ratio of the total heat transfer to the heat transfer by conduction;

$$Nu = \frac{\alpha H}{\lambda} \qquad (2)$$

Reynolds: the ratio of the inertia forces to the viscous forces;

$$Re = \frac{UH}{\mu}\varrho \qquad (3)$$

Graetz: the ratio of heat convection and heat conduction. In an extruder this means the ratio between heat transferred by the food flux and the heat transferred through the barrel to the extrudate;

$$Gz = \frac{aL}{UH^2} \qquad (4)$$

Brinkman: The ratio of heat due to conversion of mechanical energy by viscous dissipation to the heat due to conductive heat transfer;

$$Br = \frac{\mu U^2}{\lambda \Delta T} \qquad (5)$$

5.3.3 Heat transfer coefficient

Knowledge of the heat transfer encountered in food extrusion is essential for the scale-up and design of food extruders and the associated temperature control systems. Apart from the calculation used in the penetration theory (see section 5.4) only a small number of relevant papers on heat transfer coefficients in food extrusion have been found. Because of the importance of the heat transfer coefficient, two papers are considered in more detail. Mohamed et al. (1988) analyzed the Greatz-Nusselt problem for non-newtonian flow with viscous dissipation along the channel of a single screw extruder. A theoretical model was developed to study the effects of material properties, geometry, and operating conditions on heat transfer coefficients in single screw food

extruders for both heating and cooling with constant barrel temperature. Mohamed et al. found on an APV Baker MPF 50 extruder that for Brinkman numbers less than 40, viscous heating effects were dominant. For Greatz numbers less than 333 the viscous dissipation overruled the cooling capacity of the extruder. They solved numerically the energy and momentum equation to determine the temperature and velocity profiles, which were then used to determine the Nusselt number. From the Nusselt number they calculated the heat transfer coefficient, which at the fluid barrel interface was defined as:

$$\alpha (T-T_b) = -\lambda \frac{dT}{dz} \qquad (6)$$

In dimensionless terms this equation can be written as:

$$\alpha\{T-(T_0-T_b)\,T^*\} = \lambda \frac{T_0-T_b}{H} \frac{\partial T^*}{\partial \bar{z}} \qquad (7a)$$

which results in:

$$Nu(1-T^*) = \frac{\partial T^*}{\partial \bar{z}} \qquad (7b)$$

where

$$T^* = \frac{(T_0-T)}{(T_0-T_b)} \qquad and \quad \bar{z} = \frac{z}{H} \qquad (8)$$

Using multiple regression, Levine & Rockwood (1986) found a dimensionless correlation for the heat transfer coefficient. Their findings were based on the model of Tadmor & Klein (1970) and they assumed that the viscosity could be described by the power law. They concluded that the heat transfer coefficient can be described as a dimensionless equation having the following form:

$$Nu = \left(\frac{Pe\ H}{L}\right)^{k_1} (Br)^{k_2} \qquad (9)$$

and multiple regression gave:

$$Nu = 2.2Br^{0.79} \quad (10)$$

The correlation coefficient obtained was 0.88. The standard error of estimate was calculated as 12.4% of the mean value. Addition of the dimensionless group containing the Peclet number gave virtually no improvement in the percentage of variance explained. As a result, the statistical significance of the correlation was actually reduced; therefore this factor was not included in the equation.

5.3.4 Theory of Tadmor and Klein (1970)

Using the qualitative description of Maddock (1959) of the two phase flow in the melting zone, a more thorough investigation of this zone was undertaken. According to Maddock, the solid particles in contact with the hot surface of the barrel partially melt and smear a film of molten polymer over the barrel surface. This film, and probably some particles, are dragged along the barrel surface, and when they meet the advancing flight, they are mixed with previously molten material. The molten material collects at an area at the pushing flight (meltpool), whereas the forward portion of the channel is filled with solid particles. The width of the solid bed, X, gradually decreases toward the outlet of the screw. The melting process ends when the solid bed disappears. In developing a melting model for the metering section, the following assumptions were used:

(1) The most important melting mechanism takes place between the hot barrel and the solid bed;
(2) The influence of pressure gradients on the velocity profiles is negligible (highly viscous flow in very thin layers);
(3) The solid bed is semi-infinite;
(4) Heat convection is negligible;
(5) The velocity of the solid bed in the channel direction is constant;
(6) Screw and barrel temperature remain constant in the melting zone;

(7) The channel depth in the melting zone is constant;

Based on the observations of Maddock, Tadmor & Klein (1970) proposed a model which provided the equations that are required to calculate the length of the melting zone. This length depends on the physical properties of the polymer and operating conditions. The only melting mechanism takes place between the hot barrel and the solid bed. The molten mass is transported by the movement of the barrel relative to the solid bed, until it reaches a screw flight. The leading edge of the advancing flight scrapes the melt of the barrel surface and forces it into a meltpool. This meltpool needs space and moves into the solid bed; the solid bed deforms and its width decreases. It is assumed that the meltfilm thickness profile does not change in the melting zone and that the meltfilm thickness equals the flight clearance. After these assumptions and those mentioned before, analytical calculations became possible.In the past, special attention was given to the assumption of a constant meltfilm thickness because of the important role of this film thickness on the heat flux and therefore on the calculated melting length. Shapiro (1973) and Vermeulen et al. (1971) concluded that the meltfilm thickness cannot be constant and will increase. This decreases the heatflux to the solid bed and, consequently, increases the melting length. Is it important to note that the effect of viscous dissipation on the channel temperature distribution together with the flow and heat transfer in the downstream direction were completely neglected in Tadmor's model.

Over the years Tadmors model has been changed, improved and adjusted by himself and many other authors, to incorporate new developments and calculation methods with computers. A new discussion originated from the observations of Dekker (1976). His findings refuted the remaining basic concept of Tadmor's model,namely that of the deforming solid bed and the existence of a meltpool. Lindt (1976) analysed this situation and proposed another basic model. Tadmor's model and Lindt's model can be regarded as the two extremes in the field of melting zone model-

ling. Between these two, many other models for melting in the metering zone, of varying accuracy, have been published.

5.4 Boundary layer theory in the pump zone

In 1953, Jepson considered what is called the 'wiping effect for heat transfer in the pump zone': After the flight of the rotating screw has wiped a certain area on the inner barrel surface, a fresh layer of polymer becomes attached to the same region and remains there for, approximately, one revolution. The amount of heat penetrating into this layer during that time by pure conductive heat transfer is then removed with the polymer layer

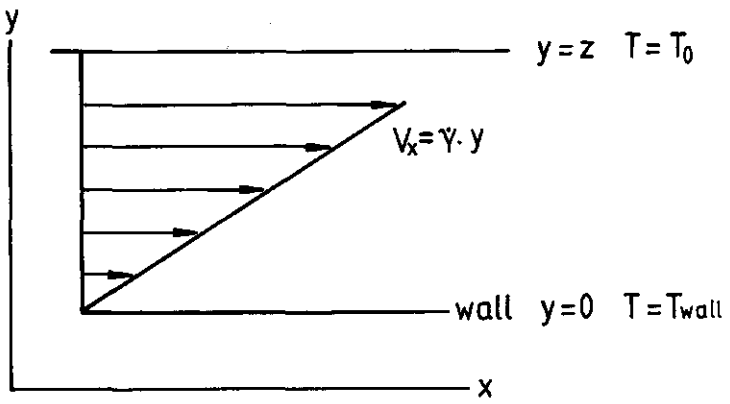

Fig. 5.4 Boundary layer (Beek, 1974)

and is thought to be homogeneously distributed throughout the bulk of the polymer in the screw channel. This process of heat penetration during extrusion can often be considered as a non-stationary penetration in a semi-infinite medium. The heat balance is given by:

$$\rho Cp\frac{\partial T}{\partial t} = \lambda\left(\frac{\partial^2 T}{\partial x^2} + \frac{\partial^2 T}{\partial y^2} + \frac{\partial^2 T}{\partial z^2}\right) \qquad (11)$$

or, in one dimension:

$$\frac{\delta T}{\delta t} = a\frac{\delta^2 T}{\delta y^2} \qquad \textbf{(11b)}$$

If the penetration depth of heat is much smaller than the height of the extruder channel, the solution of equation (11) is the well known error function:

$$\frac{T_w - T}{T_w - T_b} = \frac{2}{\sqrt{\pi}} erf\left(\frac{x}{2\sqrt{at}}\right) \qquad \textbf{(12)}$$

from which a time averaged heat transfer coefficient over one revolution time can be derived for a screw with m threat starts and a revolution rate of N RPS:

$$\langle\alpha\rangle = 2\sqrt{\frac{\lambda\rho C_p mN}{\pi}} \qquad \textbf{(13)}$$

Another approach is to consider the heat transfer to a semi infinite flowing medium for which the energy balance can be approximated by:

$$V_x\frac{\partial T}{\partial x} = a\frac{\partial^2 T}{\partial y^2} \qquad \textbf{(14a)}$$

with boundary conditions:

$x < 0$		$T = T_0$	
$x > 0$	$y \to \infty$	$T = T_0$	**(14b)**
$x > 0$	$y = 0$	$T = T_w$	

In order to solve this equation it is assumed that the velocity may be linearized over the thickness of the thermal boundary layer (Leveque solution) to:

$$V_x = \dot{\gamma} \cdot y \qquad \textbf{(15)}$$

y=0 indicates the location on the barrel wall at uniform temperature T_w.

The temperature profile in the thermal boundary layer is approximated by a parabolic function:

$$\frac{T-T_0}{T_w-T_0} = \left(1-\frac{y}{\delta}\right)^2 \qquad (16)$$

where δ is the (unknown) boundary layer thickness. Introducing equations 15 and 16 in equation 14a gives after integration an expression for the boundary layer thickness:

$$\delta = \left(\frac{36ax}{\dot{\gamma}}\right)^{\frac{1}{3}} \qquad (17)$$

and for the heat flux:

$$\phi_w' = 2\lambda\left(\frac{36ax}{\dot{\gamma}}\right)^{-\frac{1}{3}} (T_w-T_0) \qquad (18)$$

with a heat transfer coefficient on location x:

$$\alpha_x = 2\lambda\left(\frac{36ax}{\dot{\gamma}}\right)^{-\frac{1}{3}} \qquad (19)$$

5.5 Extruder model by Yacu

The first simulation model of a twin-screw corotating food extruder, was developed by Yacu (1983). The extruder is divided into three main sections:

- solid conveying zone
- melt pumping zone
- melt shearing zone

The temperature and pressure profiles are predicted for each section separately. The following assumptions were made:

(1) The rheology of the molten material is described by a non-Newtonian, non-isothermal viscosity model taking into account the effect of moisture and fat content.The extruder is operating under steady state conditions.

(2) Steady state behaviour and uniform conditions exist.

(3) The melt flow is highly viscous and in the laminar flow regime.
(4) Gravity effects are negligible and ignored.
(5) The screw is assumed to be adiabatic.
(6) The degree of cooking is assumed to be uniform over the cross-section.

5.5.1 Solid conveying section

Twin screw extruders for food processing, operate mostly under starved feed conditions and the throughput is determined by the feeding unit, the extruder's screw speed and torque. Therefore the screws in the feeding section are partially filled and no pressure is developed. The dissipation of mechanical energy is negligible because of these conditions. Heat is transferred by conduction from the barrel to the food material.

To simplify the analysis and taking into account that mixing within the channel is reasonably good in co-rotating extruders, the heat transfer is assumed to be controlled omly by convection. A pseudo heat transfer coefficient U_s is used to replace the characteristic conductivity property of the granular material in the feed section.

Constructing a heat balance across an element normal to the axial direction and solving for T with
the boundary condition at x=0, $T=T_f$ results in the equations:

$$Q_m C_{ps} T + F U_s A (T_b - T)\, dx = Q_m C_{ps} (T + dT) \qquad (20)$$

from which follows:

$$T = T_b - (T_b - T_f)\, e^{\frac{-F U_s A X}{Q_m C_{ps}}} \qquad (21)$$

The heat transfer coefficient U_s to the powder in the feedzone, for practical reasons estimated as the heat transfer coëfficient based on the penetration theory, would give irrealistic values. Phase discontinuity and the existence of additional resistance

to heat transfer between the solid particles, are the main reasons for this.

5.5.2 Melt pumping section

In this section the change of the material from solid food-powder to a fluid melt is assumed to take place abruptly. Martelli

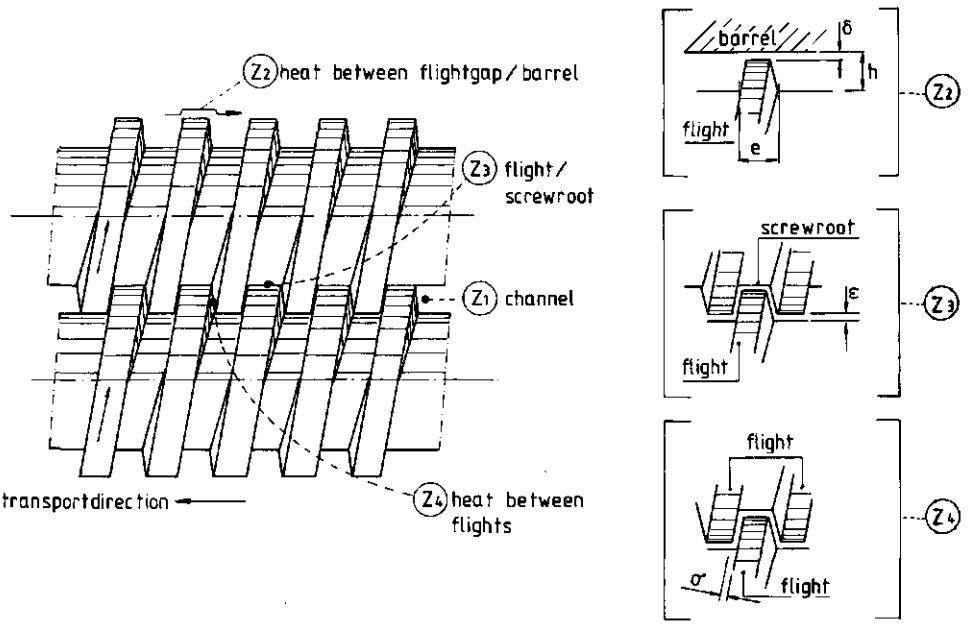

Fig. 5.5 Leakage flows in a co-rotating twin screw extruder (van Zuilichem et al., 1991)

assumed that the energy was dissipated within the channel and due to the leakage flows in the various gaps (See Fig. 5.5). He defined four locations where energy was converted:

- within the channel:

$$Z_1 = \frac{\pi^4 D_e^3 D \tan\varphi_P}{2h} \mu N^2 \qquad (22)$$

in which h is the channel depth (m) and D_e the equivalent twin

screw diameter (m). (see Figure 5.5 for the different cross sections)

- between the flight tip of the screw and the inside surface of the barrel:

$$Z_2 = \frac{\pi^2 D^2 e C_e}{\delta} m^* \mu N^2 \qquad (23)$$

where m^* stand for number of screw flights, e is the screw flight tip width in axial direction (m) and C_e stands for the equivalent twin screw circumference (m).

- between the flight tip of one screw and the bottom of the channel of the other screw:

$$Z_3 = \frac{8\pi^2 I^3 e}{\varepsilon} m^* \mu N^2 \qquad (24)$$

in which ε gives the clearance between fligth tip and channel bottom of two opposite screws and I stands for the distance between the screw shafts (m).

- between the flights of opposite screws parallel to each other:

$$Z_4 = \frac{\pi^2 I^2 h \sqrt{(D^2 - I^2)}}{2\sigma} m^* \mu N^2 \qquad (25)$$

where σ indicates the clearance between flights of opposite screws parallel to each other.

The total energy converted per channel per screw turn was therefore expressed as:

$$Z_p = Z_1 + Z_2 + Z_3 + Z_4 = C_{1p} \mu_p N^2 \qquad (26)$$

Where C_{1p} can be defined as the pumping section screw geometry-factor and is described with:

$$C_{1p}=\frac{\pi^4 D_e^3 D\tan\varphi_p}{2h}+m^*\left(\frac{\pi^2 D e^2 C_e}{\delta}+\frac{8\pi^2 I^3 e}{\varepsilon}\frac{\pi^2 I^2 h\sqrt{(D^2-I^2)}}{2\sigma}\right) \quad (27)$$

Because the length of a screw channel per screw turn equals $\pi D\tan\varphi_p$ the average amount of heat generated within an element of thickness dx can therefore be evaluated as:

$$dZ_p = C_{1p}\mu_p N\frac{dx}{\pi D\tan\varphi_p} \quad (28)$$

The overall shear rate on the product, while passing through the pumping zone, including the amount taken up by leakage flows, can be estimated by:

$$\dot{\gamma}_p=N\frac{\sqrt{C_{1p}}}{V_p} \quad (29)$$

The viscosity of the product, μ_p, is described by the power-law equation and is depending on shear rate($\dot{\gamma}$), temperature(T), moisture content (MC) and fat content (FC):

$$\mu_p=\mu_0\dot{\gamma}^{-n_1}\ e^{-a_1(MC-MC_0)}\ e^{-a_2FC}\ e^{-b_1\Delta T} \quad (30)$$

This rheology model is developed for a wheat starch. The various indices are determined by multiple regression analysis to fit the rheology model.

Constructing a heat balance across an element in the melt pumping zone, coupled with the boundary condition: $T=T_m$ at $X=X_m$, gives the relation:

$$QC_{vm}T+\alpha A(T_b-T)\,dx+\frac{C_{1p}\mu_{2p}N^2e^{-b_1T}}{\pi D\tan\varphi_p}dx=QC_{vm}(T+dT) \quad (31)$$

or

$$\frac{dT}{dX} = C_{2p}\, e^{-b_1 T} + C_{3p}\,(T_b - T) \qquad (32)$$

where

$$C_{2p} = \frac{C_{1p}\mu_p N^2}{\pi D \tan\varphi_p Q_m C_{pm}} \qquad (33)$$

and:

$$C_{3p} = \frac{FA}{Q_m C_{pm}} \qquad (34)$$

This first order, non-linear differential equation can be solved by integrating it numerically using the Simpson 3/8 rule.
One of the assumptions made by Yacu (1983), was that the moment the mass enters the melt pumping section, the screws become completely filled. In his calculation the mass is subjected to the total shear stress. However, most twin screw extruders are starved fed which results in a partially low filling degree. It would therefore be reasonable to conclude that the shear the product receives is lower than Yacu assumes.

5.6 LU Model

The LU model , developed by Van Zuilichem et. al. (1983, 1985) and later also improved by Van Zuilichem et. al. (1990), has been extended and made suitable for computer calculations. A unique feature of this model is that it calculates the total transferred heat in the extruder for every position along the screw axis. Compared to the model of Yacu (1985), the LU model gives an approximation of the heat transferred from the barrel to the foodmaterial, based on boundary layer theory using the Leveque solution. The model presented here, is composed of two major parts. The first part calculates the heat transferred from the barrel to the extrudate. This part of the calculation method is based on the findings of Van Zuilichem et. al. (1983, 1985, 1990). Part two of the model calculates the heat generated by viscous dissipation (see Fig. 5.6). With respect to this model,

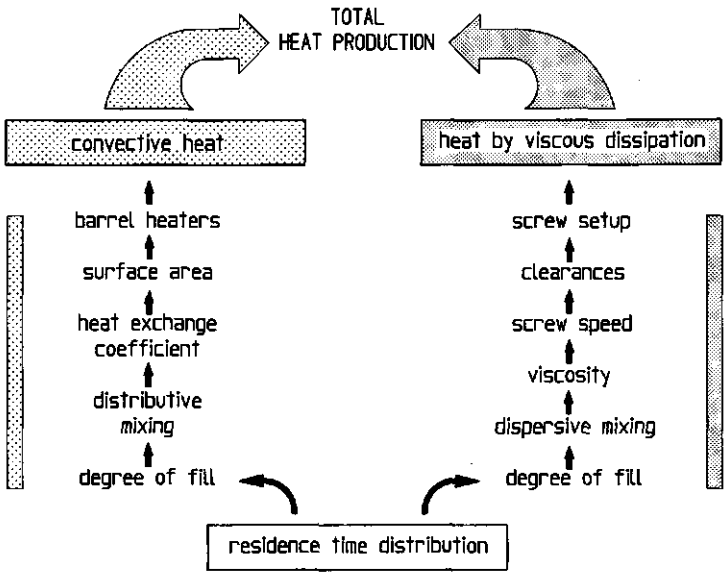

Fig. 5.6 Division of heat development in an extruder

it is important to note the following assumptions:

- Input parameters of the model are:
  * the temperature profile imposed at the barrel.
  * torque.
  * feedflow.
- Torque is converted into: pressure energy, phase transition energy and temperature increase. Hereby is is assumed that:

(1) The torque and the heat convection are linearly related to the degree of fill, according to van Zuilichem et al. (1983)

(2) The viscosity changes of the material are described by a non-Newtonian, temperature-time dependent power law model.

(3) The amount of energy necessary to gelatinize the starchy food-product is negligible compared to the energy consumed to raise the temperature of the product.

(4) The meltflow is highly viscous and in the laminar flow regime.

(5) Only the net flow in the axial direction is considered.

The calculation scheme (Fig. 5.7) shows the structure of LU model

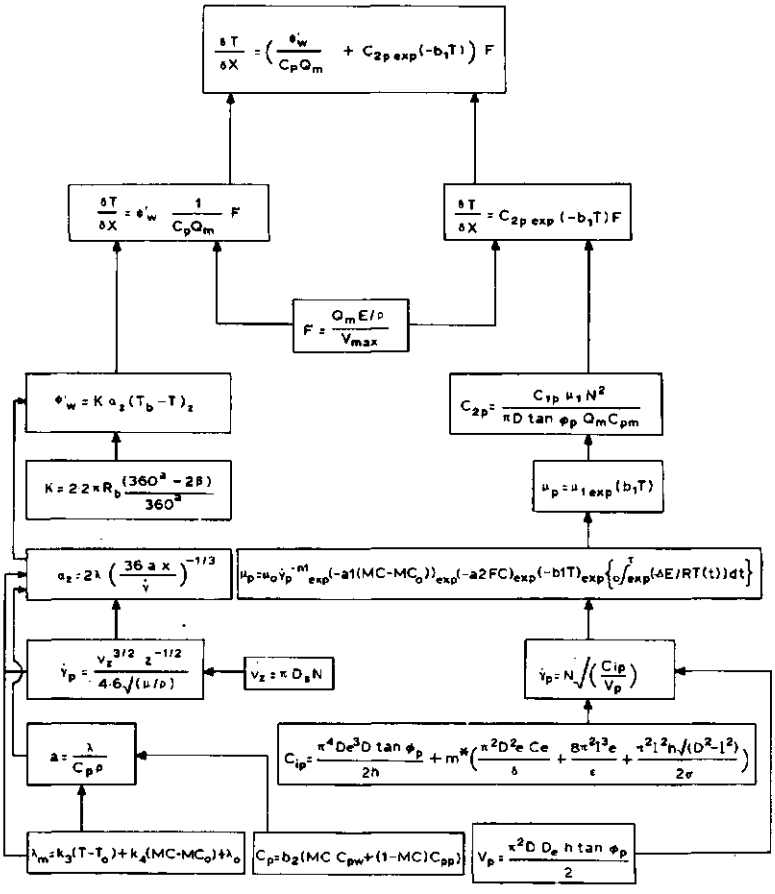

Fig. 5.7 Calculation scheme of LU model (van Zuilichem et al., 1990)

with its various components. Based on this calculation scheme, a computer model, following a stepwise procedure, was developed with the following process- and material-variables for the input:

- Material variables:
    - * C_p
    - * initial viscosity
    - * melting temperature
    - * density
    - * moisture content
- System variables:

* throughput
* initial material temperature
* length of extruder
* screw geometry
* temperature profile

The output of this computer program is a plot of the temperature of the food product versus the axial distance in the extruder. It is also possible to plot the temperature increase, due to penetration of heat and dissipation, versus the axial distance in the extruder. The calculated temperature values are also transcribed onto a datafile.

5.7 The viscosity model

The function of many operations in polysaccharide extrusion cooking is to rupture the starch particles and to gelatinize their contents to a certain extent for different applications in human food and animal feed. During this process considerable changes in the rheology of the material are occuring due to the formation and breakage of gel bonds. These changes can have their impact on processing parameters and stability criteria. Janssen and van Zuilichem (1980) suggested an equation especially for applications in food extrusion technology. This method is used in the LU model and describes the effects of the mechanism of gel-formation and -breakage on the viscosity as a function of shear rates, fat-and moisture-content. They combined a power law behaviour with a temperature dependency and an extra term for the formation of the network depending on the activation energy and the residence time. Now the apparent viscosity, μ_p, can be written as:

$$\mu_p = \mu_0 \dot{\gamma}_p^{-n_1} e^{-a_1(MC-MC_0)} e^{-a_2 FC} e^{-b_1 \Delta T} e^{\left(\int_0^t e^{\frac{-\Delta E}{RT(t)}} Dt\right)} \qquad (35)$$

where Dt is a convective derivative accounting for the fact that the coordinate system is attached to a material element as it moves through the extruder. The integration can be performed analytically as is shown in Appendix 5.1. With this model it became possible to explain certain instabilities as they occur

during the extrusion of starches.

5.8 Material

As a model food-material, standard biscuit flour (MENEBA Rotterdam) was used (Table 5.1). The experiments were done on a

Table 5.1 Physical constants of standard bisquit flour

C_p	1740	(J/kgK)
λ_0	0.303	(J/kgK)
ρ	1285	(kgm^3)
T_{melt}	348	(K)
Moisture Content	15	(%)

twin screw co-rotating extruder, type MPF-50 APV Baker with a 23 kW engine. A big advantage of this extruder is the modular screw design allowing to compose almost every desired screw configuration. Screw sections used are elements like: transportation elements and kneading elements e.g feed screw, paddles 30°/45°/90° and single lead screws (Fig. 5.8 a, b, c).

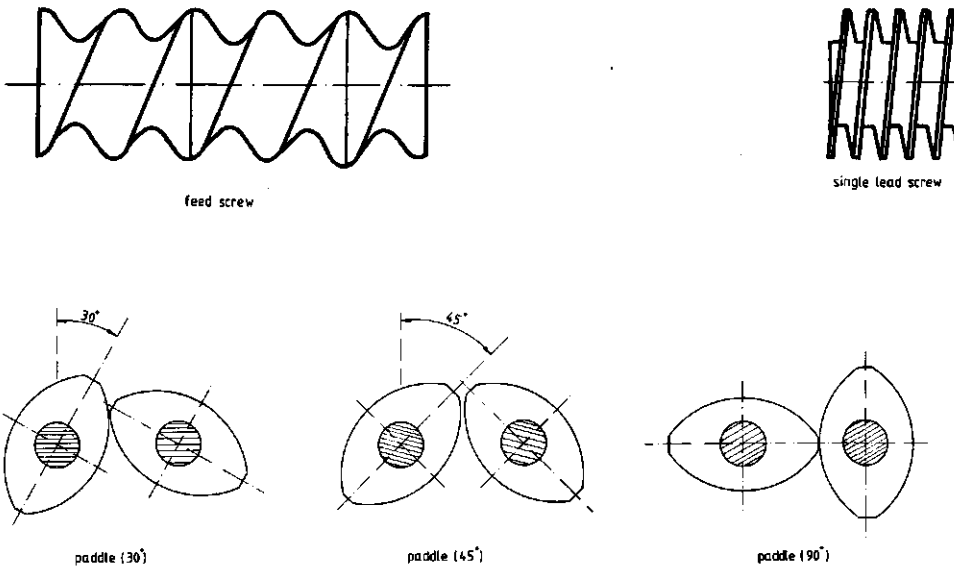

Fig. 5.8 Screw elements used for these expriments

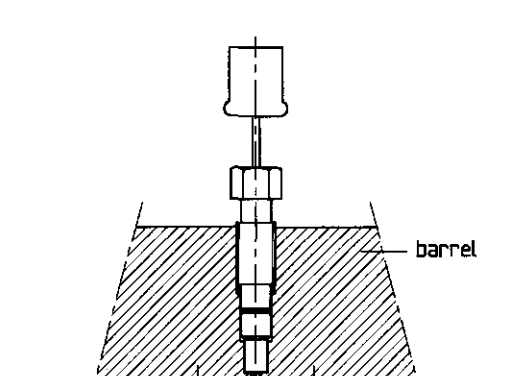

Fig. 5.9 Place of the thermal probe

Heat is supplied by 9 heating elements located on the barrel of the extruder. The experiments were done with two different

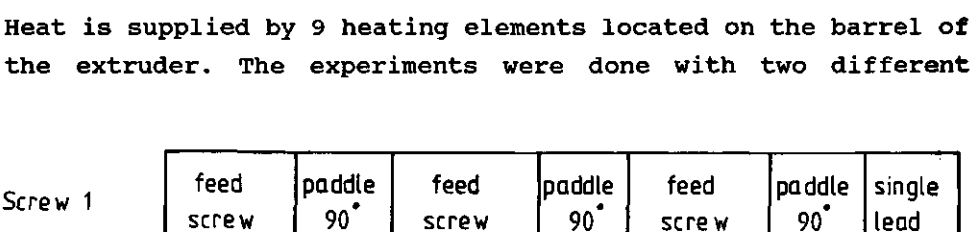

Fig. 5.10 Low and high shear screw profiles (screw 1: high shear, screw 2: low shear)

temperature profiles imposed on the barrel. To determine the temperature of the product, six thermal probes (see App. 1) were installed with the tip of the probe stuck 0.7 cm into the

Barrel Section	1	2	3	4	5	6	7	8	9
Profile „A1":	40	80	100	110	120	130	140	150	160
Profile „B2":	40	60	80	100	100	120	120	130	130

Fig. 5.11 Temperature profiles (Profile A: 160°C, profile B: 130°C)

material. (Fig. 5.9). This was accomplished by using spacer-screw elements.
It was assumed that there is no heat production by viscous dissipation at the tip of the thermocouple. To study the influence of viscous dissipation on the product temperature, two screw types were selected. In figure 5.10 screw 1 can be regarded as a "high shearing" screw because of the relatively high percentage of 90° kneading elements, whereas the screw 2 can be regarded as a "low shearing" screw. The temperature profiles imposed on the barrel are given in Figure 5.11. The measurements were carried out with different screw speeds, moisture contents and throughputs.

5.9 Results

It would go too far to present all the data acquired by measurement and prediction. Therefore the general trend will be discussed. The screw speeds used were resp. RPM 50, 150, 200, 250 and 300. At the lower RPM numbers a capacity of 0.0052 kg/s was used, steadily increasing towards 0.016 kg/s at the highest RPM (Tabel 5.1). The moisture contents applied ranged from 26.8% to 35.6%. The resulting temperature profiles calculated with the model and the corresponding thermocouple readings are collected in Tabel 5.1.

For some runs the readings and the calculated data are given in the diagrams in Figure 5.12, 5.13, 5.14. figure 5.12 shows a temperature plot for screw No.2, the low shear screw, extruding flour at 27% water content with a throughput of 0.0061 kg/s at a screw speed of 250 RPM. The imposed temperature profile was profile A. In Fig. 5.13 and 5.14, the temperature plots for screw No. 1 and No.2 are given for resp. the two different temperature profiles A and B, extruding flour at resp. 31.2% and 24.4% water content and throughput of 0.0061 kg/s at 250 RPM for both the runs.
It can be seen clearly in Fig. 5.12, that there is a slight deviation in calculated and measured values, in the order of 10 °C maximum at the metering section. In Fig.5.13 there is almost

Table 5.2 Comparison between measured and calculated data

SCREW 1.
TEMPERATURE PROFILE A.

RPM	(KG/S)	MC.(%)		T1	T2	T3	T4	T5	T6	T end
50	0.0052	26.8	MEAS	56.3	77.1	105.3	117.6	134.3	149.2	156
			MOD.	52.7	78.5	115.8	125.2	147.3	158.2	160.0
150	0.0063	29.5	MEAS	55.9	73.6	109.2	121.8	139.5	150.4	159.0
			MOD.	47.9	70.3	117.8	127.0	149.2	159.9	161.6
250	0.0072	35.6	MEAS	48.0	68.2	109.1	123.4	137.0	150.2	159.0
			MOD.	44.0	64.2	118.0	127.5	149.8	160.5	162.2

SCREW 2.
TEMPERATURE PROFILE A.

RPM	(KG/S)	MC.(%)		T1	T2	T3	T4	T5	T6	T end
200	0.016	27.4	MEAS	30.5	47.3	65.0	90.2	102.3	----	141.0
			MOD.	23.9	39.7	59.4	97.0	123.2	140.3	156.7
300	0.0165	27.8	MEAS	29.8	47.2	61.9	86.6	101.6	----	143.0
			MOD.	23.8	39.1	58.4	90.4	127.4	145.3	159.2

no measurable deviation, whereas in Fig. 5.14, there again is a deviation smaller than 10 °C; giving a measured temperature slightly lower than predicted.

5.10 Discussion

A study point of the model is, that it is capable to calculate the resulting temperature profile of the product over the viscosity-history as the key rheological parameter. In the relation used for the viscosity (eq. 23) are taken up a restricted amount of material parameters; like moisture content (MC%), fat content (F) and gelatinization energy values (ΔE). For ΔE, MC% and F are taken average values as are known for starch. It is known that ΔE is somewhat dependent on the shearrate and the moisture content and will deviate somewhat to lower apparent values due to the fact that the channel of a co-rotating extruder is open and venting of water is continuously occuring via the feed port during operation. This might explain the higher

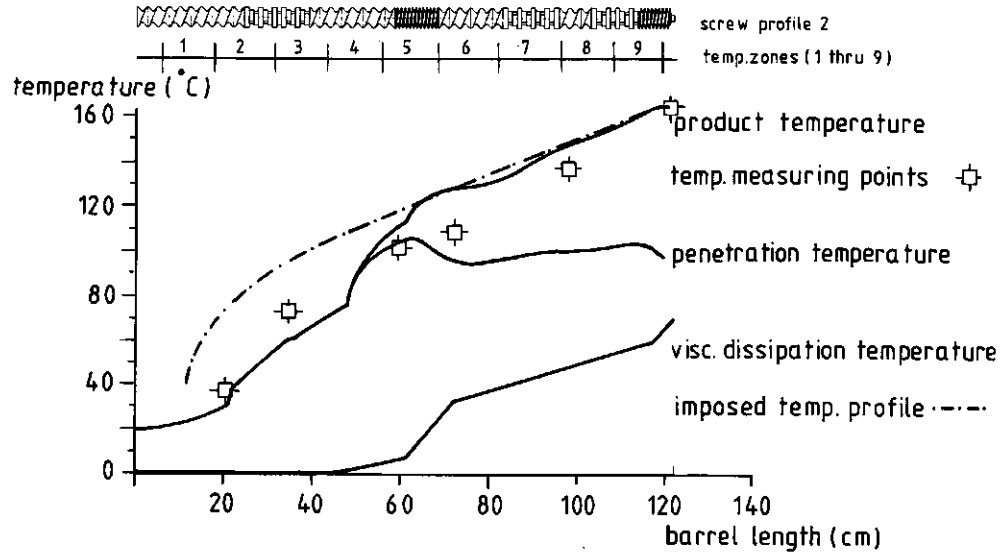

temp. profile A; moisture content 27 %; r.p.m. 250 ; throughput 0.0061 Kg/s

Fig. 5.12 Producttemperature vs. axial distance

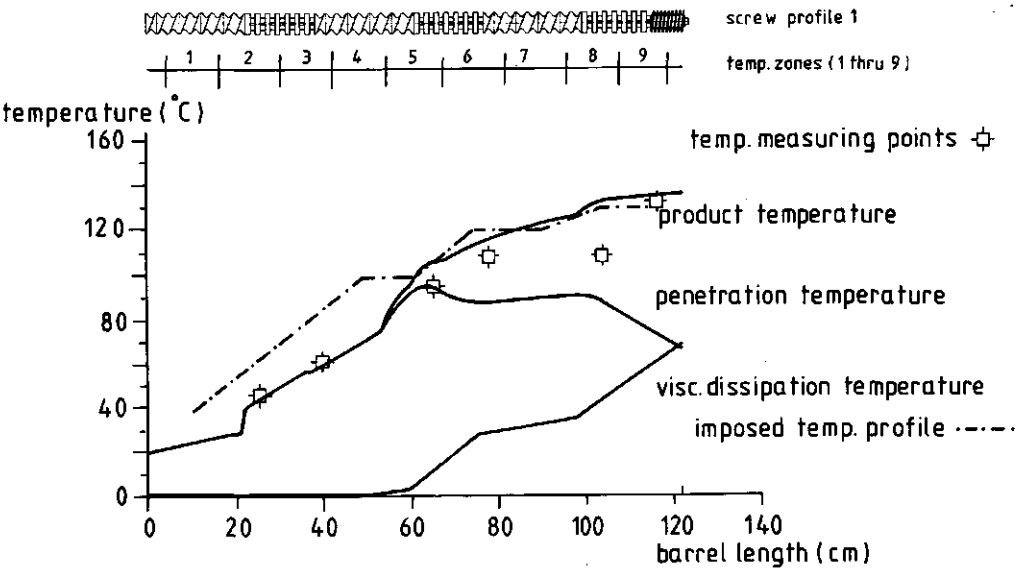

temp. profile B; moisture content 31.2 %; r.p.m. 250 ; throughput 0.0062 Kg/s

Fig. 5.13 Product temperature vs. axial distance

deviations at the 160°C temperature profile and the high RPM

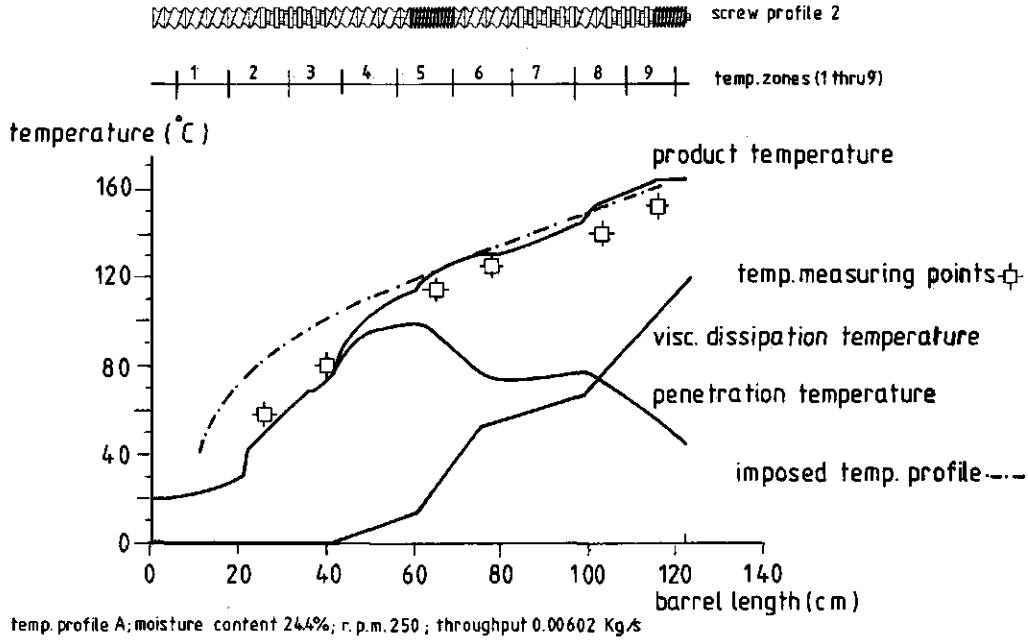

Fig. 5.14 Product temperature vs. axial distance

values, which will cause more venting of vapour and deviating ΔE values. Another fact is that the biscuitflour contains about 9% of protein, wheat gluten, which shows a different yield stress than the starch in the flour, which again will be noticable at the higher RPM values and the different temperature profiles.

It would be better in those cases to calculate the weighted shear history of the constituents of the flour, in order to optimize the rheological information and to consider slip and slip-stick phenomena in the extruder, especially in the metering section.

It must be said that the readings from the thermocouples (Figure 5.9) at high screw speeds and relatively low throughputs are not ideal because a low degree of fill in nearly all parts of the extruder can cause the effect that the thermocouples measure a mixture of melt temperature and steam temperature in the metering section, instead of a homogeneous product temperature.

With this in mind it must be admitted that there still is a lack of data and there is the nessecity to study the following aspects in the near future in more detail:

1:The impact of the chosen rheology model on the predicted viscosity values. Other models have to be considered and tested on validity.

2:Measuring and modelling the radial temperature distribution in the screw with special emphasis on the metering section in order to increase the accuracy of the predicted product temperature.

3:Studying the elongational flow of the product before the die entrance and in the die itself.

References

Beek, W.J., Fysische Technology en Polymeer verwerking, ed. W.J. Beek, Polytechnisch tijdschrift, Delft Oct. 1974, p 42-71.

Bruin, S., van Zuilichem, D.J., Stolp W. (1978). A review offundamental and engineering aspects of extrusion of biopolymers in a single-screw extruder. J. Food Process Eng., 2, 1-33.

Dekker, J. (1976). Verbesserte Schneckenkonstruction für das Extrudieren von Polypropylen. Kunststoffe, 66, 130.

Griffith, R.M. (1962). Fully developed flow in screw extruders, theoretical and experimental, Ind. Eng. Chem. Fundam., 2, 280-286.

Jepson, C.H. (1953). Future extrusion studies. Ind. Eng. Chem., 45 (5) 992.

Levine, L., Rockwood, J. (1986). A correlation for heat transfer coefficients in food extruders. Biotechnol. Progress, 2, 105-108.

Lindt, T.J. (1976). A dynamic melting model for a single screw extruder. Polym. Eng. Sci., 16, 291.

Maddock, B.H. (1959). A visual analysis of flow and mixing in extruder screws. SPE J., 15, 383-389.

Martelli, F.B. (1983). Twin-Screw Extruders. Van Nostrand-Reinhold, New York.

Martin, B., Pearson, J.R.A., Yates, B. (1969). Numerical studies of steady state extrusion process. Cambridge University, Department of Chemical Engineering Polymer Processing Research Center Report No. 5.

Pearson, J.R.A. (1966). Mechanical Principles of Polymer melt Processing. Trans. Soc. Rheol., 13, 357.

Shapiro, J. (1973). Melting in plasticating extruders. PhD Thesis, Cambridge University, 1971.

Shapiro, J., Halmos, A.L., Pearson, J.R.A. (1976). Melting in single screw extruders. Polymer, 17, 905-917.

Tadmor, Z., Klein, I. (1970). Eng. Principles of Plasticating Extrusion. Van Nostrand-Reinhold Company, New York, 185-90.

Vermeulen, J., Scargo, P.G., Beek, W. (1971). The melting of a crystalline polymer in a screw extruder. Chem. Eng. Sci., 46, 1457-1463.

Yacu, W.A. (1983). Modelling of a twin-screw co-rotating extruder. In: Thermal Processing and Quality of Foods, ed. P. Zeuthen, J.C. Cheftel, C. Eriksson. Elsevier Applied Science Publishers, London.

Yankov, V.I. (1978). Hydrodynamics and heat transfer of apparatus for continuous high speed production of polymer solutions. Heat Transfer Soviet Res., 10, 67-71.

van Zuilichem, D.J., Alblas, B., Reinders, P.M., Stolp, W. (1983). A comparative study of the operational characteristics of single and twin screw extruders. In: Thermal Processing and Quality of Foods, ed. P. Zeuthen, J.C. Cheftel, C. Eriksson. Elsevier Applied Science Publishers, London.

van Zuilichem, D.J., Tempel, W.J., Stolp, W., van't Riet, K. (1985). Production of high-boiled sugar confectionery by extrusion-cooking of sucrose: liquid glucose mixtures. J. Food Eng, 4, 37-51.

van Zuilichem, D.J., Jager, T., Spaans, E.J., De Ruigh, P. (1989). The influence of a barrelvalve on the degree of fill in a co-rotating twin screw extruder. J. Food Eng., 10, 241-254.

van Zuilichem, D.J., Janssen, L.P.B.M. (1980). In: Rheology vol.3, ed. G. Astarita, G. Marcus, L. Nicolais. Plenum Press, New York and London.

Notation

a	Thermal diffusity	$[m^2/s]$
a_1	Moisture coefficient of viscosity	[-]
a_2	Fat coefficient of viscosity	[-]
A	Surface area	$[m^2]$
b	Channel width in axial direction	[m]
b_1	Temperature coefficient of viscosity	[-]
b_2	Coefficient in heat capacity	[-]
B	Width of reverse cross-channel	[m]
Br	Brinkman number	[-]
c	General clearance width	[m]
C_e	Equivalent twin screw interference	[m]
C_p	Heat capacity	[J/kgK]
C_{pm}	Heat capacity of molten matter	[J/kgK]
C_{ps}	Heat capacity of solid matter	[J/kgK]
C_{pp}	Heat capacity of molten product	[J/kgK]
C_{pw}	Heat capacity of water	[J/kgK]
d	Thickness of boundary layer	[m]
D	Barrel diameter	[m]
D_e	Equivalent of twin screw diameter	[m]
D_s	Diameter of the screws at Z=z	[m]
e	Screw flight tip width in axial direction	[m]
E	Residence time	[s]
ΔE	Gelatinization energy of product	[J/mol]
F	Degree of fill	[-]
FC	Fat content	[%]
G	Depth of reverse cross-channel	[m]
Gz	Graetz number	[-]
h	Channel Depth	[m]
H	Characteristic height	[m]
I	Distance between screw shafts	[m]
I_2, I_3	Second and third invariants of the rate of deformation tensor	$[s^{-2}, s^{-3}]$
k_1, k_2	Exponents in Nusselt equation according to Levine and Rockwood	[-]
k_3, k_4	Coefficients in thermal conductivity	[-]

K	Twin screw circumference	[m]
L	Length of extruder	[m]
m	Parameter in power-law model	[$Ns^n m^{-2}$]
m^*	Number of flights	[-]
m_1	Number of reverse cross-channels	[-]
MC	Moisture content	[%]
n_1	Power-law index	[-]
N	Screw speed in revolutions per second	[s^{-1}]
Nu	Nusselt number	[-]
p	Pressure	[Pa]
P	Ratio between pressure flow and drag flow	[-]
Pe	Peclet number	[-]
q	Heat flux vector, components q_x, q_y, q_z	[$Jm^{-2}s^{-1}$]
Q_m	Feed rate	[kg/s]
R	Distance from screw axis to barrel	[m]
Re	Reynolds number	[-]
s	Width of flight	[m]
t	Time	[s]
T	Temperature	[T]
U	Relative velocity of barrel wall with respect to centerline of screw	[m/s]
v	Velocity vector, components v_x, v_y, v_z	[m/s]
V	Channel volume	[m^3]
w	Width of extruder channel	[m]
X	Axial distance	[m]
z	Total penetration depth	[m]
Z	Viscous heat dissipation	[N/m]
α	Heat transfer coefficient	[$Js^{-1}m^{-2}K^{-1}$]
β	Overlap angle between two screws	[-]
$\dot{\gamma}$	Shear rate	[s^{-1}]
δ	Flight clearance	[m]
Δ	Rate of deformation tensor	[s^{-1}]
ϵ	Clearance between flight tip and channel bottom of two opposite screws	[m]
η	Non-Newtonian viscosity	[Nsm^{-2}]
θ	Angle of flight	[-]
λ	Thermal conductivity	[J/smK]

μ	Newtonian viscosity	[Nsm^{-2}]
ρ	Density	[kgm^{-3}]
σ	Clearance between flights of oppsite screws parallel to each other	[m]
φ	Screw helix angle	[-]
Φ_w'	Heat flux per meter	[J/m]
Φ_w''	Heat flux per square meter	[Jm^{-2}]

Subscripts

b	Barrel
f	Feed material
h	hydrodynamic
max	Maximum
m	Melt material
0	Initial or reference condition
p	Pumping section
r	Bottom of screw channel
rs	Reverse screw section
s	Solid (powder)
T	Thermal
tot	Total
w	Heat
x,y,z	Co-ordinate indices

Appendix

The traveling observer part of equation 35 can be written as:

$$\int_{t_{min}}^{t_{MAX}} e^{-\frac{\Delta E}{bt+c}} dt \qquad \textbf{(a1)}$$

By substitution of $\frac{\Delta E}{bt+c}$ by u, dt can be expressed as:

$$u = \frac{\Delta E}{bt+c} \rightarrow bt+c = \frac{\Delta E}{u} \Rightarrow d(bt+c) = bdt = d\left(\frac{\Delta E}{u}\right) = -\frac{\Delta E}{u^2} du \Rightarrow$$

$$dt = -\frac{\Delta E}{bu^2} du \qquad \textbf{(a2)}$$

By substitution of equation a2 in equation a1, it can be found that:

$$\int_{t_{min}}^{t_{max}} e^{\frac{\Delta E}{bt+c}} dt = -\frac{\Delta E}{b} \int_{u_{min}}^{u_{max}} \frac{e^{-u}}{u^2} du \qquad \textbf{(a3)}$$

With:

$$u_{min} = \frac{\Delta E}{bt_{min}+c}$$

And:

$$u_{max} = \frac{\Delta E}{bt_{max}+c}$$

$$-\frac{\Delta E}{b} \cdot \int_{u_{min}}^{u_{max}} \frac{e^{-u}}{u^2} du = \frac{\Delta E}{b}\left(\frac{e^{-u}}{u_{max}} - \frac{e^{-u}}{u_{min}}\right) + \frac{\Delta E}{b} \cdot \int_{u_{min}}^{u_{max}} \frac{e^{-u}}{u} du \qquad \textbf{(a4)}$$

The integral on the right hand of equation a4 can be written as:

$$-\frac{\Delta E}{b} \cdot \int_{u_{min}}^{u_{max}} \frac{e^{-u}}{u} du = \frac{\Delta E}{b} \cdot \int_{u_{min}}^{\infty} \frac{e^{-u}}{u} du - \frac{\Delta E}{b} \cdot \int_{u_{max}}^{\infty} \frac{e^{-u}}{u} du \qquad \textbf{(a5)}$$

For the remaining differential equation:

$$\int_{u}^{\infty} \frac{e^{-u}}{u} du \qquad \textbf{(a6)}$$

can be solved using the approximation given by Taylor's progression in series:

$$\int_{u}^{\infty} \frac{e^{-u}}{u} du = \log u - \frac{u}{1!} + \frac{u^2}{2 \cdot 2!} - \frac{u^3}{3 \cdot 3!} + \ldots\ldots\ldots \qquad \textbf{(a7)}$$

CHAPTER 6

THE INFLUENCE OF A BARREL-VALVE ON THE DEGREE OF FILL IN A COROTATING TWIN SCREW EXTRUDER

ABSTRACT

The influence of a barrel valve on the degree of fill in a corotating, twin screw extruder (MPF-50) built by APV Baker was measured by opening the barrel and by residence time distribution measurements (RTD). The RTDs, which were measured by a radio tracer technique, were characterised by their minimum and average residence times and curve width. Measurements were made at a "low" and a "high" barrel temperature profile, two mass flows and three screw speeds. The degree of fill and the minimum and average residence time increased when the valve in the barrel was closed. When the rotational speed of the screw decreased the hold up in the extruder increased. The degree of fill during the measurements ranged from 30% to 56%, depending on the temperature, barrel-valve position, rotational speed of the screws and the feed rate. With a "low" temperature profile the width of the curve was independent of the barrel valve position. When the barrel valve was closed at "high" temperatures, only a minor increase in the curve width of the order of twice the measurement accuracy was found.

THIS CHAPTER IS BASED UPON THE PUBLICATION:

van Zuilichem, D.J., Jager, T., de Ruig, J.A.J., Spaans, E.J., (1989). The Influence of a Barrel-Valve on the Degree of Fill in a Corotating Twin Screw Extruder. J. Food Eng., 10, 241-254.

6.1 Introduction

In a co-rotating twin screw extruder, it is often difficult to make use of all the available barrel length. Approximately the first 75 % of the barrel length is being used mainly as a transport section with a low degree of fill and pressure build-up. In the remaining 25 % a more effective shear input and heat transfer are possible. A change in the process variables of the extruder such as the feed rate, rotational speed and barrel temperature, will have only a moderate effect on the extrusion cooking process. Changes in the screw configuration such as reversed pitch sections, kneading paddles and other specially designed screw sections, are widely used to modify the extrusion cooking process. A greater degree of fill and pressure build up result in a better extruder performance.

The reversed pitch section is the system most often used to shear and heat the product in the middle region of the barrel. A more

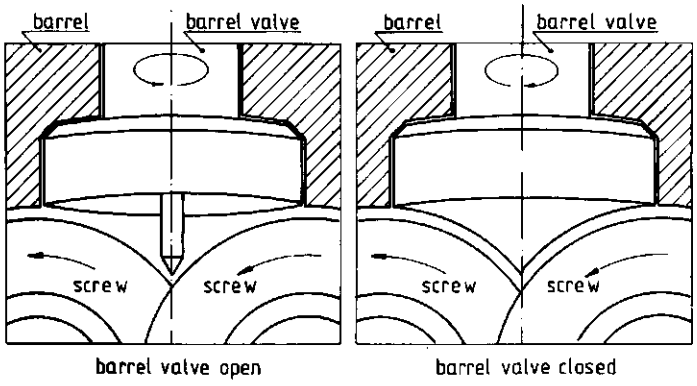

Fig 6.1 barrel-valve diagram (van Zuilichem et al., 1989)

recent component is the barrel-valve. The barrel-valve, which is shown in Fig. 6.1, should give better control of the degree of fill. Each screw is fitted with a disc which almost completely blocks the barrel cross-section. The two discs are offset axially because of the intermeshing geometry. A passageway is created in the saddle-section of the barrel, which bypasses these full-bore restrictions of the screw in which a vane valve of special shape

is placed. A 90 ° rotation of this barrelvalve in either direction allows the passageway to be fully opened (0°) or fully closed (90°). The advantage of this valve over reversed screw sections is that its position can be changed during operation. For the extrusion of plastics, Todd (1980) claims that this device influences hold up and compounding. The influence of the barrel-valve position on the degree of fill is studied by means of residence time distribution (RTD) measurements and by inspection directly after opening the horizontally split barrel. In this case the RTDs and the degree of fill of a corotating, twin-screw extruder fed with maize gritswere measured with a radiotracer technique (van Zuilichem et al., 1988) at various screw speeds, mass flows and barrel-valve positions.

6.2 Theory

Levenspiel (1972) defined the E(t) function such that E(t)dt is the fraction, at the exit, of the mass-flow which has spent a time between t and (t+dt) in a system. The F(t)-function is obtained by integration to give a cumulative RTD-function :

$$F(t) = \int_0^t E(t)\,dt \qquad (1)$$

The average residence time, τ (s), of the material in the extruder is calculated as:

$$\tau = \int_0^\infty tE(t)\,dt \qquad (2)$$

The specific feed rate , I (-), is defined by Jager et al. (1989) as:

$$I = \frac{Q}{2 \cdot z \cdot V \cdot U \cdot \rho} = \frac{Q}{Q_{max}} \qquad (3)$$

in which Q (kg/s) is the mass flow which enters the extruder, ρ

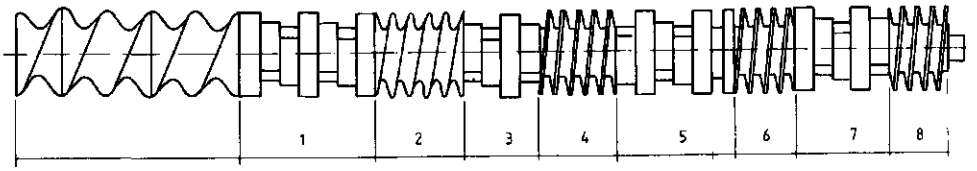

Fig. 6.2 Geometry of the screw used for the RTD experiments (van Zuilichem et al., 1989)

(kgm^{-3}) is the density of feed material when it has a zero porosity, z is the number of starts on one screw, V (m^3) is the chamber-volume of the first screw element in Fig. 6.2. U (1/s) is the rotational velocity of the screws and Q_{max} is the theoretical maximum massflow for which the chamber volume, V, is fully filled. The specific feed rate enables the effects of the rotational speed of the screw and the mass flow Q to be compared. When the average residence time τ is known, the hold up, H (m^3), and the degree of fill, D, can be calculated as follows:

$$H = \frac{\tau Q}{\rho} = DV_{TOT} \qquad (4)$$

in which D is the degree of fill and V_{TOT} is the total volume in the extruder. The curve width can be characterized by the Peclet number, the ratio of conveying and axial dispersion transport. Todd (1975) characterized the curve as the ratio of the times for 16% and 84% of the tracer to pass the detector. These RTDs had a simular shape to that of the axial dispersion model of Levenspiel. The Peclet number could be calculated with this model from the measured 16/84% ratio.
Table 6.3 contains several conflicting relations demonstrating the complexity of the axial mixing in twin-screw extruder-cookers. Hold-up and average residence time seem to be a function of at least the moisture content, feed rate, screw speed, barrel temperature and screw geometry.

6.3 Experimental

The experimental extruder was a MPF-50 APV-Baker co-rotating, twin-screw extruder with a 'K-tron' twin-screw feeder. The feed

material was maize grits with a moisture content of 23% (w/w) and with a density at zero porosity of 1200 kgm^{-3}. RTDs and degrees of fill were measured at three screw speeds (218, 326 and 432 rpm) two mass flowrates (40 and 51 kgh^{-1}) and two barrel temperature profiles (Table 6.1).

A screw configuration with ten sections was used: a transport screw, the barrel-valve discs and eight sections in which the degree of fill has previously been measured (Fig. 6.2). It contained five different elements: transport screw, single start screw, self-wiping single start screw, barrel-valve discs and kneading paddles. The barrel-valve is located at the end of the fifth zone (Fig. 6.2). The total reactor volume is 10.2 dm^3. The RTDs were measured as described by van Zuilichem et al. (1988). A coincidence detector measures the ^{64}Cu activity at the die-outlet. Maize grits (2 g d.m.) soaked in aqueous cuprous chloride ($CuCl_2$) and dried to a moisture content of 12% with a copper content of 50 mg were used as tracer. The tracer was made

Section number[a]	*Screw type*	*Length (m)*	*Temperature profile*	
			'Low' (°C)	*'High' (°C)*
1	Kneading paddles	0·088	30	51
2	Self wiping	0·050	60	93
3	Kneading paddles	0050	60	93
4	Single-start	0·050	90	121
5	Kneading paddles + barrel-valve plugs	0·100	90	121
6	Single lead	0·050	120	150
7	Kneading paddles	0·062	120	150
8	Single-start	0·050	120	150

[a]The section numbers refer to Fig. 2.

Table 6.1 Temperature profiles, the section numbers refer to Fig 6.2 (van Zuilichem et al., 1989)

radioactive by radiation in a gamma-plant. The detectors were shielded against background radiation by collimators having a slit type detection opening of 44x10 mm. The minimum distance

between the collimator and the hot extrudate was 63 mm. With the coincidence detector the average residence times and the curve shapes are not influenced by the measuring equipment (van Zuilichem et al. 1988). The average residence time was calculated from equation (1) and the degree of fill from equation (4).

6.4 Results

The procedure for the characterization of the curve width used by Todd cannot be applied to the present RTDs, as they have a combination of a peak width and a tail which does not fit any curve of the axial dispersion model of Levenspiel. The times in which 16 % and 84% of the tracer have passed the detector give only an indication of the spread of the peak which neglects the shape of the tail and would result in an unrepresentative curve spread. The ratio of the time in which 92% of the tracer has passed and the average residence time is used here as an indication of the curve width. This is more realistic as it takes most of the tail into account. One experiment was repeated in order to study the reproducibility and the accuracy of the measurements. The average residence time could be measured twice and found to be within 0.1 s.

Barrel valve: open

Fig. 6.3 gives the average degree of fill in the extruder at various feed rates and rotational screw speeds when the barrel-valve is open. When the rotational speed of the screws increases the degree of fill decreases. With a "high" temperature profile and a maximal rotational speed (U=432 RPM) the degree of fill is found to be independent of the feed rate. At the lower screw speeds, the degree of fill decreases when mass flow increases. This effect can be seen in Fig. 6.4, where a mass flow increase of 27% from 40 kgh^{-1} to 51 kgh^{-1}, results in a 23% decrease in the degree of fill from 53% to 41%. With the low temperature profile the degree of fill increases when the feed rate increases (by an increase in mass flow or a decrease in the rotational speed).

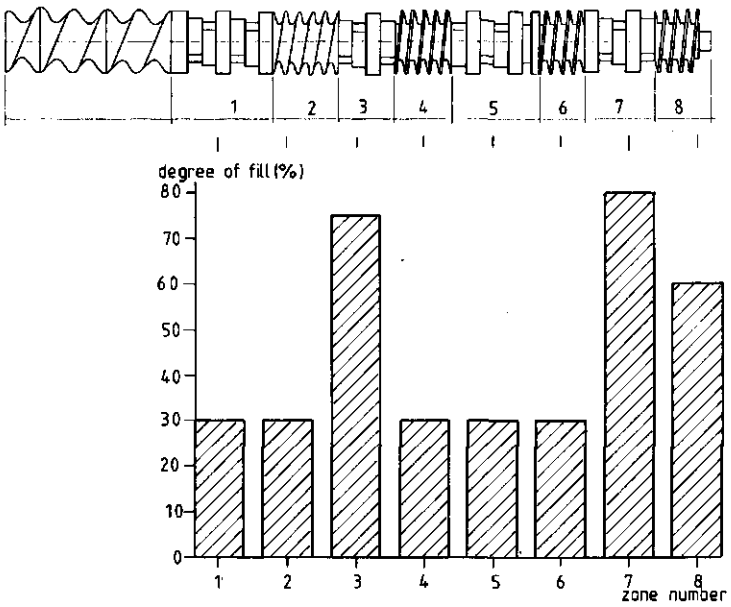

Fig. 6.3 Degree of fill in the co-rotating extruder (per zone) (van Zuilichem et al, 1989)

When the barrel valve is open, the curve spread has a maximum at a degree of fill of 37% When the mass flow increases or when the rotational speed of the screws decreases the curve spread decreases. The experiments at a low barrel temperature resulted in only small differences in their degree of fill and curve spread.

Barrel valve: closed

The minimum and average residence time increase when the barrel-valve is closed, (see Fig. 6.5) The degree of fill is 13% - 30% greater than with an open barrel-valve. The degree of fill increases when the rotational speed of the screws decreases. At the "high" temperature profile the degree of fill can decrease when the mass flow increases, which is demonstrated in Fig. 6.6 by the measurements at U=218 RPM, or remains constant, which is demonstrated by the measurements at U=326 RPM. With a low temperature profile the degree of fill increases slightly when the feed rate increases.

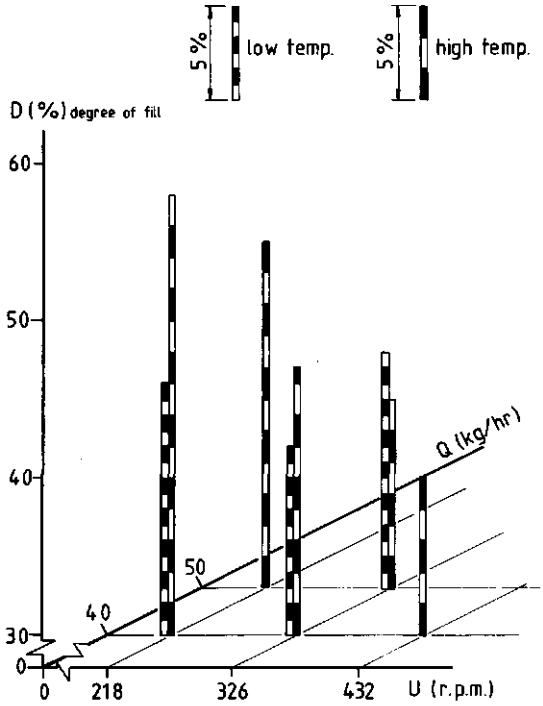

Fig. 6.4 Situation for a closed barrel valve (van Zuilichem et al., 1989)

The curve spread at the high temperature with a closed-barrel valve, depends on the screw speed and the mass flow rate. When the degree of fill increases above 46 %, the curve spread decreases. At low barrel temperatures the difference in spread of the measurements is less than the accuracy of the measurements.

The degree of fill in the extruder varies with rotational speed U and feed rate Q. An illustration is shown in Fig. 6.6 for an open barrel-valve. The position of the barrel-valve had a marked effect on the degree of fill of sections 4 and 5, just before the barrel-valve.

6.5 Discussion

In Fig. 6.7 two measured E(t)-curves with degrees of fill of 56% and 46% are compared with a curve of Altomare and Ghossi with a

degree of fill of 45%. The curves with a degree of fill of 56% and 46% are comparable for $t > \tau$. The differences between these curves before the average residence time are of minor importance

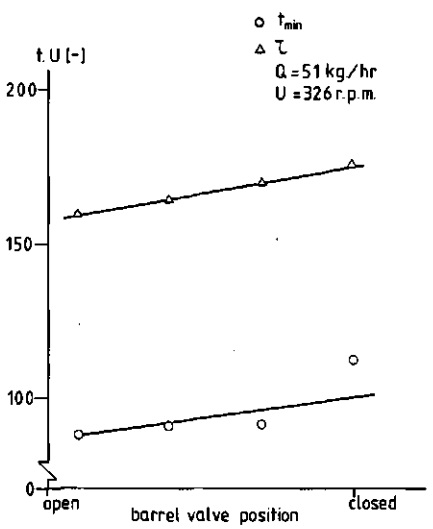

Fig. 6.5 Minimum and average residence time as a function of the barrel valve position (van Zuilichem et al., 1989)

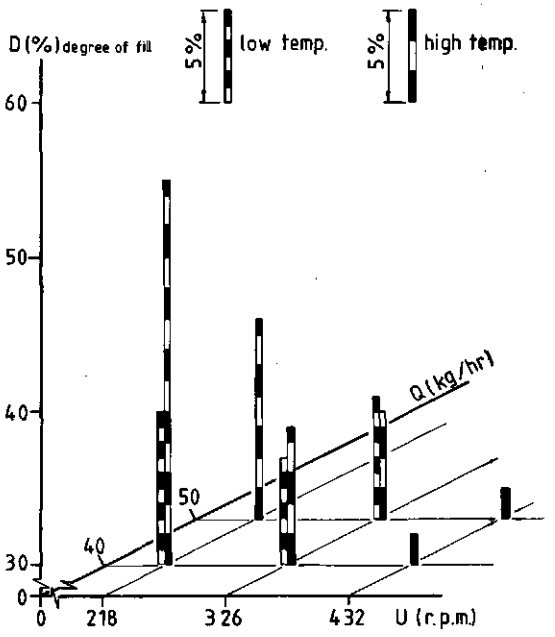

Fig. 6.6 Situation for a open barrel valve (van Zuilichem et al., 1989)

for the reactor properties of the extruder. When in the present measurements the degree of fill increases from 46% to 56%, the curve width increases considerably. The curve widths of the measurements of Altomare and Ghossi are independent of the degree of fill. The extrusion conditions of the measurements presented in this paper and that of Mosso et al. (1981) and Altomare and Ghossi (1986) are not totally comparable but show some similarities in their results. In all these measurements the degree of fill increases when the rotational speed of the screws decreases. In the measurements of Altomare and Ghossi and the one presented here, the shape of the RTD-curves are independent of the feed rate at low (107 °C) barrel temperatures. Mosso et al. and Altomare and Ghossi find an increase in the degree of fill

when the mass flow is raised. In the present measurements the degree of fill can increase, decrease or remain constant when the mass flow rate increases, depending on the screw speed, barrel temperature and barrel-valve position, which is relevant only to this type of extruder. This feature is characteristic for the investigated combination of extruder and barrel-valve.

Table 6.2 Extrusion conditions for RTD measurement in co-rotating, twin screw extrusion cooking (van Zuilichem et al., 1989)

Author(s)	Bounie (1986)	Altomare & Ghossi (1986)	Mosso *et al.* (1981)	Lim *et al.* (1985)
Extruder type	Clextral BC-45	Werner & Pfleiderer ZSK – 57	Clextral BC-45	Clextral BC-45
Length (m)	0·6	1·0	0·6	0·6
L/D ratio	9:1	16:1	9:1	9:1
Die size (mm)	22·25 × 1·5	3·2–7·9	?	?
Material	Wheat starch	Rice flour	42% wheat starch wheat flour 20% maize starch 6% sodium caseinate 11% soya protein 20% saccharin 1% salt	
Feed rate (kg h^{-1})	29·7–33·3	68·2–227·3	26–50	20
Temperature (°C)	165–200	79–177	192	?
Barrel moisture content (%w)	15–45	10–28	13–21	25
Reversed screw zone	with and without	with	with	with and without
Viscous heat dissipation (kJ kg^{-1})	300–460	350–480	?	?

The RTD and the degree of fill in co-rotating twin-screw extruders of similar design to that used in this investigation, has been measured by several investigators. They all used materials containing over 50% starch (Table 6.2) and they measured variations in the minimum residence time, the average residence time, the hold up and the curve spread when changes in the moisture content, the feedrate, the temperature and the rotational speed of the screws were made (Table 6.3). Bounie (1986) found that the introduction of a reversed pitch section increases the curve-width , the average residence time, the viscous dissipation and the minimum residence time. Altomare and Ghossi (1986) have calculated degrees of fill, and found a maximum of 46%. At increasing feed rates, the measurements of Mosso et al.(1981) and Altomare and Ghossi show an increase in the degree of fill.

The average residence time and the degree of fill seem to be dependent on a large number of variables which makes it difficult

Table 6.3 Average residence time, hold-up volume and curve spread for co-rotating twin screw extruders vs. changes in moisture content, specific feed rate, barrel temperature and die diameter (van Zuilichem, 1989)

	Change in	τ	H	Spread
Bounie (1986) with reversed screw section	-Moisture content from 15 to 45% (w/w)	p	p	p
	-Specific feed rate, constan Q, U changes from 110 to 70 rpm	i	i	i
	-Temperature in HTST zone from 165 to 200°C	i	i	i
Bounie (1986) without reversed screw section	-Moisture content from 15 to 45%	p	p	m
	-Specific feed rate, constant Q, U changes from 110 tp 70 rpm	i	p	i
Altomare & Ghossi (1986)	-Moisture content from 10 to 28% (w/w)	p	p	-
	-Specific feed rate, constant U, Q changes from 68 to 227 kg h^{-1}	p	p	-
	-Specific feed rate, constant Q, U changes from 400 to 150 rpm	p	p	-
	-Temperature in HTST zone from 79 to 177°C	p	p	-
	-Die resistance	-	-	-
Lim et al. (1985) with reversed screw section	-Specific feed rate, constant Q, U changes from 120 to 60 rpm	p	p	m
Lim et al. (1985) without reversed screw section	-Specific feed rate, constant Q, U changes from 120 to 60 rpm	p	p	m
Mosso et al. (1981)	-Moisture content from 13.4 to 21.2% (w/w)	-	-	-
	-Specific feed rate, constant U, Q changes from 26 to 50 kg h^{-1}	i	p	i
	-Specific feed rate, constant Q, U changes from 98 to 58 rpm	p	p	-
This study	-Temperature in HTST zone from 120 to 150°C	i	i	i
	-Specific feed rate, constant U, Q changes from 40 to 50 kg h^{-1}	i	i	i
	-Specific feed rate, constant Q, U changes from 432 to 218 rpm	p	p	i
	-Barrel-valve resistance, open to closed	p	p	p

p: An increase of the variable increases the value.
i: Inverse effect.
m: Mixed effect
-: No significant effect

to forecast the degree of fill, or to describe a 'standard' RTD

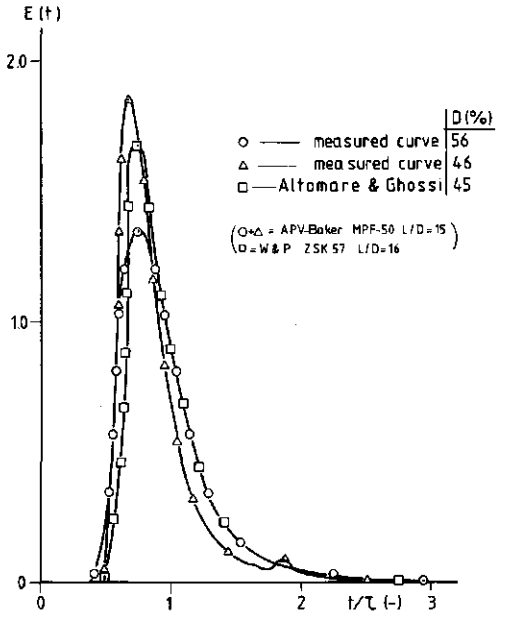

Fig. 6.7 RTD curves of co-rotating extruders (van Zuilichem et al., 1989)

in a co-rotating, twin-screw extruder.

6.6 Conclusions

The barrel-valve provides a means of varying the degree of fill and the residence time during extrusion-cooking. When the barrel-valve is closed the increase in the degree of fill and average residence time is 16% to 30%.

At the low barrel temperature the shape of the RTD curve was not influenced by the barrel-valve position. The degree of fill increased slightly when the feed rate increased. An increase in the effective feed rate either by increasing the mass flow rate or by decreasing the screw speed gave similar results.
With the higher temperature profile the degree of fill increased when the rotational speed of the screws decreased. An increase in the mass flow rate reduces the degree of fill when the rotational speed of the screws was low (218 RPM). At higher screw speeds the degree of fill was almost independent of the mass flow

rate.

The shape of the RTD curve was mainly dependent on the rotational speed, the mass flow rate and the degree of fill. When the barrel-valve was closed the increase in the curve width was about twice the accuracy of the measurement. When changes in the mass flow or the rotational speed of the screws increased the degree of fill above 37% for the open barrel-valve (or above 45% for a closed barrel-valve), the curve spread decreased. When the barrel-valve was open the curve spread decreased when the degree of fill decreased below 37%.

A barrel-valve provided on a co-rotating twin-screw extruder makes possible a most efficient utilization of the available reaction volume of a particular screw combination by a better control of the degree of fill. This implies a minimal screw length for a given extrusion process.

References

Altomare, R.E., Ghossi P. (1986). An analysis of residence time distribution patterns in a twin screw cooking extruder. Biotechnology progress, 2, 157-163.

Bounie, D. (1986). Etude de l'ecoulement et du melange axial dans un extrudeur bi-vis corotatif. These de l'Universite des Sciences et Techniques du Languedoc.

Jager, T., van Zuilichem, D.J., Stolp, W., van't Riet, K. (1988). Residence time distributions in extrusion cooking, Part 4: Mathematical modelling of the axial mixing of a conical, counter-rotating, twin-screw extruder processing maize grits. J. Food Eng., 8, 157-72.

Jager, T., van Zuilichem, D.J., Stolp, W., van't Riet, K. (1989). Residence time distributions in extrusion-cooking, Part 5: the compression zone of a conical, counter-rotating, twin-screw extruder fed with maize grits. J. Food Eng., 9, 203-218.

Lim, J.K., Wakamiya, S., Noguchi, A., Lee, C.H. (1985). Effect of reverse screw element on the residence time distribution in twin-screw extruders. Korean J. Food Sc. Technol., 17, 208-212.

Levenspiel, O. (1972). Chemical reaction engineering, 2nd ed. John Wiley and Sons. New York.

Martelli, F.G. (1982). Twin Screw Extruders: A Basic Understanding. Van Nostrand-Reinhold, New York.

Mosso, K., Jeunink I., Cheftel J.C. (1982). Temperature, pression et temps de sejour d'un melange alimentaire dans

un cuiseur- extrudeur bi-vis. Ind. Aliment. Agric., 99 (1-2) 5-18.

Todd, D.B. (1975). Residence time distribution in twin screw extruders. Polym. Eng. Sc., 15, 437-442.

Todd, D.B. (1980). Energy control in twin-screw extruders, Technical Papers, 37th Annual Technical Conference, Society of Plastics Engineers, New Orleans, 220-221.

van Zuilichem, D.J. (1987). Extrusion-cooking in retrospect. Proceedings Koch-Extrusion 87, Zentral Fachschule der Deutschen Susswarenwirtschaft, Solingen, BRD.

van Zuilichem, D.J., Jager, T., Stolp W., de Swart, J.G., (1988a). Residence time distributions in extrusion-cooking. Part 1: Coincidence detection. J. Food Eng., 7, 147-58.

Notation

D	Degree of fill	[-]
H	Hold-up	[m^3]
I	Specific feed rate	[-]
Q	Feed rate	[kgs^{-1}]
Q_{max}	Maximal feed rate	[kgs^{-1}]
t	Time	[s]
t_x	Passing time of x% of tracer along the detector	[s]
U	Rotational speed of the screws	[s^{-1}]
V	Chamber volume	[m^3]
V_{tot}	Reactor volume	[m^3]
z	Number of thread starts on one screw	[-]
τ	Average residence time	[s]
ρ	Specific density	[kgm^{-3}]

CHAPTER 7

MODELLING OF THE CONVERSION OF CRACKED CORN BY TWIN-SCREW EXTRUSION-COOKING

ABSTRACT

In the search for alternative uses for by-products of corn wet-milling, enzymatic conversion of cracked corn to fermentation substrates by means of twin-screw extrusion (tse) was investigated. The conversion was initiated with starch disclosure and liquefaction in two extrusion operations. Up to 0.5 % w/w heat-stable α-amylase was added at a mass temperature of 120 °C. The extrudate was batch-saccharified using 0.05 to 1 % gluco-amylase at temperatures ranging from 50 to 70 °C, 20 to 40 % dry matter and pH 4.5. The experiment was conducted according to the response surface analysis method, resulting in an empirical model which describes the course of the conversion into dextrose-equivalent units during saccharification at varying enzyme concentrations, temperatures and dry-matter contents. Results show that the gluco-amylase concentration is by far the most important factor in the conversion. The plot obtained for gluco-amylase concentration versus conversion time is approximately linear.

THIS CHAPTER HAS BEEN PUBLISHED AS:

van Zuilichem, D.J., van Roekel, G.J., Stolp, W., van 't Riet, K. (1990). Modelling of the Enzymatic Conversion of Cracked Corn by Twin Screw Extrusion Cooking. J. Food Eng., 12, 13-28.

7.1 Introduction

Before wet milling of corn is performed in a starch plant, it is necessary to separate cracked corn from whole corn grains before the corn enters the steeping process, as the presence of free, soluble starch in the damaged grains and dust would cause the steeping tanks to slit up. Depending on quality, origin, transport circumstances and the number of transshipments, the separated corn represents 2 - 15 % of the total volume.
This cracked corn, which has nearly the same composition as whole corn, is used in cattle-feed. In this experiment the possibilities of converting cracked corn into a fermentation substrate are investigated. This substrate would find its use in ethanol or other fermentations (Zhusman 1979; Chay et al. 1984; Park et al. 1987).
Unlike in the wet-milling process, where glucose can be obtained from pure starch, the conversion of corn starch into its dextrose units for fermentation purposes is carried out in the presence of all the other corn components. After fermentation, the ethanol must be recovered from the fermentation product. The advantage is that no separation or purification other than ethanol recovery is necessary.
The conversion investigated was carried out in a twin-screw extrusion process, using amylolytic enzymes. The required steps in breaking down raw, starchy material into glucose and oligosaccharides were primarily performed by extrusion-cooking.

The following sections describe the process variables of major importance in the conversion and how to quantify their effect on the contents of the fermentation substrate. By applying a statistical technique referred to as Surface Response Analysis [Cochran et al,1957], a model describing the course of the conversion by means of the Dextrose Equivalent (DE) value in the substrate has been calculated.

7.2 Theoretical background

The degradation of raw, starchy material into a substrate

consists of four distinct steps. First, the grain and cell structure -the rigid gluten matrix in which the starch granules are embedded- must be ruptured. Then, the crystalline structure of the granules must be broken to create access for chemical degradation. These two steps are referred to as disclosure, and require up to 1 MJ per kg of raw material. In the third step, once the amylose and amylopectin chains have been made vulnerable and can be dissolved in water, gelatinisation will occur. At this time the starch is ready for liquefaction. The α-amylase activity will be able to divide the macromolecules, thereby breaking down the macromolecular structure. Fourth and last is the conversion of the remaining starch fractions (1 to 1000 glucose units in size) into glucose and oligosaccharides by means of gluco-amylolytic enzymes, i.e. the saccharification.

The first three of the above mentioned steps can be carried out during extrusion cooking at high temperature, high shear, low moisture contents and in a short time (of the order of a few minutes) (Van Zuilichem et al. 1980; Chouvel et al. 1983). The saccharification will take one to several tens of hours, depending on the desired yield of conversion. The extrusion process cannot complete the conversion, it must be followed by a batch or continuous saccharification step.

Fig. 7.1 shows a model extruder configuration for performing disclosure, gelatinisation and liquefaction. In this investigation the model extruder configuration is simulated by two sequential runs through a single extruder.
The first extruder section operates at a high temperature (150 °C) and a high dry matter content (70-85)% wet basis), causing a very high shear rate. In the second section the dry matter content is lowered to (30-40)% by adding a heat-stable α-amylase solution in water, starting liquefaction of the gelatinising starch. The temperature in this section should enable high enzyme activity for a short period of time. The half-life of Termamyl 120L α-amylase is 15 minutes at 110 °C. Enzyme inactivation will also be high, but within the short duration of activity needed

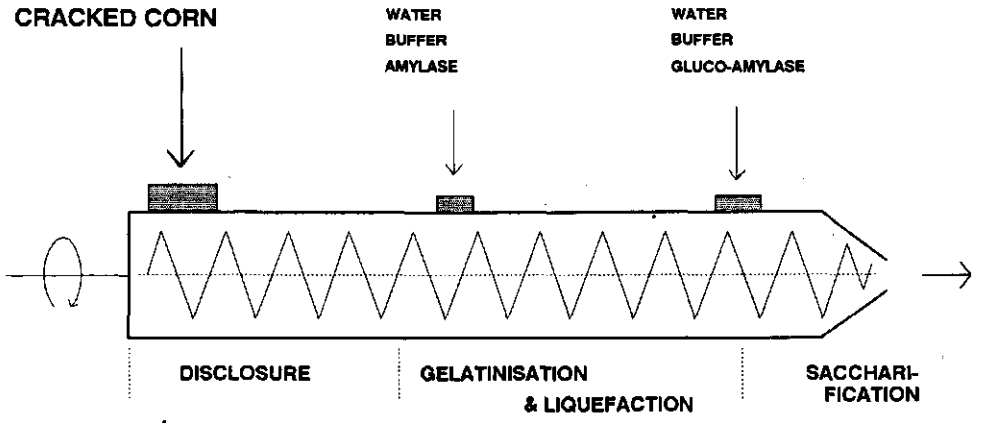

Fig. 7.1 A model extruder configuration capable of disclosing, liquefying and initialising saccharification of raw cracked corn (van Zuilichem et al., 1990)

this will not alter the effectiveness of the process. Heat-stable α-amylases have an optimum activity at 120 °C while, under the given conditions, water activity for enzyme reactions within the extruder is still close to 1 (Linko et al, 1983a). After liquefaction the starch degradation expressed in DE units is 2 to 5. The effectiveness of gluco-amylase during saccharification is higher when liquefaction results in a lower DE value (Marshall, 1980). In the third section the saccharification is started by injecting a gluco-amylase solution before the die. This is done to achieve adequate mixing and to start the reaction at a relatively high dry matter content (25-35)%. Gluco-amylase, however, is more effective at about 60 °C and at pH 4.5, so this last section of the extruder must be cooled rapidly, and the injected enzyme solution has to be buffered at pH 4.5.
The barrel lenght of such a model extruder must equal or exceed 30 diameters to be able to perform the three steps sequentially which is rather impractical.

At present, a useful model to succesfully describe the above-mentioned bioconversion is not available. The Michaelis-Menten kinetic model was developed to describe enzyme-catalysed reactions (Lehninger, 1970). However, it has not yet proved succesful in describing enzymatic conversion processes, disturbed

by the presence of a variety of other constituents, i.e. proteins, fats and cellulose in corn.
An empirical relation to fit the reaction rate r (the glucose production in $kgm^{-3}s^{-1}$) dependence on substrate- (Cs), water- (Cw), and enzyme (Ce) concentrations is as follows (Reinikainen et al. 1986):

$$r = k \cdot (Cs)^{a} \cdot (Cw)^{b} \cdot (Ce)^{c} \qquad (1)$$

This relationship can be simplified to a model describing a saccharification in terms of DE value (%w/w) during the conversion. It was found, however, that the following equation fulfills the same purpose with an equal or even smaller error. (the DE value is generally expressed in weight percents on a dry basis):

$$DE = \frac{t}{A + B \cdot t} \qquad (2)$$

where t is the time and A and B are constants. This equation is similar to the production equation with a second order rate.
Figure 7.2 illustrates the significance of A and B. This second model was chosen because of the practical use when fitting conversion data. With known DE values at certain times during the conversion, the following form of equation (2) can easily be fitted using linear regression:

$$\frac{t}{DE} = A + B \cdot t \qquad (3)$$

The constants A, (in $(\%\ w/w)^{-1}.s^{+1}$) and B, (in $\%\ w/w)^{-1}$ characterise the initial conversion rate and the final level of conversion, respectively, and as such describe the progress of a conversion.

Using surface response analysis, the effects of relevant process variables on a conversion, characterised by A and B, can be quantified.

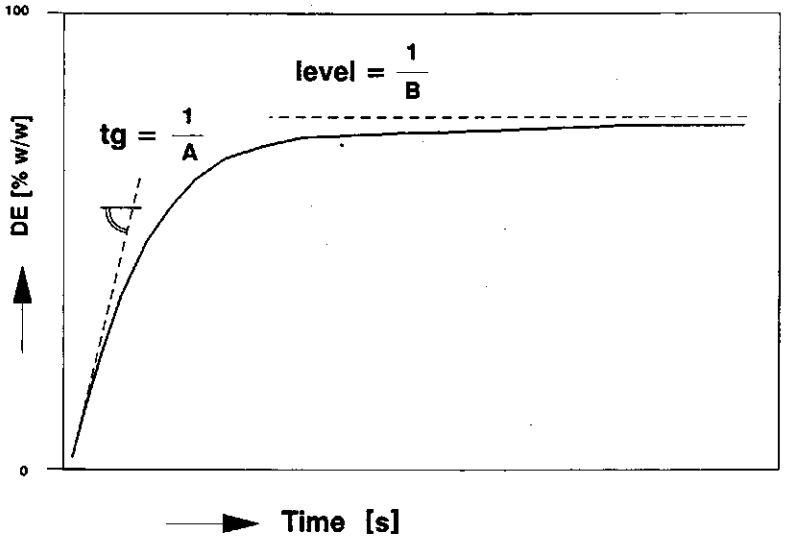

Fig. 7.2 Typical plot of the progress of a saccharification reaction. The constants 1/A and 1/B characterise the initial conversion level and the final conversion level, respectively (van Zuilichem et al., 1990)

Previous work (Linko et al, 1983a,b) revealed that during extrusion the effect of temperature, dry matter content, screw geometry, feed rate and other variables showed certain optima, often dictated by the optimum conditions for use of α-amylase. In this investigation, therefore, the α-amylase dosage was selected as the only variable in the liquefaction process. Other variables were selected from results of investigations on starch extrusion in the presence of amylolytic enzymes (Linko et al, 1980; Hakulin et al, 1983; Linko et al, 1983 a,b). During saccharification, the effect of the gluco-amylase dosage is of major economic interest: in a saccharification process the gluco-amylase cost largely determines the process cost. In order to confirm the suggested linearity of the reaction rate with the gluco-amylase concentration, the temperature and dry matter content of the substrate during saccharification were selected as variables to be investigated. Because of the relatively long residence time in the saccharification, these variables have great influence on enzyme activity, and thus on process cost.

7.3 Experimental

7.3.1 Setup

The experiment was set up to determine the effect of the α-amylase concentration during liquefaction, and of the gluco-amylase concentration, temperature and dry matter content during saccharification. The statistical model uses a mean variable X_0, and four coded variables for the variables in the experiment. Each of these variables was set at five different levels. Table 7.1 shows the combinations of different levels for each variable used in the 31 conversion experiments.
The variables were coded using the following relations :

α-Amylase :

$$X_1 = 2.8\log[\alpha\text{-}amylase] + 3.7 \qquad (4)$$

Gluco-amylase :

$$X_2 = 3\log[gluco\text{-}amylase] + 2 \qquad (5)$$

Temperature :

$$X_3 = \frac{T-60}{5} \qquad (6)$$

Dry matter content :

$$X_4 = \frac{DM-30}{5} \qquad (7)$$

7.3.2 Methods and materials

The extrusion part of the experiment could not be performed on one long-barrel extruder. Therefore disclosure and liquefaction were carried out sequentially in a Cincinnati Milacron CM 45 conical counter-rotating twin-screw extruder (screw type SK 1552/100B).

The disclosure step was the same for all experiments, so a large quantity of disclosed cracked corn was prepared at 85 % DM (1.5 h, 130 °C) and 150 ° C barrel temperature. At 84 kgh^{-1}, 83 RPM

Table 7.1 Experimental design (van Zuilichem et al., 1990)

Exp. No.	Coded variables					Actual physical values[b]			
	X_0	X_1	X_2	X_3	X_4	[α-am] (% w/w)	[g-am] (% w/w)	Temp. (°C)	DM (% w/w)
1	1	−1	−1	−1	−1	0·03	0·1	55	25
2	1	1	−1	−1	−1	0·105	0·1	55	25
3	1	−1	1	−1	−1	0·03	0·47	55	25
4	1	1	1	−1	−1	0·105	0·47	55	25
5	1	−1	−1	1	−1	0·03	0·1	65	25
6	1	1	−1	1	−1	0·105	0·1	65	25
7	1	−1	1	1	−1	0·03	0·47	65	25
8	1	1	1	1	−1	0·105	0·47	65	25
9	1	−1	−1	−1	1	0·03	0·1	55	35
10	1	1	−1	−1	1	0·105	0·1	55	35
11	1	−1	1	−1	1	0·03	0·47	55	35
12	1	1	1	−1	1	0·105	0·47	55	35
13	1	−1	−1	1	1	0·03	0·1	65	35
14	1	1	−1	1	1	0·105	0·1	65	35
15	1	−1	1	1	1	0·03	0·47	65	35
16	1	1	1	1	1	0·105	0·47	65	35
17	1	−2	0	0	0	0	0·214	60	30
18	1	2	0	0	0	0·262	0·214	60	30
19	1	0	−2	0	0	0·053	0·047	60	30
20	1	0	2	0	0	0·053	1·0	60	30
21	1	0	0	−2	0	0·053	0·214	50	30
22	1	0	0	2	0	0·053	0·214	70	30
23	1	0	0	0	−2	0·053	0·214	60	20
24	1	0	0	0	2	0·053	0·214	60	40
25	1	0	0	0	0	0·053	0·214	60	30
26	1	0	0	0	0	0·053	0·214	60	30
27	1	0	0	0	0	0·053	0·214	60	30
28	1	0	0	0	0	0·053	0·214	60	30
29	1	0	0	0	0	0·053	0·214	60	30
30	1	0	0	0	0	0·053	0·214	60	30
31	1	0	0	0	0	0·053	0·214	60	30

[a]Central composite rotatable second-order design for four variables at five levels.
[b]α-am: alpha-amylase, g-am: gluco-amylase.

and approximately 23 kW mechanical power, a little water (4 kgh^{-1}) was added to prevent the extruder from plugging. The product, fractionated using a 8 x 4mm diameter die with cutter, was crispy, yellow and fluffy. These particles were ground in a Condux pin-grinder and stored at room temperature.

Liquefaction was carried out using 5 different concentrations of

α-amylase (NOVO Termamyl 120 L). The disclosed meal, 85 % DM, was extruded at a mass temperature of 120 °C. About 0.1 m from the feed-point the enzyme solution was injected. These solutions were prepared so as to bring the DM content down to 30 % and to attain the correct α-amylase concentration. The solutions were buffered with a Sodium acetate/acetic acid buffer at pH 6, but liquefaction without buffer showed no variations from pH 6 greater than 0.5 pH. During liquefaction, solid matter throughput was only 11 kgh^{-1} with 21 kgh^{-1} enzyme-solution added at 32 RPM and approx. 2 kW mechanical power. The samples were collected in plastic boxes and stored at 0 °C.

Saccharification was then carried out over 48 h in a shaking incubator. The 31 saccharification solutions were prepared by adding acetic acid to bring the pH to 4.5, adding water to correct to the right DM (DM determination at 105 °C overnight), blending for 1 minute and allowing the mixture to heat up for exactly 45 min before injection of the glucoamylase (Gist brocades Amigase GM) Samples were taken at 0, ¾, 1½, 3½, 8 and 48 h after injection. These 30 ml samples were frozen at -6 °C immediately. Problems arose preparing experiment nr. 24 and the liquefied sample had to be vacuum-dried for ten hours up to 40 % DM. During saccharification DM increased 0.5 % at most. DE analyses were carried out according to Nierle-Tegge, preceded by a 10 minutes 80 % ethanol extraction.

7.3.3 Calculation

The constants A and B were then calculated for each conversion using the Gauss linear regression algorithm. In regression, t=0 was taken to be 15 min before injection of the enzyme. This virtual starting point was taken to correct for the start of conversion during extrusion. Then for both A and B a surface response analysis was performed. In this analysis the reciprocal values of A and B were used, as they appear in the denominator in eqn. (2).

RESULTS

Table 7.2 shows the results of the analysis. The columns '1/A' and '1/B' give the calculated first and second order effects for each variable, and all interaction effects. Significance (90 % confidence level) was designated by the effect being greater than the corresponding standard error. The columns 'S' show the significance of each effect ('-' denoting insignificance). The

Table 7.2 Results of surface response analyses (van Zuilichem et al., 1990)

Effect		*1/A*	*S*	*1/B*	*S*
First-order:					
Mean	b_0	137·1		67·7	
α-Amylase	b_1	28·5		0·3	—
Gluco-amylase	b_2	83·8		3·0	
Temperature	b_3	23·3		−2·0	
Dry matter	b_4	−19·7		−0·1	—
Second-order:					
(α-Amylase)	b_{11}	−10·9		1·3	
(Gluco-amylase)	b_{22}	17·2		−0·1	—
(Temperature)	b_{33}	2·5	—	0·7	
(Dry matter)	b_{44}	18·3		−0·1	—
Interactions:					
α-Amy./Gluco	b_{12}	34·0		−1·4	
α-Amy./Temp.	b_{13}	24·6		−0·4	—
α-Amy./Dry mat.	b_{14}	−3·4	—	0·8	
Gluco/Temp.	b_{23}	16·8		1·6	
Gluco/Dry mat.	b_{24}	−9·9		−0·1	—
Temp./Dry mat.	b_{34}	−9·9		0·3	—
Means of squares:			*f*		*f*
First-order		52 548·1	17·7	80·6	22·1
Second-order		5 830·1	2·5	15·1	4·1
Exp. error		230·9		1·7	
Lack of fit		2 827·5		3·5	
Standard errors (i, j = 1,..., 4):					
Per observation		14·07		1·49	
s.e. b_i		2·87		0·25	
s.e. b_{ii}		2·60		0·23	
s.e. b_{ij}		3·52		0·30	

'f' values for 'first order' and 'second order' are statistical

values expressing the validity of the analyses for both 1/A and 1/B. The critical value at 90 % confidence level are 2.61 (first order effect) and 2.32 (second order effect). Table 7.2 shows that first and second order effects are significant for both analyses at 90 % confidence level.
For details concerning the statistical analysis, see Cochran and Cox (1957).

The effects in Table 7.2 are constants in the following equations, with which a conversion of cracked corn into a fermentation substrate can be described. Only significant effects are taken into account.

$$1/A = 137.1 + 28.5\,X_1 + 83.8\,X_2 + 23.3\,X_3 - 19.7\,X_4 - 10.9\,X_1^2 + 17.2\,X_2^2 + 18.3\,X_4^2 + 34.0\,X_1X_2 + 24.6\,X_1X_3 + 16.8\,X_2X_3 - 9.9\,X_2X_4 - 9.9\,X_3X_4 \quad (8)$$

$$1/B = 67.7 + 3.0\,X_2 - 2.0\,X_3 + 1.3\,X_2^2 - 0.7\,X_3^2 - 1.4\,X_1X_2 + 0.8\,X_1X_4 + 1.6\,X_2X_3 \quad (9)$$

With (8) and (9) 1/A and 1/B can be found for a certain combination of variables. With known A and B, the progress of a conversion, is described by equation (2). For instance a conversion with all variables set to 0 ; 0.053 % Termamyl, 0.214 % Amigase, 60 °C at 30 % DS, is described by :

$$DE = \frac{t}{0.00729 + 0.0148\,t} \quad (10)$$

Where t is expressed in hours and DE is expressed in (%w/w).

7.5 Discussion

7.5.1 Extrusion (disclosure & liquefaction)

In extrusion two major sources of error are recognised. The first is in the grinding of the expanded and cooled extrudate after disclosure. The exposure of the disclosed material to air, the cooling down after disclosure and the reheating during liquefaction probably cause formation of some structure in the disclosed extrudate which is again destroyed by grinding. Also, exposure to oxygen is known to inhibit native α-amylase activity. Second, storage of the liquefied extrudate at 0 °C did not fully stop enzymatic activity.

DE determinations immediately after extrusion and just before saccharification varied from 0 to 7 % w/w in one experiment. Because of the orthogonal setup of the experiment the small significance of the α-amylase effect does not affect the value of the other three effects.

Figure 7.3(a) shows a far from linear effect of α-amylase on 1/A (the continuous drawn line incorporates both first and second order effects, the dotted line shows the first order effect only). This agrees with the general theory that the use of α-amylase during liquefaction followed by saccharification prevents retrogradation (the formation of inhomogeneties during liquefaction) rather than actually initialising conversion. Using high α-amylase concentrations during liquefaction does not result in higher initial conversion rates 1/A. Figure 7.5(a) shows the effect of α-amylase concentration on the final conversion level 1/B. The derived relationship is significant, but stays within a range of four DE-units, which is in the same range as the combined error of regression (1%) and DE-determination (2.1%). Figure 7.4(a) shows a decreasing activity of gluco-amylase with increasing α-amylase concentrations at low gluco-amylase concentrations.

7.5.2 Saccharification

The gluco-amylase effect on 1/A (Fig. 7.3(b)) obviously is partially a second-order effect. The decrease in the effect at concentrations of 0.5 % and upwards corresponds to the manufactu-

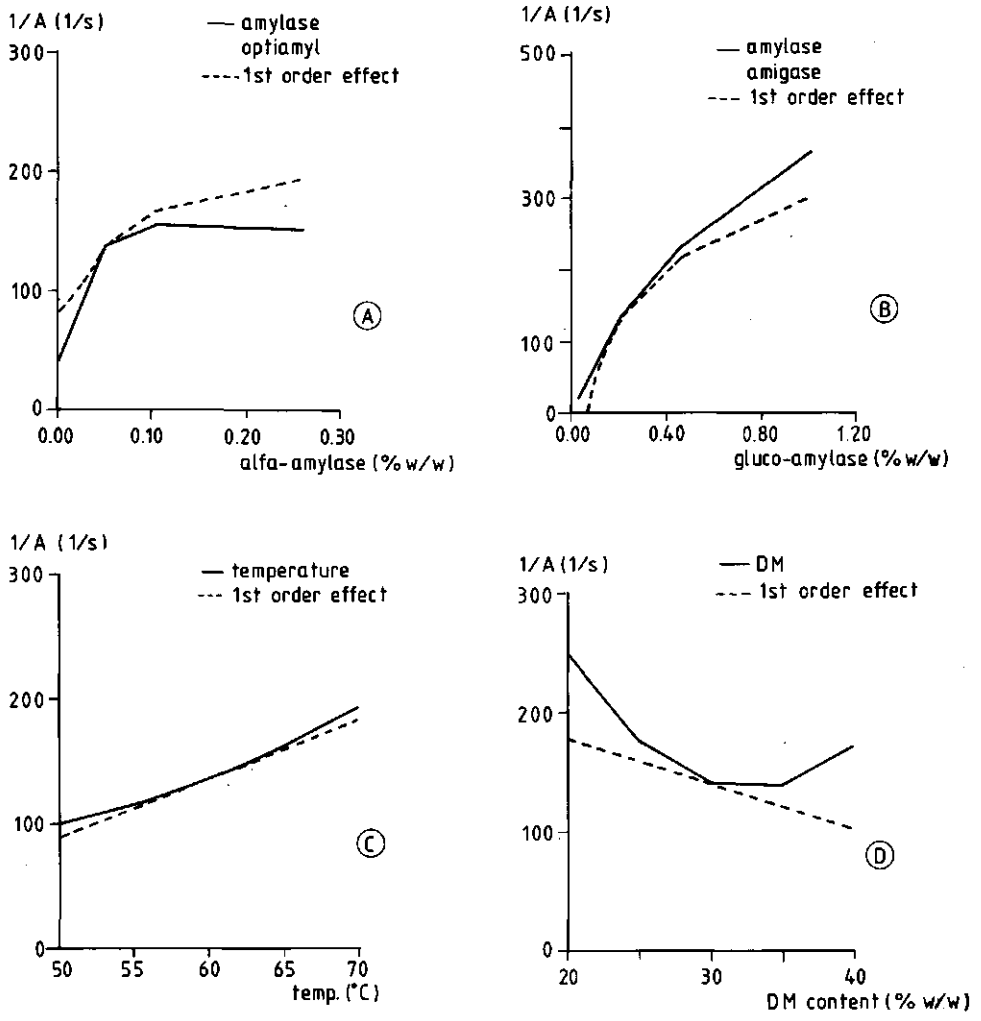

Fig 7.3 The effects of the four conversion variables on the initial conversion rate 1/A. All scales are linear (van Zuilichem et al., 1990)

rer's data. At low concentrations the effect can be considered linear. Fig. 7.3(c) shows a linear increasing temperature effect. This can be explained by the fact that this is the effect on the initial conversion rate 1/A, where no inactivation has yet occured.

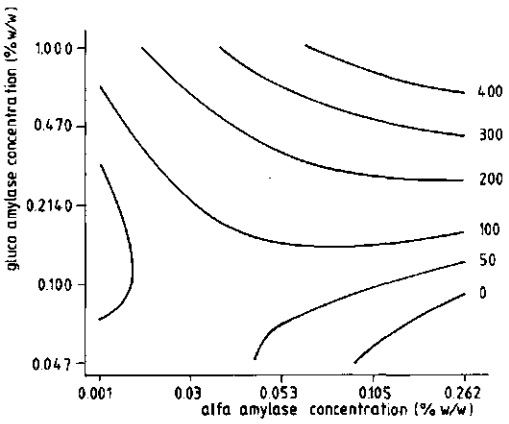

Fig. 7.4a The combined effects of α-amylase and glucoamylase on the initial conversion rate 1/A. Both scales are logarithmic (van Zuilichem et al., 1990)

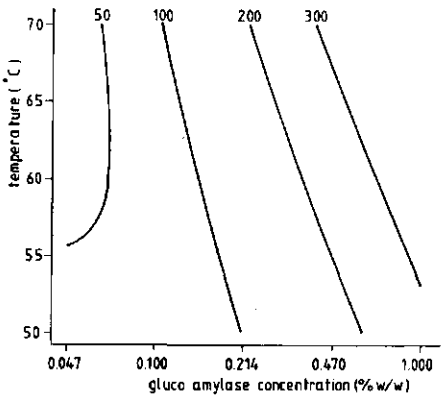

Fig. 7.4b The combined effects of glucoamylase and temperature on the initial conversion rate 1/A. The horizontal scale is logarithmic (van Zuilichem et al., 1990)

The significant effect of dry matter content (Fig. 7.3(d)) is declining steadily. The insignificant increase at DM greater than 35% is due to the vacuum drying before incubation in experiment no. 24.

Figure 7.4b clearly shows the combined linear effect of temperature and gluco-amylase on 1/A. In the linear regression calculations, A was found as the intercept. This intercept was relatively small, causing an estimated error of 30% (mean regression error for 1/A in the 31 regressions). Nevertheless the total first order effect is significant. The total second order effect is significant at 0.87 confidence level.

The gluco-amylase effect on the final conversion level (Fig. 7.5(b)) shows a declining slope. The temperature effect (Fig. 7.5(c)) shows severe gluco-amylase inactivation over the period of saccharification. The dry matter content (Fig. 7.5(d)) does not affect the final conversion level.

Figure 7.6(a), the combined effect of gluco-amylase and α-amylase, shows that at high α-amylase concentrations the effect of gluco-amylase decreases, due to the lower activity of gluco-amylase on more degraded starch. Figure 7.6(b) shows that the

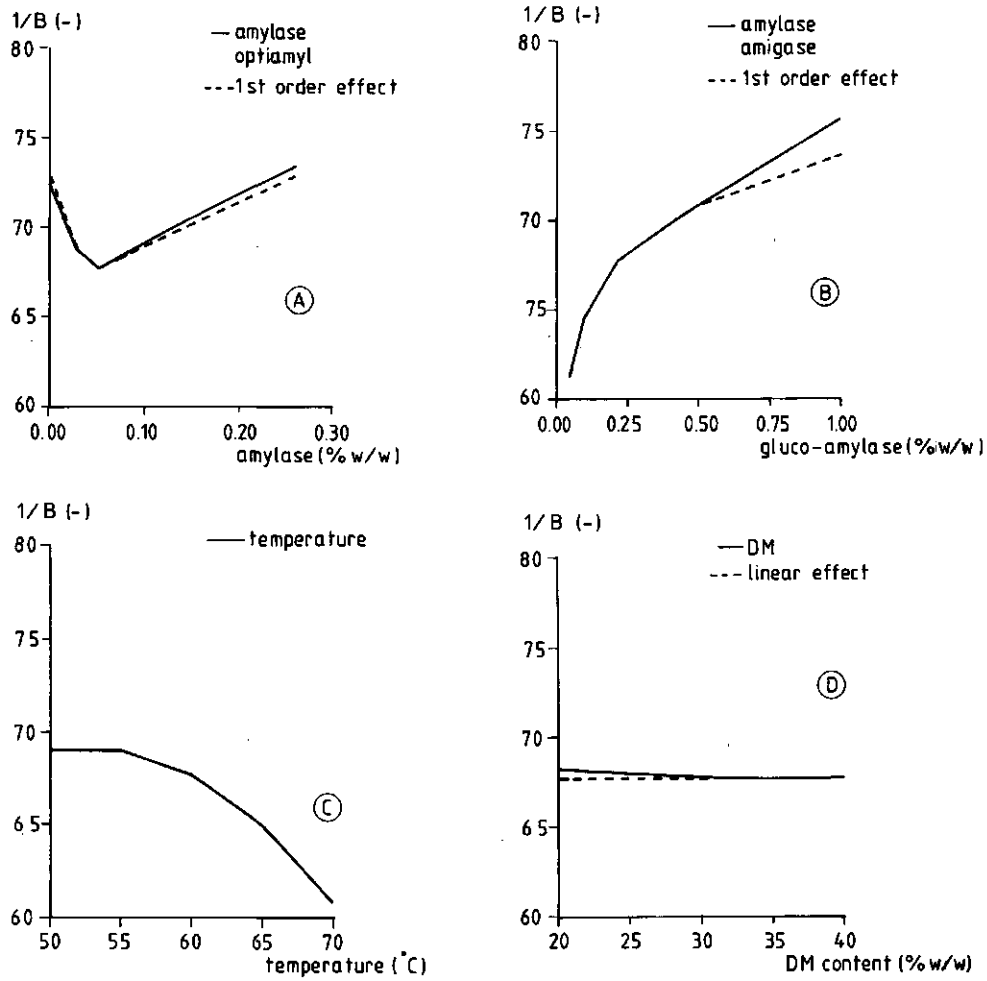

Fig. 7.5 The effects of the four conversion variables on the final conversion level 1/B. All scales are linear (van Zuilichem et al., 1990)

inactivation of glucoamylase over a period of time (denoted by the level 1/B) is more severe at low glucoamylase concentrations. B was calculated from the slope in linear regression. The accuracy of that calculation was approximately 1%.

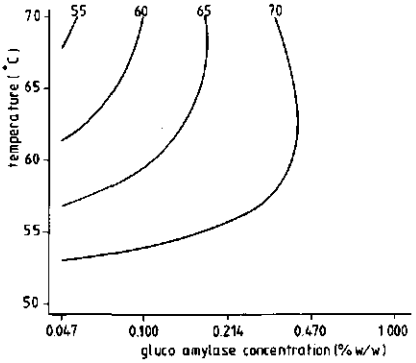

Fig. 7.6a The combined effect of α-amylase and glucoamylase on the final conversion level 1/B. Both scales are logarithmic (van Zuilichem et al., 1990)

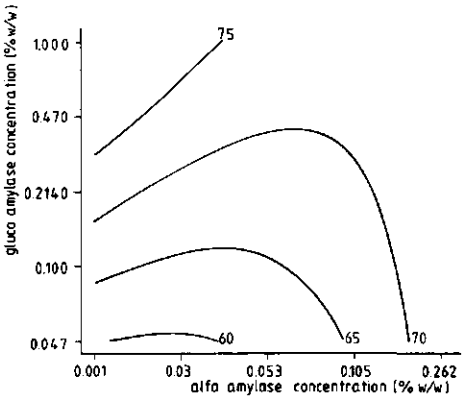

Fig. 7.6b The combined efect of glucoamylase and temperature on the final conversion level 1/B. The horizontal scale is logarithmic (van Zuilichem et al., 1990)

7.6 Proposed process

Figure 7.7 shows a proposed process design for cracked corn conversion, followed by a cell-recycle fermentation process. The cracked corn is extruded and saccharified in a continuous reactor. A separating operation (i.e. sieving) removes solids from the dextrose mass before it enters the fermentor. The biomass in the fermentation product is separated by centrifugation and recycled into the fermentor. The remaining fluid is destilled, producing ethanol.

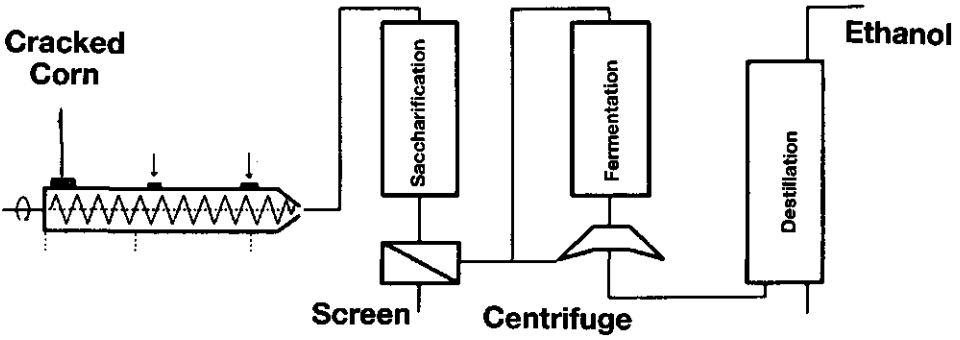

Fig 7.7 A proposed process for conversion and fermentation of raw cracked corn (van Zuilichem et al., 1990)

The estimated cost of this simplified process, with capital

depreciation over three years, is approximately $ 130,- per tonne substrate for the conversion process. This results in an attractive raw material cost for the fermentation process.

7.7 Conclusions

The described conversion was proven to be possible. The use of one continuous extrusion process instead of the two steps described would however improve the process.

Conversion of cracked corn (70% of DM starch) into a fermentation substrate using extrusion under the given circumstances (0.053% Termamyl α-amylase during extrusion, 0.214% Amigase gluco-amylase, 60 °C and 30% DM during saccharification) results in a DE 40 substrate within 1 h, and DE 60 in approximately 4 h. The total process cost for such a DE 40 substrate (including depreciation, excluding raw material cost) would be around $ 15,- per tonne substrate.

The presented method of investigation provided a useful tool for calculating and optimising such a conversion process.

References

Chay, P.B., Chouvel, H., Cheftel, J.C., Ghommidh, C., Navarro, J.M. (1984). Extrusion of hydrolysed starch and flours to fermentation substrates for ethanol production. Lebensm. Wiss. & Technol., 17, 257-267.

Chouvel, H., Chay, P.B., Cheftel, J.C. (1983). Enzymatic hydrolysis of starch and cereal flours at intermediate moisture content in a continuous extrusion-reactor. Lebensm. Wiss. & Technol., 16, 346-353.

Cochran, G.W., Cox, G.M. (1957). Experimental Designs, 2nd. ed.. Wiley, New York.

Hakulin, S., Linko, Y.Y., Linko, P., Seiler, K., Seibel, W. (1983). Enzymatic conversion of starch in twin-screw HTST extruder. Starch, 35, 411-414.

Lehninger, A.L. (1970). Biochemistry: The molecular basis of cell structure and function. Worth Publishers, Inc., New York, 153-157.

Linko, P., Linko, Y.Y., Olkku, J. (1983a). Extrusion cooking and bioconversions. J. Food Eng., 2, 243-257.

Linko, P., Hakulin, S., Linko, Y.Y. (1983b). Extrusion cooking of barley starch for production of glucose syrup and ethanol. J. Cereal Sci., 1, 275-284.

Linko, Y.Y., Vuorinen, H., Olkku, J., Linko, P. (1980). The effect of HTST extrusion on retention of cereal α-amylase activity and on enzymatic hydrolysation of barley starch. In: Food process Engineering Vol. II: Enzyme Engineering in Food Processing, ed. P. Linko, L. Larinkari. Applied Science Publishers, London, 210-223.

Marshall, J.J. (1980). Some aspects of Glucoamylase action relevant to the enzymatic production of dextrose from starch. In: Food process Engineering Vol. II: Enzyme Engineering in Food Processing, ed. P. Linko, J. Larinkari. Applied Science Publishers, London, 224-236.

Park, Yong K., Sato, H.H., San Martin, E.M., Ciacco, C.F. (1987). Production of ethanol from extruded corn starch by a non-conventional fermentation method. Biotechnology letters, 9, 143-146.

Reinikainen, P., Suortti, T., Olkku, J., Malkki, Y., Linko, P. (1986). Extrusion cooking in enzymatic liquefaction of wheat starch. Starch, 38, 20-26.

Zhusman, A.I. (1979). Extrusion of starch products from maizeprocessing waste at the Korenovskii experimental factory. Sakharnaya Promyshlennost, 12, 33-35.

van Zuilichem, D.J., Bruin, S., Janssen, L.P.B.M., Stolp, W. (1980). Single screw extrusion of starch- and proteïn-rich materials. In: Food process Engineering Vol. I: Food processing systems, ed. P. Linko, Y., Malkki, J., Olkku, J. Larinkari. Applied Science Publishers, London, 745-756.

van Zuilichem, D.J., van Roekel, G.J., Stolp, W., van 't Riet, K. (1990). Modelling of the Enzymatic Conversion of Cracked Corn by Twin Screw Extrusion Cooking. J. Food Eng., 12, 13-28.

Notation

r	Reaction rate glucose	$[kgm^3s^{-1}]$
C_s	Substrate concentration	$[kgm^{-3}]$
C_w	Water concentration	$[kgm^{-3}]$
C_e	Enzym concentration	$[kgm^{-3}]$
k	Reaction rate constant	$[s^{-1}]$
DE	Dextrose equivalent	[%w/w]
A	Constant	$[(\%w/w)^{-1}s]$
B	Constant	$[(\%w/w)^{-1}]$
X_0-X_4	Coded variables	
X_1	Concentration α-amylase	[%]
X_2	Concentration glucoamylase	[%]
X_3	Temperature	[°C]
X_4	Dry matter content	[%]

Appendix 7.1

$$r_s = \frac{dC_s}{dt} = kC_s^2 \qquad (1)$$

$$C_s = \frac{1}{B} - DE = \frac{1}{B} - \frac{t}{A+Bt} = \frac{A+Bt-Bt}{B(A+Bt)} = \frac{A}{B} \cdot \frac{1}{A+Bt} \qquad (2)$$

$$\frac{dC_s}{dt} = \frac{A}{B} \cdot \frac{-1}{(A+Bt)^2} \cdot B = \frac{-A}{(A+Bt)^2} \qquad (3)$$

$$kC_s^2 = k \cdot \frac{A^2}{B^2} \cdot \frac{1}{(A+Bt)^2} \qquad (4)$$

Substitution of equations 4 and 3 in 1 gives:

$$k = \frac{B^2}{A} \qquad (5)$$

which suggests that the kinetics of the reaction are second order.

CHAPTER 8

GENERAL DISCUSSION ON EXTRUSION-COOKING

8.1 Gain in knowledge

As explained in chapter 1 the so called HTST processes are prefered for processing of food because of their ability to maintain upmost the original food quality. High temperatures combined with attractive short processing times (HTST) can be realised in most extruder types,but the realisation at the same time of a good residence time distribution (RTD) is not always possible. In some cases the chosen extruder design is limiting , in other cases the specifications of the wanted product may be too narrow. How the hardware can be limiting will be understood when an extruder-user has to decide between a single screw or a twin screw extruder with respect to the RTD. As explained in chapter 2 for single screw extruders and in chapter 3 for twin screw extruders both types of equipment have possibilities but especially the tail in the RTD-curve for a single screw extruder may be an unacceptable feature in combination with the unavoidable slip phenomena. A good example is the preparation of some baby food products and dietetic food with narrow specifications in cooking extruders. Here it is extremely important that each food particle is treated almost in the same way, with respect to the amount of heat, shear energy and residence time. If the food is containing starchy material, it is unacceptable if non-gelatinized, native starch particles will be detected in the food. The philosophy of the extruder manufacturer may cause such a defect as will be explained. Trials performed with Clextral corotating extruders in the beginning of the eighthies learned that always a certain amount of native starch particles arrived at the die. This was caused by the "house concept" of the screw layout as was advised by Clextral, where at the tip of the screw set always a so called counter-

pitch element is mounted in order to bring the wanted pressure level and to create at last the shear and mixing. This concept works out quite acceptable for product specifications which are not so definitely set as is for baby food and dietetic purposes. The clearances for screw and barrel and the more or less open screw channel path still allow some particles to travel fast and untreated to the reverse screw element which again will allow some particles to arrive at the die in native state. The same trials, performed with Baker Perkins equipment in Raleigh (U.S.A.), where the corotating extruder was provided with a barrel valve, as described in chapter 6, learned that the product was homogeneously treated and no untreated individuals could be traced. At the same time the extra advantage is cashed, that the variance in RTD will not increase so much by using the barrelvalve as is the case when the concept of the reversed pitch element is used.

In comparison with the beginning of the eighties knowledge has gained considerably about the effects of changed screw lay-out for single and twin screw cooking extruders on the RTD. At the same time the real effects of rooted prejudices advertised by some cooking extruder manufacturers how special screw elements should be used are investigated in the chapters 2/3 and 6 and are evaluated further by Jager in his thesis (1992).
Data are available now for a number of cooking extruders, at different working points and for various raw materials, e.g soy and some starches, which allow to predict the expected over-treatment for a calculable part of the product, using simple equations. For these denaturations the severity can be estimated using equations, constructed in analogy with the Arrhenius model, like e.g is done in chapter 4 describing the coloration of starch syrup and sucrose mixtures. Recently, comparable calculations have been made for the animal-feed branch where the inactivation of anti nutritional factors (ANF) in legume seed during extrusion cooking could be described successfully (van der Poel et al., 1991a, in press).
For a safe use of raw materials in this branch, like feeding peas

from different origin, broad beans, field beans and other pulses, the extruder cooker will be an appreciated process tool, when the cooking effects can be predicted, as is stated by van der Poel et al., (1991b).
How important a gain in knowledge is reached by developing a good fitting heat transfer model for cooking extruders as is done in chapter 4 and 5, is demonstrated by the Arrhenius model, in general written as:

$$\frac{\Delta L}{\Delta t} = k_\infty e^{\frac{-\Delta E}{RT}} \cdot L \qquad (1)$$

In which K is reaction rate constant (1/s), T is absolute temperatuur (K), R is the gas constant and ΔE is the activation energy (kJ/mol). ΔL/Δt is the derivative of e.g nutritional value to time. This means that for each residence time step Δt, the loss of ANF present in the extruder, at the product temperature T now can be calculated, assuming a certain thermohomogeneity over the extruder channel cross section after a residence time t from the feed port. As is demonstrated in chapter 5 there is some inaccuracy between measured and predicted temperatures of the cooking extruder at the higher throughputs. This is a subject which will be part of the research program in order to optimize the calculation procedure as soon as possible.
The most striking gain in knowledge about extrusion cooking since the eighties is found in the tooling offered in the chapters 1 through 7, leading toward calculations where combined efforts of heat, residence time, product moisture and screw layout on product quality now can be performed. At the same time this knowledge leads to a procedure of product development, if more data are collected and stored in expert systems for the different food branches. The collection of such data is a craft, the use of the data with help of the science leads to a more full-grown-extrusion-cooking technology.

8.2 Market

When considering the results of the investigated subjects one can conclude that the understanding of the behaviour of extruder

cookers has increased. In several cases it had led to an increase of the number of applications of extruder cookers in the branches of food industry but mostly market questions have given a big push in technology development. Janssen and van Zuilichem forecasted in 1976 at the Dutch Machevo-fair in Utrecht a six fold increase of the number of food extrusion cooking applications over a period of 15 years (Fig. 8.1). The figure of 1990, foreseen in 1976, tells that the extruder snack market and pasta food market would not grow so much, whereas at the same

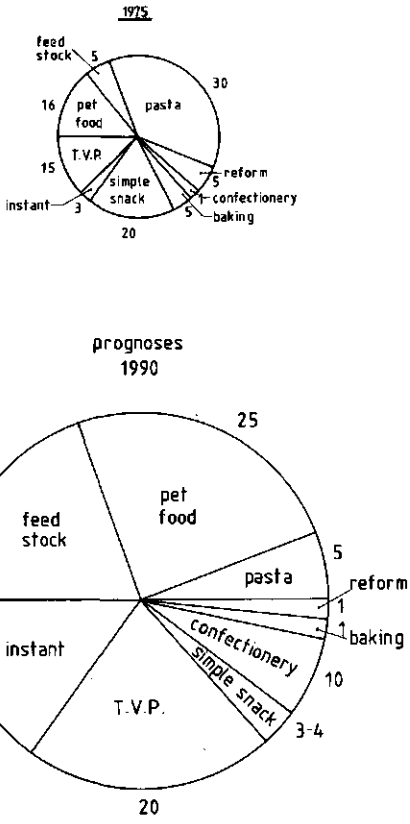

Fig. 8.1 History and forecast of extrusion-cooking applications in western Europe, 1975-1990 (van Zuilichem et al., 1978)

time the market for instant products and convenience products like petfood would expand heavily. Having some results available for the extruded food and feed market in 1990 it can be conducted that the forecast for e.g. the petfood industry has even been to

pessimistic.

8.2.1 Petfood

In Europe the market for extruded petfood is still steadily growing. In comparison with the figure of 1975 the number of applications is more than a tenfold and the extruded petfood has

year	1975	1980	1985	1990
sales in billion dollars	1.5	2.4	3.5	4.4

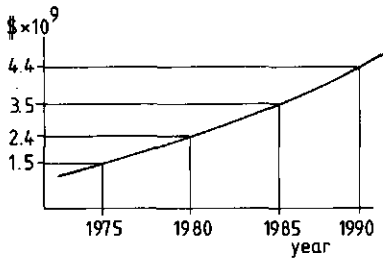

Fig. 8.2 Expected growth for the petfood market (van Zuilichem et al., 1978)

become a severe competitor of the canned, so called "wet" petfood (Fig. 8.2). As a general figure can be said that about 55-60% of all petfood is now an extruded dry product. The petfood industry tries to produce well shaped, multi coloured "fancy" products, facing, with a time delay of approximately twenty years, identical technological problems as are known in the snack industry, which are not only restricted to die design. The time for only simple expanded dry petfood has passed by and the lack of knowledge what really happens in extruder-cookers becomes obvious. Manufacturers, who can afford to buy sophisticated twin-screw extruders can come up more easily to the expectations set by the marketeers and the customers, making use of the flexibility of the twin-screw extruder equipment. The users of single screw extruder equipment will have more problems as they are condemned to the so called bulk-market, which is big, but

with smaller profits. This means that single screw extruder equipment of the most economical design will be chosen for the production (see chapter 1 Fig. 1.9.a), as than the depreciation of the lower investment will allow better profits. However, the more important now will be the knowledge of the impact of process variables like residence time, heat transfer, viscosity behaviour, mixing, etc., on product properties. Another factor, which starts playing an important role is the scale of production per unit. In petfood production as well as in fish feed production and animal feed production hourly capacities of (5-10) metric tons will be quite normal (Veenendaal, 1990). At the moment only the expander-extruder equipment mentioned in chapter 1 (Fig. 1.9.a) will be capable to perform this job, and to bring the wanted capacities, which means that we have to accept the limited performances of the expander-extruder equipment.
The limitations mentioned concern respectively:

- A greater dependence of flow patterns and residence time distribution of material properties, including moisture.
- Less positive displacement.
- Less heat transfer homogeneity.
- Less flexibility, in terms of fixed screw length/geometry.
- Difficult to scale up.
- Somewhat dependent of the craftsmanship of the operator.

However, we have to admit that considerable advantages can be gained which turn the scale for industrial applications easily, like:

- Easy maintenance.
- Low spare part costs.
- Suitable for steam injection.
- Acceptable mixing by mixing pins.

Especially the use of steam injection is of particular value as it increases the production per unit considerably due to the combined influence of controllable heat input and decreased viscosity.
It overcomes the limited heat transfer from the barrel to the

bulk. Of course the use of the amount of steam in the expander is limited since one will avoid too high water contents in the product and too low viscosities. It is remarkable to notice that this branch of food industry has started in the past with single-screw extruders, that has made quite often use of twin-screw extruders in the seventies and the eighties. They are now, however, back again with the most simple design of a single screw extruder possible; the expander extruder. As stated before the main reason for this is the simple question: "Who pays the second screw?", but the increasing know how of extrusion cooking processes has made the use of the expander extruder possible, since now we understand much better the combined effects of heat transfer, shear, mixing and viscosity behaviour.

8.2.2 Coextrusion

On the other hand this better understanding allows to develop the more complicated products as they are produced in the snack industry, mostly with twin screw extruders (See Fig 8.3 and 8.4). In the years 1985 to 1987 so called coextruded products were very popular in the U.S.A, disappeared from the market, but are back again over there, made by M&M and start to come in Europe (Bass, 1986). One

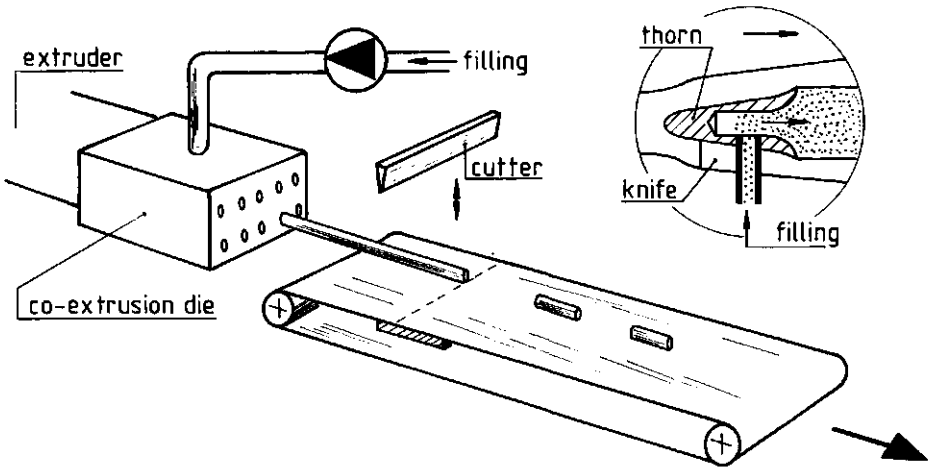

Fig. 8.3 Co-extrusion filled bisquits (demo APV-Baker, Interpack 1984; van Zuilichem et al., 1987)

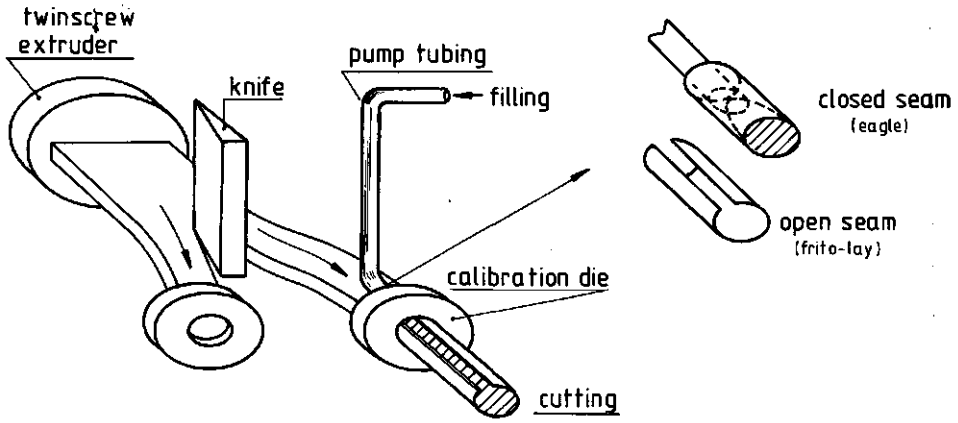

Fig. 8.4 Alternative for co-extrusion: post-die-head filled snack (van Zuilichem et al., 1987)

should not underestimate the complexity of this process, reason to discuss here some of the problems.

Coextrusion is a redesigned process found in the bakery and confectionery industry. The coextruded product is mostly of the tubular type, in which the outer component is produced by a cooker-extruder and the inner component is a pumpable product which will not flow freely at ambient temperatures. The two components are extruded simultaneously to produce a continuous filled tube, which is later cut to size.
Earlier products on the English market, like Cadbury's "Criss Cross" and Mars "Cornquistos" consisted out of an extruded tube and a "post-filled" center. In the U.S.A. however Herschi produced a liquorice type product, which is die-filled with a dried fruit containing chewable inner filling.
For each product development a number of problems have to be solved; including die design; recipe-restrictions; pumping the illing; post extruder processing and the cutting, which is explained below.

Die design: The best arrangement is to bring the center filling over 90 degs. in the extruded outer tube, giving the center a more restrictive path but allowing the outer tube to be

consistent. The outer tubing is mostly forced through a restriction formed by a number of small holes or by an annular ring. It is desirable to have the center entry point as far away from the final die as possible, in practice a distance of about 40 mm. An imporatant problem is manufacturing a die-arrangement which will maintain the accurate gaps between center die -and outer parts, during the die lifetime.

Size restrictions: When the minimum dimension of the outer annulus is about 1 mm thickness and the wall-thickness of the center tubing is also chosen 1 mm , the restriction will be clear. The outer shell easily expands to twice the diameter of the die annulus, giving way to a certain pumping area cross section. It does not appear to be practical to work with a ratio greater than 10, giving a minimum inside diameter of a finished product of about 10 mm, whilst the outside is about 14 mm. Reduction of the expansion can be achieved by changing the raw material properties and the product moisture, Multiple outlets are perfectly possible as demonstrated by Demo APV-Baker at Interpack Fair Dusseldorf BRD in 1984, where 10 tubes were extruded simultaneously.

Recipe restrictions: Crisp extruded wheat based outers can be directly produced in a twin screw extruder at 5% moisture. A problem for the center filling will be the equilibrium moisture content which will ultimately exist, but enough knowledge is available from the biscuit, wafer and confectionery industry to develop attractive center formulations for cheese, meat pastes, onion/nuts, caramel, gums, jellies and sugar/fat creams.

Density-influence: If a round tube is extruded and filled the weight of the center will be 2 or 3 times that of the outer, which makes the center to dominate. This can be overcome by:

- alteration of the cross section after extrusion from circular tubing to a flattened cross section.
- adding finely ground extruded and expanded starchy material to the center filling, in order to reduce the density.

- aeration of the center filling, which brings the density back for a straight cream from 1,2/1,3 towards 0,7/0,8 $kg.dm^{-3}$.

Center pumping: Usually each tube, produced by the twin screw extruder is provided with its own metering-pump, in order to match the weights in the two streams exactly. The temperature, at which the cream is pumped depends on several factors. Very viscous creams must be preheated, but normally pumping at ambient temperatures should be preferred. For such a cream a typical temperature curve would be:

- hopper 22°C
- pump outlet 24°C
- die entry 25°C
- die exit 50°C
- post die (60S) 65°C

Post processing: Several technological solutions are in use like rolling, the use of secondary dies, cooling provisions, drying and toasting. It should be mentioned that most products have a memory for the original die shape and more than one roller passage is needed for an alteration of the cross section.
Since long secondary dies are impractical to operate, these dies are only in use for outer recipes that set quickly. Those dies must be adjustable, in much the same way shaping jaws are used for flat-bread production. Since the outer tube cools faster than the inner center, the outer tubing acts as an effective insulator. Nevertheless, in practice 2% moisture loss can be reached by cooling.
For drying purposes warm air is suitable and will help to give a final texture to the outer tube. Finally the products in the toasting section should be rotated in order to create an evenly distributed colour and taste.

Cutting: If closed product ends are needed the cutting/crimping device must be close to the die. If a symmetrical crimp is needed a pair of cutting rolls is essential. When the product end-planes

are to be open, allowing the center to be seen, the tube must be set prior to the cutting, and at the same time the center cream must be cool enough not to flow out.
It is difficult to see how the family of coextruded products will develop but product makers will handle this technology as a strong tool in the future. One has to admit that this coextrusion in the stage where it is described here, is more a craft than a science.

8.2.3 Feed industry

As is mentioned above the expectation is confirmed that the feed industry has discovered cooking extruders for part of their production, especially for weaning feed. The extruder will be used as a preconditioner in their pellet lines, just before the press.
It is a wise decision using the extruder in this way as the processing reactor, in which unwanted ANF can be inactivated, whereas the conventional shaping and economical forming-equipment like pelletizing mills will be maintained. For the feed industry the gain in knowledge, described above, can be of immediate help to solve some ANF-problems and allow to "engineer" product quality. Also here the marginal profits in this industry will exclude at a first glance the costly twin screw extruders and will favor single screw equipment, as is the case in the pet food industry. This tendency also counts for the fish feed industry where the gross margins are small and a good balance must be found in caloric value of the products and the total process costs, including the drying costs. This will direct this branch as well to the use of expander equipment

8.2.4 Other Food-branches

In the remaining branches of the food industry, mentioned by Janssen and van Zuilichem in 1975, the cooking extruder will be used as a processing reactor capable to produce products with certain unique rheological properties, such as watersorption, watersolubility, wateractivity or a certain consistency. This counts for the pasta industry as well as for the convenience food

branch, where people understand that an extruder cooker is capable to "engineer" rheological properties. A survey of products, made by extruder cookers is given in Table 8.1. For this purpose the extruder cooker is used to create a product with a complicated texture and structure, which cannot be produced with conventional equipment. Here the die is an important part of the hardware and the die construction mostly is very vulnerable and crucial for the end result as is e.g the case for instant products.

8.2.5 Agrochemicals

The marketshare for extrusion cooking applications is not limited to food alone, since the extruder cooker, as a process reactor,

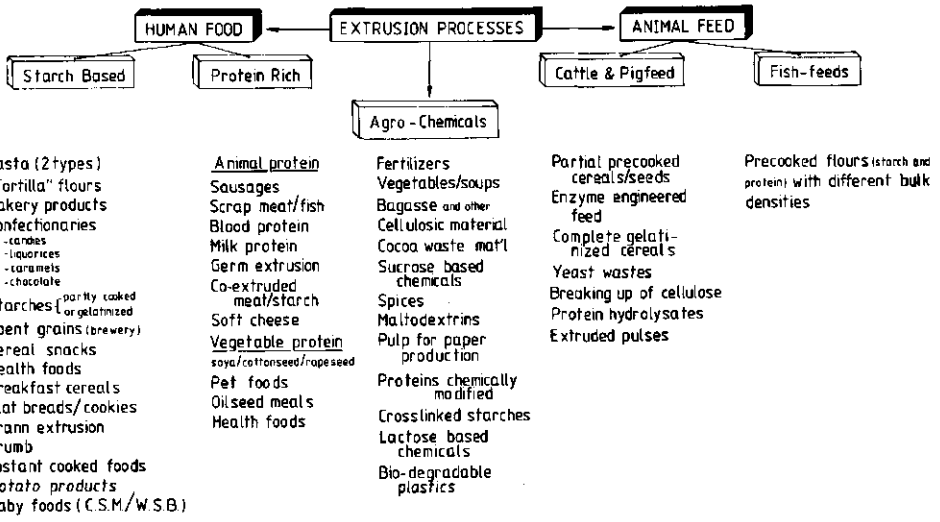

Fig. 8.5 Survey of products made by extrusion cooking (van Zuilichem et al., 1987)

proves to be a good piece of equipment for so called agrification purposes. In the survey of Fig. 8.5 appears a third group agro-chemicals, ranging e.g. from chemically modified starches, used in the paper industry as paper coating, to wood chips and plant fibre extrusion. The number of applications in this field is still increasing. The knowledge however to develop such processes is limited, since the thorough descriptions of extruder cookers as processing reactors are scarce available.

8.3 Equipment manufacturers

Many expectations in extrusion-cooking have not come up, quite some equipment manufacturers have held out great hopes to their customers, promising irrealistic throughputs, product qualities and savings when using extruder cookers. Especially those among the manufacturers, who had none or too little experience with food, non-newtonian food properties and with the food market were bad advisors.
Not all of them are to blame, esp. those companies specialised in food equipment for which extruder cookers only are one interest amongst others, since they are very much familiar to the difficult behaviour and sometimes remarkable rheological properties of food products.

Most failures have been made by companies which are used to construct equipment for the plastic polymer industry. They underestimated the effect of the presence of water and oil as normal constituents in agricultural produce and had no knowledge about the behaviour of not well defined bio-polymers in food, such as different starches and proteins.
With the knowledge presented above, the equipment manufacturers will be able to advise their clients more properly about technological questions related to product development. On the other hand they should equip themselves with the knowledge that is available now and use it for the development of better food extruders. Time has passed in which a food-extruder lay-out was made by a design staff, educated in mechanics and chemical polymer science. When extrusion cooking operations will be performed more efficient in the future, the existing design teams will have to include well educated food process engineers with a substantial amount of science in their luggage.

8.4 Technology, Final Remarks

RTD

General knowledge is available how axial mixing works out in a

RTD. This is quite exact for the co- and counter-rotating, twin-screw extruders. This knowledge is still incomplete for different designs of single screw extruders, like expander equipment. This should be studied further.

Heat transfer

Knowledge is available now about the calculation of the heat flow in single and twin-screw extruders. Here the peculiar region near the barrel inside diameter appears to be a limitation in the understanding of the radial mixing and the flow patterns in different kinds of screw geometries. This fundamental knowledge will help to optimize the heat transfer calculations. Also this is a subject for further studies.

Biotechnology, consequently mixing

It is common to use extruder equipment quite successfully for dispersive mixing applications in the plastic and rubber industry, however the study in chapter 7 shows directly that the restrictions in using extruders as reactors in food/biochemical operations are of a different nature.

Integration

When an attempt is made to integrate models of a RTD, heat transfer and mixing in one extruder model the predictions on extruder performance can be improved. This will not diminish the "craft" part in extrusion cooking as the complexity of such a model will guarantee the question "craft or science" to remain, but now for the use of this model.

References

Bass, C.P. Co-extrusion: The problem and some of the solutions. Pasta and extrusion cooked foods, proceedings of symposium held in Milan 25-26 march, 1985, p159-166.

Poel, A.F.B. van der, Blonk, J., Huisman, J., den Hartog, L.A. Steam processing methods for pheasolus vulgarus beans. Livestock production science. 1991a, p305-319.

Poel, A.F.B. van der, Doorenbos, J., Huisman, J., Boer, H., Evaluation of Techniques to determine the protein digestibility in heat processed beans for piglets, Animal feed science and technology, 1991b, p331-341.

Veenendaal, J. Extrusion in the compound feed industry. Moritz Schaeffer Detmold, Advances in Feed technology, 1990, p 63.